Author/s:
Penna, Vanessa

Title:
Understanding and promoting the functional integration of neural transplants in Parkinson's disease

Date:
2019

Persistent Link:
https://hdl.handle.net/11343/240400

UNDERSTANDING AND PROMOTING THE FUNCTIONAL INTEGRATION OF NEURAL TRANSPLANTS IN PARKINSON'S DISEASE

Vanessa Penna

UNDERSTANDING AND PROMOTING THE FUNCTIONAL INTEGRATION OF NEURAL TRANSPLANTS IN PARKINSON'S DISEASE.

Vanessa Penna

0000-0003-0963-3106

August 2019
Submitted in total fulfillment of the requirements of the degree of Doctor of Philosophy

Department of Medicine, Dentistry & Health Sciences
The Florey Institute of Neuroscience and Mental Health
The University of Melbourne

Abstract

Clinical trials have provided evidence that the transplantation of new dopamine neurons (DAn) into the striatum of Parkinson's disease (PD) patients can survive, integrate and restore motor function. Demonstrated first using fetal donor tissue isolated from the developing ventral midbrain (VM), the procedure was hindered by challenges of poor tissue standardisation, limited availability and ethical considerations. Recently, studies have seen a rapid advancement in the use of human pluripotent stem cells (hPSC), differentiated into dopamine progenitors, as a viable alternative and standardized donor source. Despite recently advancing to clinical trials, several questions remain regarding the safety, predictability and efficacy of these cells. While fetal tissue has an estimated 20% cell survival and just 10% of cells within the graft are DA neurons, hPSC-derived neural transplants are notably poorer – remaining highly heterogeneous with a high proportion of non-dopaminergic cells and display inferior reinnervation of target tissues compared to their fetal counterpart. Such observations suggest that a more conducive environment, reminiscent of the developing brain, to support newly integrate fetal and hPSC-DA progenitors could improve the differentiation and functional capacity of neural transplants for PD. The present thesis had focused on improving the host environment into which cells are delivered by using a tissue-specific hydrogel/biomaterial to mimic the extracellular matrix (ECM). The employed biomaterial was capable of signalling to the cells by presenting a high density of a laminin epitope (the main brain ECM component) capable of influencing not only cell adhesion but also survival, differentiation and plasticity. In addition, the biomaterial was utilised to sustain the delivery of trophic proteins, absent in adult brain. This thesis demonstrated the synergistic capacity of the tissue-specific hydrogel, sustaining the delivery of stromal derived factor1 (SDF1) or glial cell-derived neurotrophic factor (GDNF) to enhance grafting outcome for rodent fetal tissue grafts and human pluripotent stem cell derived grafts, respectively, in rodent models of PD. Finding demonstrated these functionalised scaffolds promoted graft survival, improved the specification of A9 dopaminergic neurons (the subpopulation of DA neurons responsible influencing motor function) and enhance plasticity – resulting in restoration of motor deficits.

Recognising the heterogeneity of hPSC-derived VM grafts to date, yet with little knowledge of the cellular composition, the work within this thesis also developed a new method to rapidly and efficiently transcriptionally profile xenografts. The method employs bulk tissue dissection, inclusive of the graft and surrounding host tissue, and utilises differences in the RNA sequences between the species to discriminate the xenograft from host gene expression -using either real-time qPCR (qPCR) or whole RNA sequencing (RNAseq). The technique is validated and demonstrated by assessing and comparing the composition of undifferentiated hPSC grafts/teratomas to hPSC-derived VM progenitor grafts in the rodent brain. The approaches enable identification of known and novel genes and provides the first complete characterisation of human VM grafts to date.

Collectively, this thesis provides new insight into improving the functional outcomes of VM progenitors' grafts, as well as a means to screen grafts for both safety and predictable efficacy. Such knowledge will be of critical important as these cells continue to move into clinical trials.

Declaration

This is to certify that:

I. This thesis comprises only my original work towards the PhD except where indicated in the preface,

II. Due acknowledgement has been made in the text to all other material used,

III. This thesis is fewer than 100,000 words in length, exclusive of tables, bibliographies and appendices.

Vanessa Penna

03/09/2019

Preface

Others who have contributed to the studies of this thesis. Contributions include:

- Prof Clare Louise Parish for the *in vitro* testing of release kinetics and activity of proteins released from the hydrogels.
- Ms Mong Tien for assistance with immunohistochemistry staining, animal perfusion and tissue processing.
- Ms Isabelle de Luzy for the human stem cells maintenance, ventral midbrain differentiation, *in vitro* staining, cell sorting and collaboration with animal behaviour.
- Dr. Carlos Gantner for the human stem cells maintenance, ventral midbrain differentiation, sorting, immunohistochemistry staining, and assistance with microscopy.
- Mrs. Charlotte Ermine for assisting with animal surgery, collaborating immunohistochemistry staining and synaptic density quantifications.
- Mrs. Jessica Kauhausen for assisting and collaborating with animal surgery and immunohistochemistry staining.
- Dr. Christopher Bye for contributing to the development of the methodological technique described in chapter 5.
- Dr. Cameron Hunt for collaborating with some qPCR results
- Ms. Brianna Xuereb for assistance with animal surgery, animal husbandry, behaviour testing and transcardial perfusions.
- Dr. David Nisbet for providing the biomaterials/hydrogels
- Ms. Yi Wang for the hydrogel fabrication, and ELISA for protein release from hydrogels, and transmission electron microscopy of hydrogels
- Melbourne International Fee Remission Scholarship
- Melbourne International Research Scholarship

The publication status of this thesis is as below:

- No part of this thesis is currently published. It is anticipated that the 3 results chapters will form 3 publications, with chapter 5 currently under review.

Publications related to the Ph.D.

D.R. Nisbet, T.Y. Wang, K.F. Bruggeman, J.C. Niclis, F.A. Somaa, **V. PENNA**, C.P.J. Hunt, Y. Wang, J.A. Kauhausen, R.J. Williams, L.H. Thompson, C.L. Parish. Shear Containment of BDNF within Molecular Hydrogels Promotes Human Stem Cell Engraftment and Post infarction Remodeling in Stroke. *Advanced Biosystems* (2018) Jul; 2(9): 1-13. doi: 10.1002/adbi.201800113

Alsanie WF, Niclis JC, Hunt CP, De Luzy IR, **PENNA V**, Bye CR, Pouton CW, Haynes J, Firas J, Thompson LH, Parish CL. Specification of murine ground state pluripotent stem cells to regional neuronal populations. *Scientific Reports.* 2017 Nov 22;7(1):16001. doi: 10.1038/s41598-017-16248-x.

Alsanie, W.F, **PENNA, V**, Schachner, M., Thompson, L.H, Parish, C.L. Homophilic binding of the neural cell adhesion molecule CHL1 regulates development of ventral midbrain dopaminergic pathways. *Scientific Reports.* 2017 Aug 24;7(1):9368. doi: 10.1038/s41598-017-09599-y.

Manuscripts under peer-review

Bye, CR*; **PENNA, V***; R de Luzy,I; C. P. Hunt; Gantner, CW; and Parish, CL. Transcriptional profiling of xenogeneic transplants: a case study examining human pluripotent stem cell-derived neural grafts in the rodent brain. *Stem Cell Reports* (minor revisions submitted 20/8/19). *Equal contribution

Gantner, CW; Kauhausen, JA; R de Luzy,I; Niclis, JC; **PENNA, V**; Hunt, CP; Bye, CR; Ermine, CM; Pouton, CW; Kirik, D; Thompson, LH; and Parish, CL. Viral Delivery Of GDNF Improves The Functional Integration Of Human Pluripotent Stem Cell-derived Dopamine Grafts in Rodent Models of Parkinson's disease. *Cell Stem Cell* (revisions in progress, 20/8/19).

Acknowledgements

There are many people I would like to thank for the help and support during my Ph.D. First to my family: My mother for the unconditional love and faith in me, in my choices and for supporting me throughout the most difficult health issues times in my life. My father (*in memoriam*) that sadly could not see (at least in physical presence) my Ph.D. completion but is the person responsible for my love in science and for my love in cooperation and ethics. My sister, for the emotional support, for knowing me better than I know myself and for listening to so many of my presentations in English. My husband who was so essential in my Australian life, that faced and helped me with my psychological and physical challenges. My godfather and godmother, you two are so essential in my life, your support and existence changes (and changed) my life for good. My grandma and grandpa that have taught me, through their difficult life history, what resilience and faith are.

Second to my friends: Carla Garcia (sister in my heart), Bianca Zanetti (friendship and help in science and professionally), Charlotte Ermine and Jessica Kauhausen (Stojcevski) - you have taught me so much at the lab and especially for being my most important mental health keeper, Serena Viventi - for the emotional support, the Brazilian gang (Roberta, Johnny, Pedro, Flavia, Marcela, Akira, Lucas, Carol, Larissa, Lilian, Andrea, Luciana, Rubens, Natasha, Leandro, Sasha) for the millions of barbecues, laughs and for being my Australian family.

I would like to express my deepest gratitude to my main supervisor Prof Clare L. Parish for her guidance in academia and in life. For teaching me so much about neuroscience, for her contribution to my academic growth, her patience throughout my candidature. To have never doubted my scientific, surgical and laboratory capacities.

I would like to thank my co-supervisor A/Prof Lachlan Thompson particularly for the support in immunohistochemistry.

Also, I would like to thank my co-supervisor Dr. Christopher Bye for his patience and support in teaching most of my molecular biology knowledge.

To my PhD committee chair, A/Prof Mirella Dottori and Steven Petrou, for taking the time to discuss my PhD project and collaborating to my scientific growth.

To the members of the Parish and Thompson labs, past and present, thank you for your assistance and for making the lab an enjoyable workplace. In particular, I would like to thank Dr Carlos Gantner for his friendly help, patience and guidance, you are brilliant.

Table of Contents

ABSTRACT ..... **II**

DECLARATION ..... **IV**

ACKNOWLEDGEMENTS ..... **VII**

TABLE OF CONTENTS ..... **IX**

LIST OF FIGURES ..... **XII**

LIST OF TABLES ..... **XV**

LIST OF ABBREVIATIONS ..... **XVI**

CHAPTER 1 - LITERATURE REVIEW **1**

1.1 Dopamine neurons and axons projections 2
1.2 Parkinson's Disease 4
1.3 Cell Replacement Therapy for PD 5
1.3.1 Grafting fetal dopaminergic neurons 5
1.3.2 Grafting hPSC-derived dopaminergic neurons 7
1.3.3 Challenges to surpass as we move to the clinic 9
1.3.4 Biomaterials – A recent and future approach to overcome the challenges facing cell transplantation for PD 15
1.4 Thesis overview 18
1.4.1 Hypothesis and aims of the thesis 18

CHAPTER 2 - MATERIALS AND METHODS **19**

2.1 Animals and Ethics 20
2.1.1 Stereotaxic Surgery 20
2.1.2 Lesion and Transplantation 21
2.2 Cells 23
2.2.1 Ventral Midbrain Primary Cultures 23
2.2.2 Maintenance of human pluripotent stem cells 23
2.2.3 Fluorescence-activated cell sorting 25
2.3 Biomaterials 25
2.3.1 Preparation of self-assembling peptide scaffolds 25
2.4 Immunohistochemistry 26
2.5 Microscopy and Quantification 28
2.6 RNA Isolation and qPCR 28
2.7 RNA sequencing 29
2.8 Statistical Analysis 30

CHAPTER 3 - EXTRACELLULAR MATRIX BIOMIMETIC HYDROGELS, ENCAPSULATED WITH STROMAL DERIVED FACTOR-1, ENHANCE THE

A9 DOPAMINERGIC SPECIFICATION OF FETAL TISSUE GRAFTS IN A RODENT MODEL OF PARKINSON'S DISEASE 31

3.1 ABSTRACT 32
3.2 INTRODUCTION 33
3.3 MATERIALS & METHODS 35
3.3.1 Self-assembling peptide hydrogel preparation and functionalisation 35
3.3.2 Ventral midbrain specification of human pluripotent stem cells 36
3.3.3 Surgical Procedures 37
3.3.4 Tissue Processing & histochemistry 37
3.3.5 Statistical Analysis 38
3.4 RESULTS 39
3.4.1 Laminin-based IKVAV hydrogel fabrication and sustained SDF1 delivery 39
3.4.2 SDF1 functionalised scaffolds increases DA differentiation 41
3.4.3 Functionalised scaffolds have no impact on the density of dopaminergic innervation of the host striatum 44
3.4.4 Functionalised scaffold increases the fate acquisition of A9 DA neurons, a subpopulation critical for motor function 45
3.5 DISCUSSION 47

CHAPTER 4 - PROLONGED GDNF RELEASE FROM TISSUE-SPECIFIC HYDROGELS IMPROVES THE FUNCTIONAL INTEGRATION OF HUMAN STEM CELL-DERIVED PROGENITOR GRAFTS IN A RODENT MODEL OF PARKINSON'S DISEASE 51

4.1 ABSTRACT 52
4.2 INTRODUCTION 53
4.3 MATERIALS AND METHODS 55
4.3.1 Self-assembling peptide hydrogel preparation 55
4.3.2 Assessment of GDNF release, and function, from SAP hydrogel 56
4.3.3 Ventral midbrain specification of human pluripotent stem cells 57
4.3.4 Surgical Procedures 57
4.3.5 Behavioural testing 58
4.3.6 Tissue Processing and histochemistry 58
4.3.7 Statistical Analysis 60
4.4 RESULTS 60
4.4.1 Tissue-specific scaffolds deliver functional GDNF to promote DA survival and plasticity in vitro 60
4.4.2 GDNF-Functionalized scaffolds promote functional recovery and increased graft survival in Parkinsonian rats 64
4.4.3 Functionalized scaffolds promote survival of DA neurons and bias A9-specification 69
4.4.4 Functionalized scaffolds support the integration of hPSC-derived VM graft 71

4.5 Discussion 74

CHAPTER 5 -TRANSCRIPTIONAL PROFILING OF XENOGENEIC TRANSPLANTS: A CASE STUDY EXAMINING HUMAN PLURIPOTENT STEM CELL-DERIVED GRAFTS IN THE RODENT BRAIN 79

5.1 Abstract 80
5.2 Introduction 81
5.3 Materials and Methods 82
5.3.1 Cell culture, differentiation and Sorting 82
5.3.2 Cell transplantation 85
5.3.3 Tissue Processing and histochemistry 85
5.3.4 RNA Isolation and qPCR 86
5.3.5 RNA sequencing 89
5.3.6 Statistical Analysis 90
5.4 Results 90
5.4.1 Design and validation of xenograft-specific primers for qPCR 90
5.4.2 Characterisation of xenografts using species-specific qPCR 93
5.4.3 Unbiased characterisation of xenograft composition and identification of novel transcriptional changes using RNAseq 100
5.5 Discussion 107
5.5.1 Conclusion 110

CHAPTER 6 - DISCUSSION 111

6.1 Where are we now? 112
6.2 Summary of research findings, significance and future directions. 113
6.2.1 Improving fetal tissue grafts for PD 113
6.2.2 What is the future for hPSC-derived transplants in PD 115
6.2.3 Understanding graft composition 117
6.3 Future directions 120

REFERENCES 123

List of Figures

Figure 1. Schematic picture showing the distribution of the DA neuron cell 2

Figure 2. Midbrain coronal section in the adult brain 3

Figure 3. Nigrostriatal and Mesocorticolimbic pathway 3

Figure 4. Diminished number of pigmented DAn of the substantia nigra in PD .. 4

Figure 5. Overview of fetal tissue transplantation into the Parkinsonian rodent brain. 6

Figure 6. Spatial and temporal expression of morphogens and transcription factors contributing to the development of ventral midbrain DAn 8

Figure 7. Comparison of former xenogenic and the newly recently established xenogenic-free (NEW) protocol for the DA differentiation of hESCs. 9

Figure 8. Diagram illustrating the various phases of cell death of DA progenitors within a cell transplantation study 10

Figure 9. Horizontal brain sections illustrating a homotopic TH-GFP fetal graft within the VM with GDNF over-expression 11

Figure 10. Schematic illustration of gels assembling peptide IKVAV 17

Figure 11. Hydrogel involving and protecting the cells from shear during the injection. 17

Figure 12. Laminin-based IKVAV hydrogel fabrication and sustained SDF1 delivery 40

Figure 13. SDF1 functionalised scaffolds increase DA differentiation. 42

Figure 14**.** Functionalised scaffolds have no impact on the density of dopaminergic innervation of the host striatum. 44

Figure 15. SAP scaffold, and sustained SDF1, increase A9 fate acquisition of DA neurons, a subpopulation critical for motor function. 46

Figure 16**.** Generation of SAP hydrogel biomaterial and hESC-derived Vm progenitors suitable for transplantation 60
Figure 17. Implantation of human ESC-derived VM progenitors together with a GDNF functionalised tissue-specific scaffolds improves motor function in Parkinsonian rats. 65
Figure 18. Tissue specific scaffolds show in vivo biocompatibility. 67
Figure 19. Tissue specific scaffolds show in vivo biocompatibility acutely after implantation. 67
Figure 20. Human PSC-derived VM progenitor grafts show modest vascularisation that was not influenced by the presence of GDNF and/or the SAP hydrogel. 68
Figure 21. Functionalized scaffolds increase graft size, consequential DA neuron yield and bias A9-specification. 70
Figure 22. Functionalized scaffolds support the integration of hPSC-derived VM graft. 73
Figure 23. Characterization of undifferentiated and DAn progenitors in vitro ... 83
Figure 24. Experimental design chapter 5 87
Figure 25. Screening of xenograft-specific reference (housekeeping) genes... 89
Figure 26. Graph of the specificity of xenograft-specific primers for human transcript relative to rodent host transcript in vitro 91
Figure 27. Graph representing the in vivo specificity of xenograft-specific primers 92
Figure 28. In vivo validation of a xenograft profile using species-specific qPCR. 95
Figure 29. Capacity for qPCR technique to detect graft composition. 96

Figure 30. Validation of midbrain dopaminergic identity of xenografts using qPCR. 98
Figure 31. Unbiased Characterisation of xenograft composition 103
Figure 32. Identification of novel transcriptional changes using RNAseq. 105

List of Tables

Table 1. Stereotaxic coordinates 21

Table 2. List of primary antibodies..... 27

Table 3. Table of human xenograft-specific primers designed 88

List of Abbreviations

AFP - Alpha Fetoprotein

ALDH1L1 - Aldehyde Dehydrogenase 1 Family Member L1

Calb - Calbindin 1

CD11b - Integrin

cFOS - AP-1 Transcription Factor Subunit

CHAT - Choline O-Acetyltransferase

CHMP2A - Charged Multivesicular Body Protein 2A

DA - Dopamine

DAn - Dopaminergic neurons

DAPI - 4’,6-diamidino-2 phenylindole

DAT (SLC6A3) - Solute Carrier Family 6 Member 3

DBH - Dopamine Beta-Hydroxylase

DRD2 - Dopamine Receptor D2

EAAT1 (SLC1A3) - Solute Carrier Family 1 Member 3

EAAT2 (SLC1A2) - Solute Carrier Family 1 Member 2

ECM - Extracellular Matrix

EN1 – Engrailed 1

FACS - Fluorescent Activated Cell Sorting

FEV - FEV Transcription Factor, ETS Family Member

FOXA2 - Forkhead Box A2

GAD1 - Glutamate Decarboxylase 1

GAT-1 (SLC6A1) - Solute Carrier Family 6 Member 1

GATA6 - GATA Binding Protein 6

GCH1 - GTP Cyclohydrolase 1

GDNF - Glial cell line-Derived Neurotrophic Factor

GFAP - Glial Fibrillary Acidic Protein

GFP- Green Fluorescent Protein

GIRK2 - G-protein-gated inwardly rectifying K+ channel subunit 2

GLS - Glutaminase

hESC - Human Embryonic Stem Cells

HNA - Human Nuclear Antigen

HPRT1 - Hypoxanthine Phosphoribosyltransferase 1

hPSC - Human Pluripotent Stem Cells

IGSF8 - Immunoglobulin Superfamily Member 8

IPSC - Induced Pluripotent Stem Cells

KI67- Marker of Proliferation Ki-67

LMX1A - LIM Homeobox Transcription Factor 1 Alpha

MBP - Myelin Basic Protein

MCM2 - Minichromosome Maintenance Complex Component 2

MTHFD1 - Methylenetetrahydrofolate Dehydrogenase, Cyclohydrolase And Formyltetrahydrofolate Synthetase 1

NeuN - Neuronal Nuclei Antigen

NEUROG2 - Neurogenin 2

NLGN3 - Neuroligin 3

NURR1 - Nuclear Receptor Subfamily 4 Group A Member 2

OCT4 - POU Class 5 Homeobox 1

Olig1- Oligodendrocyte Transcription Factor 1

Olig2 - Oligodendrocyte Transcription Factor 2

OTX2 - Orthodenticle Homeobox 2

PCNA - Proliferating Cell Nuclear Antigen

PD - Parkinson's Disease

PITX3 - Paired Like Homeodomain 3

PSA-NCAM - Neural Cell Adhesion Marker

PSC - Pluripotent Stem Cells

PSMB4 - Proteasome Subunit Beta 4

qPCR - Real-Time Polymerase Chain Reaction

RECA1 - RecA-Like Protein 1

RNAseq – RNA sequencing

SAP - Self-Assembling Peptide

SDF1- Stromal Cell-Derived Factor 1

SEMA5a - Semaphorin 5A

SERT (SLC6A4) - Solute Carrier Family 6 Member 4

SLC5A7 - Solute Carrier Family 5 Member 7

SNCA - Synuclein Alpha

SNpc - Substantia Nigra Pars Compacta

SOX2 - SRY-Box 2

SYN - Synaptophysin

SYNB - Synaptobrevin

TH - Tyrosine hydroxylase

TPH2 - Tryptophan Hydroxylase 2

VAChT (SLC18A3) - Solute Carrier Family 18 Member A3

VGAT (SLC32A1) - Solute Carrier Family 32 Member 1

VGLUT2 (SLC17A6) - Solute Carrier Family 17 Member 6

VM - Ventral Midbrain

VMAT (SLC18A2) - Solute Carrier Family 18 Member A2

VTA - Ventral Tegmental Area

Chapter 1 - Literature Review

1.1 Dopamine neurons and axons projections

Dopamine (DA) is one of the most intensely studied neurotransmitters in the brain due to its critical involvement in important functions such as motor control, motivation, arousal, reinforcement, and reward - and also because of its association with a number of psychiatric, neurodevelopmental and neurodegenerative disorders. Dopamine neurons (DAn) belong to a subgroup of catecholamine neurons and are distributed among 17 nuclei within the brain, classified as A1- A17 [1]. These populations are anatomically distributed from medulla oblongata to the hypothalamus (A1-A12) and in diencephalon, olfactory bulb and retina (A13-A17) [2]. DAn project axons into defined brain areas. The nine principal DAn groups and their projections are shown, in a sagittal view of embryonic and adult rodent brain below, **Figure 1**.

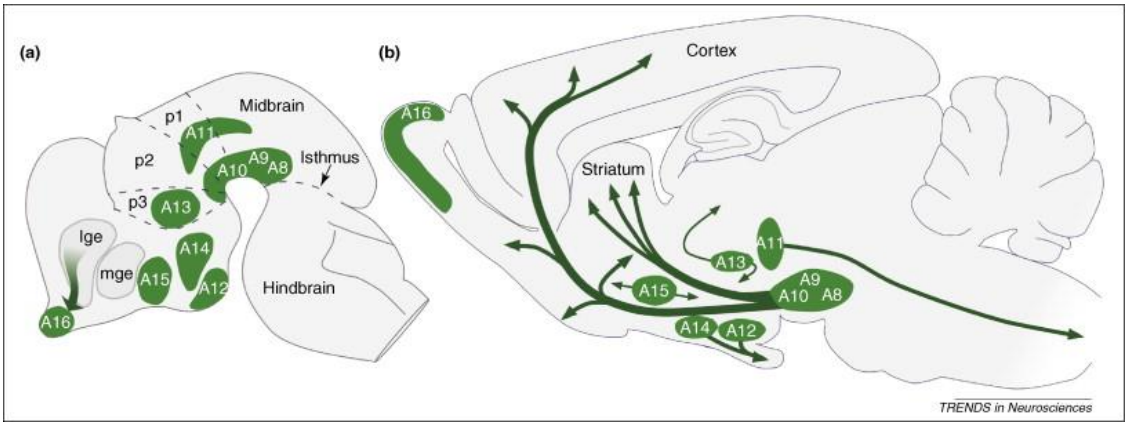

Figure 1. Schematic picture showing the distribution of the DA neuron cell groups within the (a) developing, and (b) adult rodent brain. The A8-A10 DA neurons within the ventral midbrain project to the striatum and cortex to regulate motor and cognitive function [2], *lge (lateral ganglionic eminence) and mge (medial ganglionic eminence).*

Relevant to this thesis are the midbrain dopamine populations, their involvement in control and modulation of motor function and the consequence of loss of these neurons in Parkinson's disease [3][4].

In the mammalian brain, the ventral midbrain dopaminergic neurons are the main source of dopamine with an estimated 500,000 neurons existing bilaterally in the human adult midbrain DA system [5]. The two main midbrain populations include A9 neurons of the substantia nigra pars compacta (SNpc), and the A10 neurons

of the ventral tegmental area (VTA) [1]. Note, a small population of A8 DAn reside within the Retrorubral field but will not be discussed further within this thesis. These A9 and A10 subclasses of DAn are identified and categorized regarding their morphology, location within the midbrain (**Figure 2**) and efferent projection patterns (**Figure 3**) [3][6].

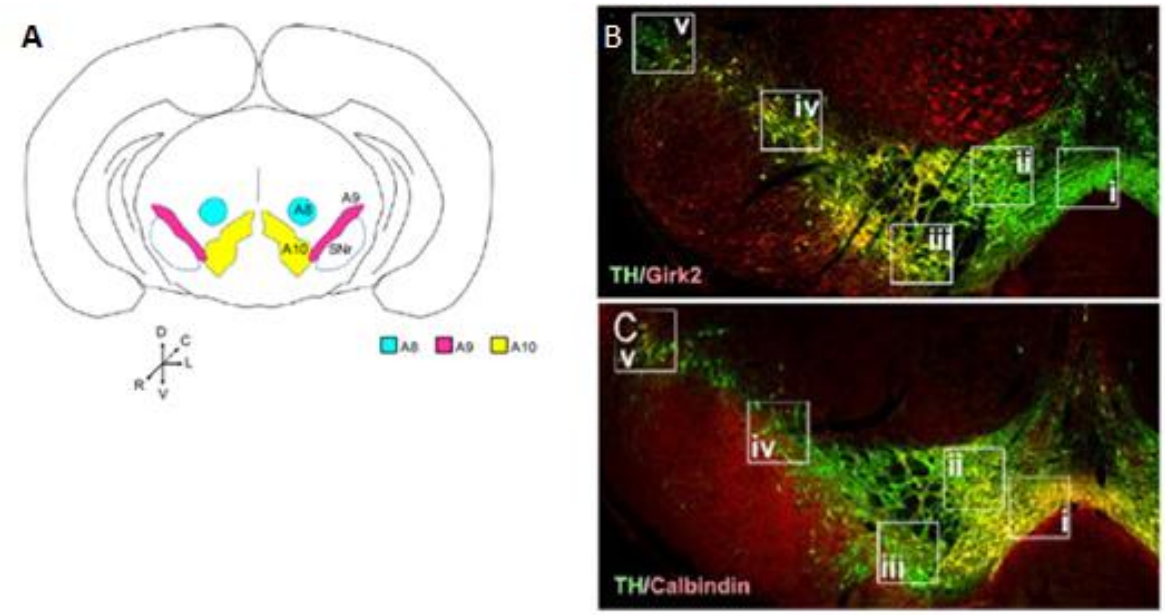

Figure 2. (A) A midbrain coronal section in the adult brain, showing the position of the three mDA nuclei -A8, A9 and A10. Relevant to the thesis, SNpc/A9 (pink) and VTA/A10 (yellow). (B) Midbrain Immunostaining for A9 (TH/Girk2) showing a higher expression in SNpc region (iii, iv, v) and lower expression in VTA (i,ii). (C) Midbrain Immunostaining for A10 (TH/Calbindin) showing a higher expression in VTA region (i, ii) and lower expression in SNpc (iii, iv, v) – Adapted from [3][5].

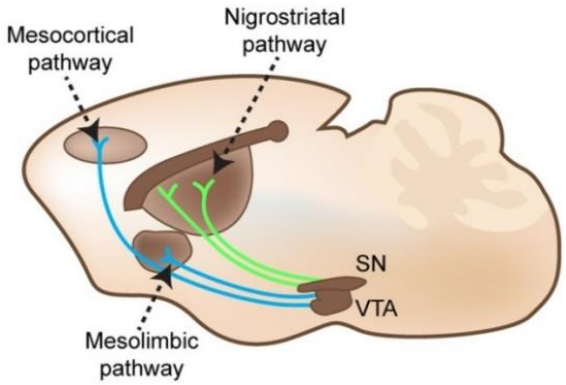

Figure 3. Nigrostriatal pathway- projection from the SNpc to the dorsal striatum (green). Mesocorticolimbic pathway – projections from the VTA to cortical and limbic structures (blue) [6].

The A9 neurons, located lateral to the midline, can be identified based upon their expression of G-protein-gated inwardly rectifying K+ channel subunit 2 (Girk2). These DAn project via the nigrostriatal pathway to predominantly

innervate the dorso-lateral striatum and regulate motor function. The A10 neurons are the more medial population of the ventral midbrain VM DAn. These neurons express Calbindin (Calb) and project via the mesocorticolimbic pathway to cortical and limbic structures to regulate reward-related behaviour [6][7].

1.2 Parkinson's Disease

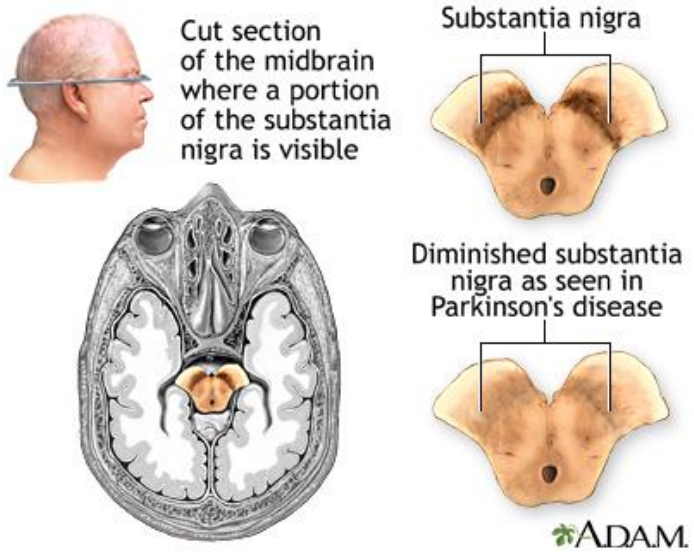

Figure 4. Horizontal section of the brain at the level of the midbrain showing the diminished number of pigmented DAn of the substantia nigra in PD (https://medlineplus.gov/ency/imagepages/19515.htm)

One of the major neurodegenerative disorders associated with dopaminergic cell loss is Parkinson's disease. PD is a progressive neurodegenerative disorder that affects as much as 2% of the population over the age of 65 years [8]. The symptoms of PD are commonly confounded by comorbidities that normally occur in the elderly and the number of people affected by PD is possibly larger. In Australia, the health system financial costs were $478.5 million in 2011, mainly borne by federal government (39%) [9].

Pathologically, the A9 DAn within the SNpc are one of the most vulnerable DAn to degenerate (**Figure 4**), resulting in reduced DA release within the striatum, altered signalling through the basal ganglia and consequently a reduction of motor cortex output. The consequence of this loss is the classical movement anomalies associated with the disease, namely bradykinesia, tremors at rest, postural imbalance and limb rigidity [10].

This loss of DA in PD guided the development of treatments focused on relieving the motor-complications by administration of dopamine-modulating drugs

inclusive of L-DOPA (the precursor in DA synthesis capable of crossing the blood brain barrier), DA agonists (to manage side-effects as motor fluctuations) as well as inhibitors of dopamine degradation (including monoamine oxidase and COMT inhibitors). While capable of providing relief of motor symptoms in the vast majority of patients in early stages of the disease, overtime these drugs starts to fail. This was, in part, due to their reliance on residual dopamine neurons (a population that continue to degenerate) to convert the precursor, L-DOPA, to dopamine. Added to this were side-effects, such as dyskinesia, often associated with the systemic delivery of these drugs [11][12]. Consequently, a long-term treatment to focally restore and regulate DA neurotransmission in order to treat motor symptoms is needed. Thus, the idea of cell replacement emerged, and is the focus of the present thesis.

1.3 Cell Replacement Therapy for PD

1.3.1 Grafting fetal dopaminergic neurons

The first successful rodent study showing the possibility of dopamine cell replacement therapy was performed in the late 1970s [13]. While earlier efforts had attempted to use alternative sources of dopamine cells, this study implanted VM tissue isolated from the developing embryo - a tissue source known to be rich in VM DA progenitors. The donor tissue was isolated at the peak of DA neurogenesis (approximately embryonic day E14.5 in rats) and ectopically transplanted into the denervated striatum (the target tissue of the VM DA neurons), as depicted in **Figure 5**. Cells were purposefully implanted into the target tissue to circumvent the necessity for long-distance axonal growth, had the cells been implanted into the site of cell loss [14][15]. These cells were capable of surviving, innervating the striatum, releasing dopamine and restoring motor function.

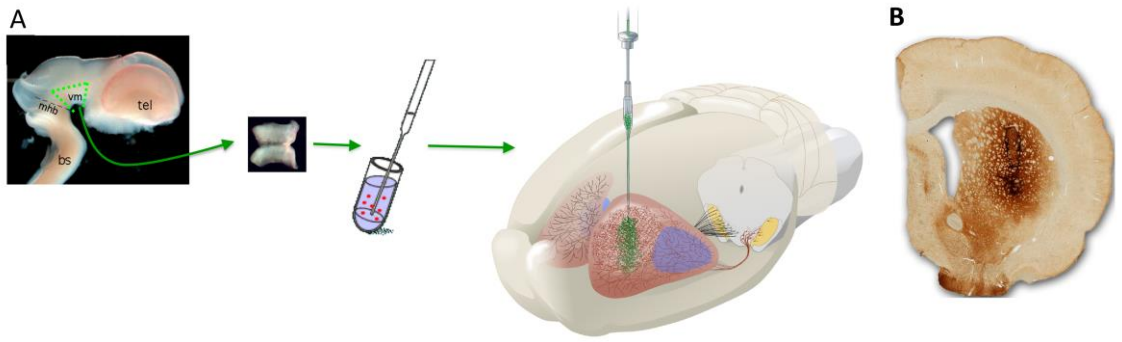

Figure 5. Overview of fetal tissue transplantation into the Parkinsonian rodent brain. (A) Donor tissue was isolated from the ventral midbrain (VM) of embryos, a cell suspension prepared, and subsequently ectopically implanted into the denervated striatum. (B) Coronal section of the rodent brain showing a VM fetal tissue graft in the striatum. Staining against tyrosine hydroxylase (a marker of DAn) highlights the graft and extensive innervation of the host striatum. Figure adapted from [11].

Due to the positive outcomes of the rodent studies, several clinical trials using human fetal tissue were performed, but the results within and across studies were highly variable. While some patients presented symptomatic relief for more than 2 decades, a significant proportion of the patients presented modest or no benefits, and an estimated 20% developed side effects such as graft-induced dyskinesias [16].

Retrospective assessment of the open label and double blinded studies from the 1990's provided important insight into the variability [17]. In particular, a notable lack of standardization such as: donor tissue processing, dissection method, variation in donor age, number of donors, implantation site, immune suppression employed and patient age, disease onset and disease duration. Added to this was the conundrum of using human fetal tissue that presented not only ethical issues but was limited in supply.

The neural transplantation community recognised that a more standardised and sustainable donor tissue was required for the cell replacement therapy to be a realistic treatment for PD [17]. One promising option is the use of pluripotent stem cells, including embryonic stem cells or inducible pluripotent stem cells.

1.3.2 Grafting hPSC-derived dopaminergic neurons

The generation of the first human embryonic stem cell (hESC) lines in the late 1990s generated significant excitement for regenerative medicine [18]. This embryo-derived immortal cell line, generated from the inner cell mass of the human blastocyst, has unlimited developmental potential, opening a range of possibilities not only for cell replacement therapy but additionally tissue engineering, disease modelling and drug development. Almost 10 years later, in 2007, the same possibilities for regenerative medicine treatments were brought by the generation of induced pluripotent stem cells (IPSCs). Free from the ethical concerns that have continued to shroud the use of hESC (due to their source of origin from fertilised embryos), these IPSCs are obtained by 'reprograming' adult cells into naive pluripotent stem cells by the forced expression of a cocktail of transcription factors [19].

Aimed at not only providing a sustainable donor cell source for transplantation in PD, but also new models to study the disease, great efforts have been made to generate *bona fide* ventral midbrain dopamine progenitors and neurons from these pluripotent stem cells. Despite extensive efforts over the past 2 decades, only recent years have protocols emerged that generate VM DA neurons. Two key discoveries underpinned this advancement: 1) Recognizing the necessity to inhibit two major signalling pathways, TGFß and BMP (that both utilize downstream Smad for transduction), in order to rapidly transition the Pluripotent Stem Cells (PSC) into an early neuroectoderm fate [20] (a process referred to as 'dual Smad inhibition' and verified in culture by PAX6/OTX2 co-expression); 2) Second, was understanding that regional patterning of the cells, using morphogens such as sonic hedgehog (SHH) to control dorso-ventral, as well as WNT and Fibroblast growth factor 8 (FGF8) to modulate rostro-caudal identity (**Figure 6A**) [11], needed to occur at the time of neural induction, rather than subsequently, as had previously been believed [21]. The resultant new protocols generated developmentally relevant cells that progressively expressed: OTX2 (a forebrain-midbrain transcription factor), FOXA2 (a marker of ventral identity), LMX1A (an early intrinsic determinant of DA progenitors), PITX3 (a late DA

progenitor gene), NURR1 (expressed in post-mitotic DA precursors), and TH (the rate limiting enzyme in DA syntheses and marker of differentiated DA neurons) – **Figure 6** [11]. Importantly, these cells were shown to integrate into the brain and alleviate motor deficits in neurotoxin-induced models of Parkinson's disease [21][22] .

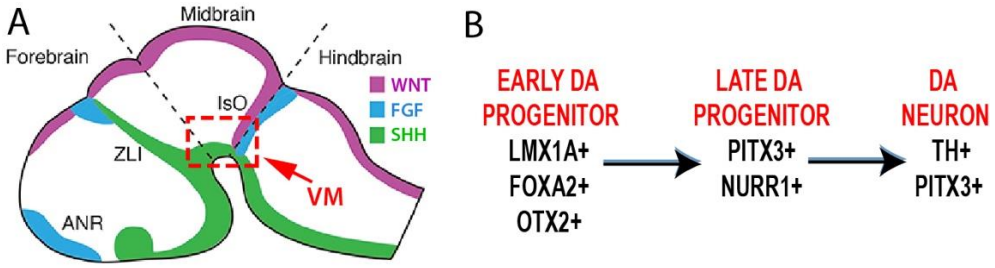

Figure 6. Spatial and temporal expression of morphogens and transcription factors contributing to the development of ventral midbrain DAn. (A) Sagittal schematic of the developing rodent brain illustrating the forebrain, midbrain and hindbrain regions and the expression of the key dorso-ventral morphogen, Sonic hedgehog (Shh), and antero-posterior morphogens, Fibroblast growth factor8 (FGF8) and Wnt1. ANR - anterior neural ridge; ZLI - zona limitans intrathalamic and IsO - isthmic organizer (B) Schematic of some of the key transcription factors progressively expressed in maturing VM DA progenitors and DA neurons.

The next task for the field was ensuring these protocols were amenable to clinical transfer. This included removal of all animal-based products in the media and substrates (xenogeneic-free), ensuring scalability and establishing procedures for the storage of differentiated progenitors, thereby enabling an 'off the shelf' product for clinical use. In recent years, the Parish laboratory generated a xeno-free protocol for the differentiation of VM DA progenitors and mature VM DAn derived from hPSC. Through the removal of feeders and xenogeneic reagents, we not only established a transferable protocol of high reproducibility, but also demonstrated improved homogeneity and efficiency, reflected in significantly increasing yield of correctly specified OTX2/FOXA2 progenitors and subsequent DA neurons (identified by tyrosine hydroxylase expression, the rate limiting enzyme in DA synthesis)- **Figure 7**. In addition, the new xeno-free protocol allowed scalability and cryopreservation with no impact on viability, culture

progenitor composition or DAn maturation potential – critical attributes for future clinical application. Moreover, transplantation of these xeno-free VM DA progenitors into PD rodent model improved engraftment outcome [23].

Where some have held doubt over the true capacity of (neuronal) cell replacement therapy – i.e. that new dopamine neurons can survive and structurally integrate, recent work by Lorenz Studer has utilised optogenetics to silence these grafts, leading to loss of motor recovery such observations provide unequivocal evidence of human stem cells-derive DA grafts synaptically integrating into existing circuit to modulate motor function [23].

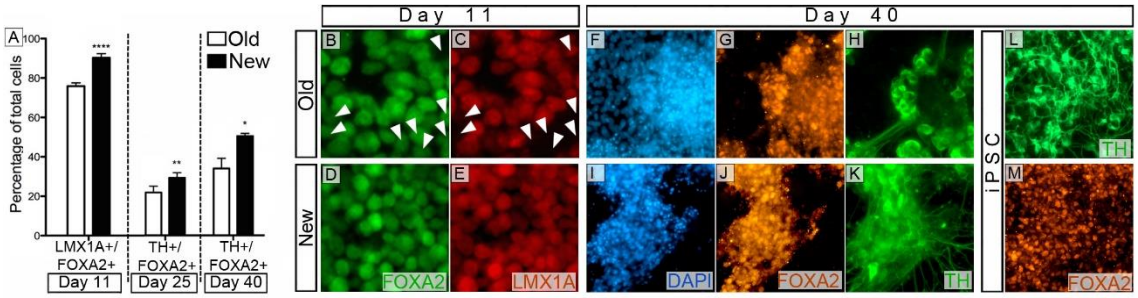

Figure 7. Comparison of former xenogenic (OLD) and the newly recently established xenogenic-free (NEW) protocol for the DA differentiation of hESCs. (A) At 11 days in vitro (DIV) markers for the early VM progenitors (LMX1A+/FOXA2+) are increased, as well as TH+/FOXA2+ in maturing DA neurons at both 25 & 40 DIV. (B-C) Not only were yields increased but correct specification, with notably more incorrectly specified cells using the former protocols (cells failing to co-express LMX1A & FOXA2, arrowheads), (D-E) that are not visible with our revised xenogeneic-free protocol. Unpublished data and data adapted from [23].

1.3.3 Challenges to surpass as we move to the clinic

Whilst the functional integration of hPSC-derived DA progenitors has been demonstrated, with these cells now advancing to clinical trial (the first patient transplanted in Japan in October 2018), we continue to recognise the need for ongoing research into optimising cell transplantation and refinement in the use of these cells for treating PD. Key persistent challenges for the field are the poor survival of the DA neurons, low proportions of DA neurons within the grafts and

sub-optimal plasticity and innervation of the host tissue by the DA neurons within the graft.

1.3.3.1 Challenge #1 – Survival

One of the most important factors for a transplant success is the graft survival. The number of DAn that survives to the transplantation directly affects the improvement of PD symptomatology in the patients. Studies have shown cell survival rates <20% for fetal tissue grafts and ranging from 3-9% for hPSC-derived DA progenitors grafts [24][25]. Key events that impact on survival (and are illustrated in **Figure 8**) include: (I) - handling of the donor cells prior to implantation inclusive of their dissociation, preparation medias, cell sorting (if employed) and storage; (II) - the physical process of implantation (noting the shear forces exerted on the cells during injection); and (III) - integration into the host tissue, noting that the adult brain into which transplants are placed lack many neurotrophic cues that are normally present when DA progenitors/neurons and their axons navigate their way in situ during development. Such observations highlight the need for strategies to improve cell survival at all stages in cell transplantation. This has and continues to be a key focus for the field and will be addressed in greater detail below.

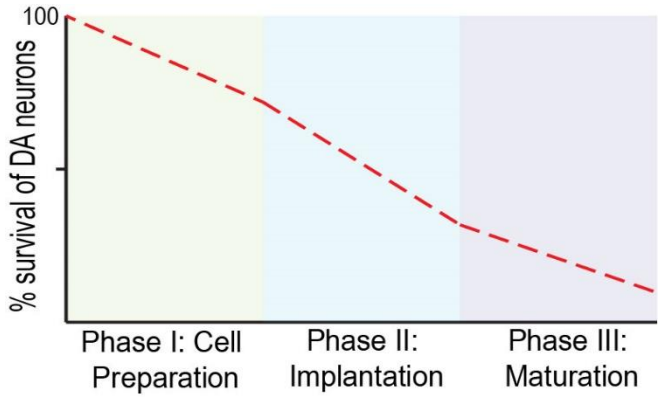

Figure 8. Diagram illustrating the various phases of cell death of DA progenitors within a cell transplantation study. Adapted from [24].

In an effort to promote survival, a raft of anti-apoptotic and pro-survival proteins have been trialled – for more extensive detail see review [24]. Most extensively studies showing the greatest promise has been achieved using GDNF. This molecule was first identified in 1980 and subsequently, in 1993, GDNF was demonstrated to promote the survival and plasticity of embryonic ventral midbrain-derived rodent DAn *in vitro* [26]. With this knowledge, a series of pre-

clinical and clinical studies examined the potential for GDNF to slow the progression of Parkinson's disease, by promoting survival and influencing DA metabolism [27][6][28]. In parallel work, recombinant GDNF protein was also used to promote DA progenitor survival, by addition to the cell preparations prior to in vivo transplantation [29]. Subsequent studies infused GDNF [30][31][32][32][32][32], showing beneficial effects on graft survival and function and finally viral delivery of GDNF in the rodent host tissue was adopted to sustain delivery of the protein (**Figure 9**) . These studies, by us and others, showed enhanced survival, plasticity and functionally appropriate integration of DA-rich fetal VM tissue grafts [32][33][34][35].

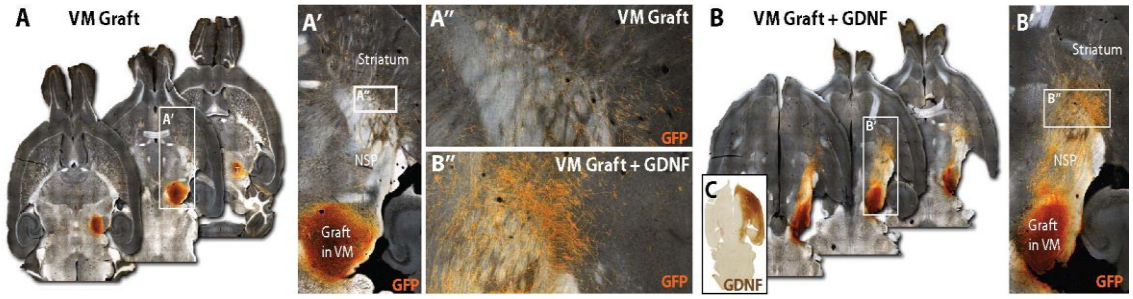

Figure 9. (A) Horizontal brain sections illustrating a homotopic TH-GFP fetal graft within the VM with (A') GFP+ DA fibers extending along the nigrostriatal pathways and (A") terminating in the striatum. (B) GDNF over-expression (via adenovirus) in the striatum enhances graft integration. Note the increased number of GFP+ fibers in the nigrostriatal pathway (B') and striatal innervation (B"). (C) Section adjacent to 2B, illustrating GDNF expression. Image adapted from [36].

Most recently we have demonstrated benefits of GDNF for hPSC-derived grafts (manuscript under review), highlighting that the timing of onset GDNF delivery is a critical variable. The early cell exposure to a GDNF-rich environment, via viral delivery, promoted survival but decreased the capacity of innervation into the host striatum. On the other hand, a delayed onset of GDNF delivery (3 weeks after implantation) had no effect on survival but leaded to better DAn maturation, innervation and function. These findings suggest the timeframe is imperative for survival and integration. Whilst these findings have been important and exciting for the field, a key limitation of viral delivery of proteins is the challenge of controlling the protein dose and the inability to turn off the transgene. An

alternative for a time-controlled protein delivery is the use of biomaterials, discussed further below (section 1.3.4).

1.3.3.2 Challenge #2 – Graft composition:

Another challenge to be addressed before moving to the clinic is identification of the graft composition, still largely unknown – particularly in the context of human pluripotent stem cell derived VM progenitor grafts. Understanding the full compilation of the graft will be critical to not only predict functional efficacy but also guarantee safety. Advanced protocols now exist for the for *in vitro* specification of VM DAn progenitor's – as described above. Despite high yield of correctly specified cells after extended periods of time in vivo, less than 5% of the graft is in fact mature DA neurons DAn [21][22][37]. This poor *in vivo* outcome raises important questions such as the impact that the non-DAn population may have on function. For example, prior studies have reported the detrimental effect of serotonergic neurons within preclinical and clinical grafting studies, highlighting their involvement in graft induced dyskinesias [38], [39]. Added to this is the potential for proliferative cells remaining within the grafts that pose a risk of neural overgrowth and/or tumours.

Several studies have attempted to understand graft composition. The most common approach has been low throughput histochemical assessment, revealing that grafts are often rich in neuronal fate [21][37], [21][37], but more specific subpopulations and non-neuronal populations have been harder to ascertain – as one needs to know what protein to look out for, and is reliant on antibody availability and/or requires availability of antibodies capable of discriminating the grafted cells from the host tissue to ensure assessment are in fact of graft composition. This is particularly relevant in the current context of assessing DA grafts, where efforts to discriminate graft-derived DA innervation patterns from residual host DA fibers is not possible with commercially available tyrosine hydroxylase antibodies. Alternative approaches to characterise grafts have relied on more high throughput techniques, involving transcriptional profiling of the grafts. In this context reporter cells lines are commonly adopted to generate the donor tissue/cells that can then be identified and selectively isolated from the

host by gross tissue dissection or laser capture. Unfortunately, such approaches present their own challenges. A tight tissue dissection can selectively isolate the grafted reporter cells yet fails to include cells at the graft-host boundary, noting that, at least in the context of VM progenitor grafts, are often the most mature cells and of DA neuronal identity. By contrast broader dissection to include this boundary population will invariably also include contaminating host cells. An alternative approach, also commonly reliant on a reporter to identify the graft, involves performing single cell analysis [40][41][42]. This is a powerful technique but due to the labour intensive aspect, only a small fraction of the graft can typically be analysed (for example, it is not uncommon for hPSC-derived VM grafts to contain up to 1 million cells, and hence single cell analysis of 1000 cells represents just 1% of the total graft [25][43][44]. To address these challenges and advance our knowledge and understanding of graft composition we have developed an alternative method, described in chapter 5.

Even with an improved understanding of graft composition, strategies to overcome the poor *in vivo* outcome are still needed, to guarantee safety and anticipation of the graft composition, and thereby function. One approach is to select for correctly specified VM progenitors prior to transplantation, by magnetic or fluorescent activated cell sorting (MACS and FACS, respectively). We have shown that LMX1A, an early VM determinant [45][46], is a good candidate marker for the enrichment of DA progenitors and have generated a hPSC reporter line expressing GFP under the LMX1A promoter. FACS isolation and transplantation of LMX1A-eGFP+ progenitor lead to a greater density of DAn within grafts, improvement in PD rodent motor function, elimination of proliferative cells population and serotonergic populations from the grafts. Isolation of LMX1a ventral midbrain progenitors improves the safety and predictability of human pluripotent stem cell-derived neural transplants in parkinsonian rodent model disease (de Luzy et al., minor revisions submitted 25 June 2019).

An additional key consideration for improving the functional efficiency of VM DA grafts is to ensure maximal specification of the appropriate DA subtype. In cell replacement therapy targeted at alleviating the motor deficits in PD, this is

reflected by the contribution of A9-like DAn (the subpopulation that regulated motor function, as described on page 3) within the graft. The scientific field has been exploring what determines A9 specification and has demonstrated that the transplantation of a younger donor tissue (isolated from the developing fetus) not only resulted in better survival and larger grafts but also an enrichment in A9 DAn with a better host innervation [47]. Later, it was hypothesised that these results were derived from the presence of the meninges, tightly attached to the younger (but not older) donor tissue. Additionally, numerous studies have highlighted the positive impact of meningeal cells on neural development and repair, effects mediated by secretion of trophic factors such as SDF1 (Stromal cell-derived factor 1) as well as the laying down of ECM proteins including collagen, laminin and fibronectin [48][49]. It was confirmed in vitro that, at least in part, the secretion of SDF1 was responsible for improving dopaminergic differentiation and neurite growth [50]. With this collective knowledge, in this thesis (chapter 3), we looked to directly assess the impact of the SDF1 protein on graft outcomes.

1.3.3.3 Challenge #3 – Graft integration.

The therapeutic validity of a graft is commonly assessed using behavioural test after transplantation into animal models of neurological diseases. This symptoms amelioration, for Parkinson's disease, had been demonstrated to be directly dependent on circuit integration. This circuitry connection importance was demonstrated by using an optogenetics approach where VM DAn grafts were reversibly silenced and influenced directly the animal motor behaviour [51]. Thus, the success of a transplant was established to be dependent on the ability of the graft to appropriately extend and integrate into the existing circuitry to reinnervate the target striatum.

In recent years numerous studies have observed that hPSC-derived DA transplants show notably poorer innervation of the target striatum than their human VM fetal counterparts, a considerable 4-fold reduction [52]–[55]. We propose that inferior innervation (also observed in fetal tissue grafts compared to the intact brain) is likely underpinned by the lack of trophic support in the adult host brain. During development, the sequence of axon extension and guidance

is orchestrated by the rearrangement of microtubules and actin filaments driven by the growth cone's response to the local environment of guidance proteins and its receptor/ligand interaction. Guidance molecules can influence chemoattraction [56], inducing growth towards the signal or chemorepulsion, directing growth away from the target [57][58]. Interestingly, axons can react differently to the same signals at different time-points along intermediate targets. For example, signals could attract Immature neurites, but became repulsive over time in order to pass through an intermediate target en route to a final target destination [59]. The influence of these molecules is partially determined by ligand-receptors interactions, with four families of classical guidance: Ephrins (ligands) and Eph (receptors); Netrins (ligand) and DCC/UNC (receptors); Slits (ligands) and Robo (receptors) and Semaphorins (ligands) and plexins/neuropilins (receptors). Additionally, morphogen inclusive of WNTs, Hedgehogs/Shh and FGFs as well as neurotrophic factors, such as GDNF (section 1.3.3.1) have been shown to regulate axon growth and influence plasticity [33][34].

With this knowledge of developmental regulators of axonal plasticity, efforts have been made to recapitulate these events to promote axon guidance, growth and integration of transplanted neurons. This thesis work strived to mimic key aspects of the developing neural circuit formation, by sustaining the delivery of GDNF or SDF1, targeted at promoting hPSC-derived DA graft integration in a model of PD.

1.3.4 Biomaterials – A recent and future approach to overcome the challenges facing cell transplantation for PD

The scientific community has been extensively trying to identify and understand the trophic cues such as growth factors, morphogens and transcriptions factors that regulate neuronal differentiation and integration. However, the physical environment, notably the extracellular matrix, has been largely overlooked. In more recent years it has been demonstrated cell renewal, migration, differentiation and plasticity of cells, including neurons, is dependent on signals generated by the ECM and its complementary cell receptors [60]–[62]. In the context of the nervous system, it was demonstrated that laminins, one of the

major ECM proteins in the brain, also influences proliferation, survival, differentiation and plasticity [62]. Of particular relevance, laminin has been shown to promote the survival and differentiation of midbrain DA neurons in vitro, derived from fetal tissue and mouse embryonic stem cells [63]. Added to this, new protocols for neuronal (and dopaminergic) specification of hPSC have highlighted the benefit of culturing on laminin substrates [23][44].

These finding have confirmed the benefit of an ECM-like environment for DA differentiation and has raised attention for the importance in transplantation. Thus, a range of different biomaterials mimicking the 3D physical ECM-like scaffolding neural microenvironment have been developed. For example, we have developed an electrospun scaffold, delivered as short nanofibers within a thermo-sensitive xyloglucan hydrogel, to demonstrate the capacity for improving the physical and trophic environment for transplanted DA progenitors [64] [65].

Currently, hydrogel-based biomaterials have been receiving great attention – due the ability to mimic the modulus of the host tissue, ease of incorporating donor cells within gels, and their ability to deliver in vivo through fine cannulas. Hydrogels are composed by hydrophilic polymer networks from natural or synthetic origins and present a great versatility, allowing modifications with ECM components, stiffness alterations, and more importantly, they allow the delivery of trophic cues with spatiotemporal control [66], much needed for the potential to improve PSC-derived grafts outcomes. Recently our team developed a peptide-based hydrogel- named self-assembling peptide hydrogel (SAP) - to present a laminin-based epitope (amino acid sequence DDIKVAV – **Figure 10**). This laminin-epitope has been shown to promote neural adhesion, differentiation and axonal growth of neural progenitors with more efficiency than the laminin protein itself due to its high density of presentation on the surface, compared to the full-length protein. We have also shown that this hydrogel promoted human pluripotent stem cell neuronal graft differentiation, integration and functionally support neural grafts in a stroke model [50].

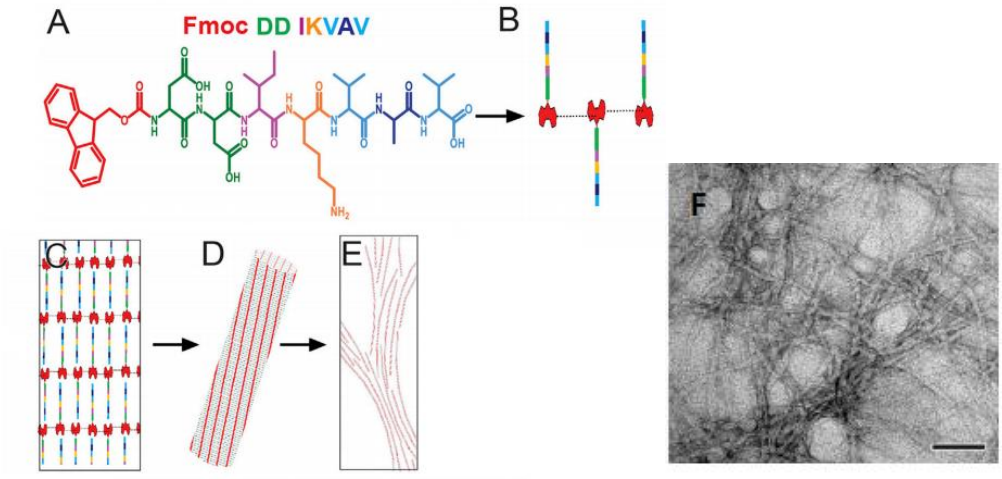

Figure 10. (A-E) Schematic illustration of gels assembling peptide IKVAV. (F) Electron microscopic image of the gel fibres. Scale bar, 100 nm [50].

In addition, the SAP scaffolds enable simple physical state change from gel to liquid by shear forces (titration) and spontaneously self-assemble within minutes when the forces are removed. This characteristic is attractive for transplantation since cells can be mixed to the liquid hydrogel just prior to injection and protected from damaging caused by the transplant injection, increasing cell survival (**Figure 11**).

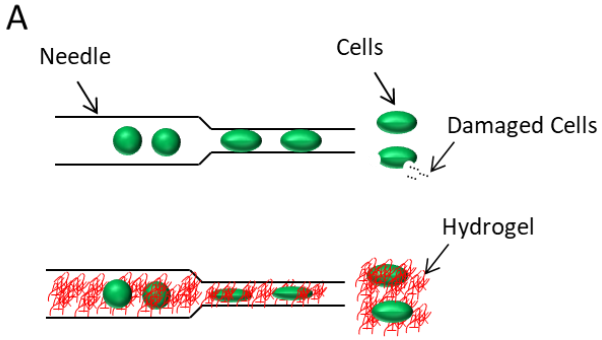

Figure 11. Hydrogel involving and protecting the cells from shear during the injection.

Moreover, the gel provides physical support to the cells and can shield the cells from the host inflammatory response [67][67]. Furthermore, a hydrogel can be utilised to control the temporal release of small molecules, proteins and drugs in the adult brain, thereby influencing neuronal fate and plasticity/integration into the host [68] [69]– for more details see [70].

1.4 Thesis overview

The capacity of the cells to survive, differentiate, integrate and restore motor function in PD provides proof-of-principle that cell replacement therapy is a reality that is moving fast to clinical applications. Nonetheless, clinical trials have shown limitations that remain to be addressed to ensure maximal predictability and functionality from these transplants, whilst simultaneously ensuring safety.

This thesis work aimed to improve the graft outcomes using biomaterials that signal to the cells by the presence of the laminin epitope, the main brain ECM component, as well as a controlled-deliver of key guidance molecules absent in the host adult brain. With surprisingly little knowledge of the composition of the VM progenitor grafts (noting DA neurons comprise <5% of all cells in the graft), the following work also describes the development of a new methodology to transcriptionally profile xenografts. Pre-clinical testing and insight into graft composition will be critical to understanding graft function and safety – prior to the clinical translation of donor preparations for patient treatment.

1.4.1 Hypothesis and aims of the thesis

Hypothesis 1: Modification of the host environment, through modulation of the physical and trophic scaffolding will result in superior grafting outcoming.

Aim1: To determine if sustained SDF1, delivered by a tissue specific hydrogel, improve the survival, differentiation and integration of VM fetal grafts in a mouse model of PD.

Aim 2: To establish whether a laminin-based tissue specific hydrogel, capable of prolonging GDNF delivery, will enhances the survival, plasticity and functional integration of hPSC-derived DA progenitors grafts.

Hypothesis 2: Establishment of a new methodology to transcriptionally profile xenografts will prove critical in understanding graft composition, function and safety.

Aim 3: To develop a new method that enables the easy, rapid and standardised transcriptional profiling of xenografts (specifically of human cells transplanted in rodent).

Chapter 2 - Materials and Methods

2.1 Animals and Ethics

All procedures were conducted in accordance with the Australian National Health and Medical Research Council's published Code of Practice for the Use of Animals in Research, and experimentation was approved by the Florey Institute for Neuroscience and Mental Health animal ethics committee. All mice and rats were house in a 12-hour light/dark cycle with ad libitum access to food and water. Adult (8-12 weeks) swiss mice as well as athymic ($Foxn1^{nu}$) nude mice and (CBH^{rnu}) nude rats were purchased from Animal Resource Center (Australia).

2.1.1 Stereotaxic Surgery

Stereotaxic surgery enables the precise targeting of nuclei within the brain and was employed to perform discrete lesions of neuronal populations and deliver replacement cells. To ensure minimal non-specific mechanical damage to the brains cytoarchitecture, all substances (i.e.: toxin, cell suspension) were injected into the brain using a fine-glass capillary (with a final internal diameter of approximately 100µm) coupled to a Hamilton syringe. Shrink-wrap was then used to secure the glass capillary to a 5ul Hamilton syringe.

Mice and Rats were initially anaesthetised in an induction chamber using 2-5% isoflurane (Baxter; Deerfeild, IL, USA) mixed with oxygen at 1-2 litres per min. Anaesthetic was subsequently maintained at 1-2% for the remainder of the surgery, with the absence of a reflex response (ie: eye and/or paw reflex) indicating an adequate level of unconsciousness. Subsequently the head of the rodent was shaved, when necessary, and analgesia administered (3mg/kg, meloxicam). The rodent was then placed into a stereotaxic frame with care being taken to ensure that the ear bars were secured in the external acoustic meatus, the nose was adequately secured in the nosecone, and the surface of the skull horizontal to the bars. A midline incision, 1-1.5cm in length, exposed the surface of the skull and the landmark junction of the occipital and parietal bones (Bregma) from which all stereotaxic coordinates were made. Refer to **Table 1** for the stereotaxic coordinates for all injections.

A benchtop microscope was used to magnify the skull, align the tip of the glass cannula above the coordinated position and drill a small burr hole in the skull.

The cannula was flushed with saline, to check for any blockages and subsequently the solution to be injected drawn into the end of the cannula. the capillary was then slowly implanted into the brain until it reaches the appropriate distance below the Dura mater (refer to **Table 1**). All injections were carried out at a flow rate of 1ul/min, with the cannula left in place for 2 minutes upon completion of the injection in order to minimise backflow. Following withdrawal of the cannula, the skull was sutured, antiseptic applied to the wound and animals returned to a warmed cage for recovery.

Mouse coordinates

Location	***Anterior-Posterior[i]***	***Mediolateral[i]***	***Dorsolateral[ii]***
Dorsal Striatum	*+1.0mm*	*-2.3mm*	*-3.2mm*
Substantia Nigra	*-3.2mm*	*-1.4mm*	*-4.5mm*

Rats coordinates

Location	***Anterior-Posterior[i]***	***Mediolateral[i]***	***Dorsolateral[ii]***
Dorsal Striatum	*+0.5mm*	*-3.0mm*	*-4.0mm*
Medial Forebrain Bundle	*-3.4mm*	*-1.3mm*	*-6.8mm*

Table 1. Stereotaxic coordinates. i: coordinates relative to bregma; ii: Coordinates relative to the Dura mater surface

2.1.2 Lesion and Transplantation

Lesion: Animals received unilateral 6-OHDA lesions (rats: 3.5ul, 3.2µg/µl; mice: 1.5ul, 1.6 ug/ul) of the medial forebrain bundle (MFB; rat) or substantia nigra (mouse), as previously described [33].

2.1.2.1 Transplant

Study I- 4 weeks after 6-OHDA lesioning, mice were implanted with dissected cells from the ventral midbrain of E11.5 TH-GFP mouse embryos (100,000 cells in 1ul). The groups were: Cells only (100,000 cells in 1ul); cells+ SDF1 (100000 cells + 100 ng of SDF1 in 1ul); Cells + hydrogel (100,000 cells combined with

hydrogel in 1ul) and Cells+hydrogel+SDF1 (100,000 cells + 100ng of SDF1 combined with hydrogel in 1ul).

Study II: 4 weeks after 6-OHDA lesioning, rats were implanted with FACS isolated VM progenitors differentiated from the H9 LMX1A-eGFP hESC line (100,000 cells in 1ul). The groups were: Cells only (100,000 cells in 1ul); cells+ GDNF (100,000 cells + 4 ng of GDNF in 1ul); Cells + hydrogel (100,000 cells combined with hydrogel in 1ul) and Cells + hydrogel+ GDNF (100,000 cells + 4 ng of GDNF combined with hydrogel in 1ul).

Study III: Mice were implanted with FACS isolated VM progenitors differentiated from the H9 LMX1A-eGFP hESC line, the groups were: (10,000; 30,000, 100,000 and 300,000 cells in 1ul). The next experimental phase, mice were implanted with the same line and the groups were: Undifferentiated cells to be assessed in 1 month (100,000 cells in 1ul); FACS isolated VM progenitors to be assessed in 1 month and FACS isolated VM progenitors to be assessed in 5 months (100,000 cells in 1ul).

2.1.2.2 Behavioural Analysis

Four weeks after lesioning, the rat's unilateral DA function was assessed using the amphetamine-induced rotation, and stepping tests, as previously described [50], with re-testing performed at various intervals following transplantation (16 and 20 weeks). Amphetamine rotations: net rotations over 60 minutes were analysed 10 minutes after intraperitoneal injection of D-amphetamine sulfate (5mg/kg; Tocris Bioscience). Stepping test: Stepping test was performed as described previously [71]. Rats were restrained by the experimenter, allowing them to make unilateral forepaw weight-bearing contact with the bench, and were assessed for their ability to make stepping adjustments with the paw when moved laterally over a 1 m distance. Number of steps made by weight-bearing forepaws was recorded in both the forehand and backhand direction, with testing repeated 3 times/day over 5 days. Upon completion of initial testing 4 weeks post-lesioning, animals displaying a functional deficit (>300 rotations in 60 min) were ranked in order of the percentage rotational asymmetry and evenly distributed across the

groups (Lesion, Lesion+Graft, Lesion+GDNF, Lesion+Graft+SAP and Lesion+Graft+SAP+GDNF).

2.2 Cells

2.2.1 Ventral Midbrain Primary Cultures

2.2.1.1 Embryos collection

A GFP reporter, under the tyrosine hydroxylase promoter (TH-GFP) mouse strain was used to generate time-mated embryos that were utilized for transplantation. The TH-GFP mice were generated and obtained from Hideyuki Okano (Fukushima Medical University, Japan) [72]. Embryos were isolated from time-mated transgenic TH-GFP Swiss mice. Animals were time mated overnight and visualized for a vaginal plug on the following morning was considered as day (E) 0.5.

2.2.1.2 Tissue isolation

The ventral midbrain of E11.5 mouse embryos were dissected under dissecting microscope in ice-cold L15 media (GIBCO). The telencephalon–mesencephalon boundary as well as the isthmic organizer was cut to isolate the midbrain tissue. The overlying meninges was removed from the mesencephalic tissue. The ventral third of the midbrain tissue was dissected and used to enrich the dopaminergic population in culture. The isolated VM tissues were incubated in papain (10u) for 16 minutes at 37 °C and after, it was added 500mL of NBB27 (a 1:1 mix of Neurobasal media and DMEM/F12+Glutamax, supplemented with 2% B27,1% ITS-A, 0.5% glutamax and 0.4% Penicillin-Streptomycin) + 10% FBS to stop the enzyme action. The tissues were dissociated to single cells and 4.5ml of NBB27 added to wash the cells and centrifuge the cells at 1500 rpm for 5’ for the supernatant remotion. The cells were resuspended, counted and prepared in 200.000/1ul with NBB27+ rock inhibitor (1:100) – **Figure 5.**

2.2.2 Maintenance of human pluripotent stem cells

The generated human embryonic stem cell line H9 LMX1a-eGFP [73] were cultured xenofree conditions. The cell line was confirmed to be karyotypically normal and frequently tested for absence of mycoplasma (MycoAlert detection

kit, LONZA). Undifferentiated stem cells were cultured on Laminin-521 (Biolamina), in xeno-free TeSR2 (STEMCELL Technologies) supplemented with 0.4% Penicillin-Streptomycin and maintained for >20 passages. Media was changed daily and EDTA used to passage every 4-6 days. Cultures were maintained at 37oC with 5% CO2.

2.2.2.1 Human PSCs VM Differentiation

Confluent hPSC cultures were disassociated with EDTA to generate small aggregates. hPSC suspensions were collected in TeSR2 media and plated at the above densities on plates coated with Laminin-521 (10µg/ml). Differentiation to VM DAn was performed as described previously [23]. Specifically, differentiation commenced 24 hours post-seeding with the addition of serum replacement media (SRM; DMEM/F12+Glutamax with 15% KSR (xeno-free variant), 1% NEAA and 0.2% β-Mercaptoethanol) and supplemented with SMAD inhibitors LDN193189 (100nM or 200nM, Stemgent) and SB431542 (10µM, R&D Systems) for neural induction. SB and LDN were removed at day 5 (d5) and d11, respectively. SRM media was gradually replaced with N2 media, (DMEM-F12 with 1% N2 and 1% ITS-A (Life Technologies) from d5-d11. Sonic hedgehog C25II (SHH; 100ng/ml, R&D Systems) and the smoothened receptor agonist purmorphamine (PM; 2µM, Stemgent) were added from d1-d7 to promote ventralization. GSK3β inhibitor CHIR99021 (CHIR; 3µM, Stemgent) was added from d3-13 to promote caudalization. At d11 media was switched to NBB27 (a 1:1 mix of Neurobasal media and DMEM/F12+Glutamax, supplemented with 2% B27,1% ITS-A, 0.5% glutamax and 0.4% Penicillin-Streptomycin) with recombinant human brain-derived neurotrophic factor (BDNF, 20ng/ml, R&D Systems), recombinant human glial cell line-derived neurotrophic factor (GDNF, 20ng/ml, R&D Systems), ascorbic acid (AA, 200nM, Sigma-Aldrich), recombinant human transforming growth factor type β3 (TGFβ3, 1ng/ml, Peprotech), dibutyryl cAMP (dcAMP, 0.05mM, Tocris Bioscience) and the notch inhibitor DAPT (10µM, Sigma-Aldrich), henceforth known as ‘maturation media’. Maturation media was maintained until d21.

2.2.3 Fluorescence-activated cell sorting

At 19 DIV, cultures rich in VM progenitors were dissociated in Accutase (Innovative Cell Technologies) to a single-cell suspension and resuspended into a sorting buffer containing 90% maturation media, 10% knockout serum replacement, and ROCK inhibitor Y-27632 (10μM, Tocris Bioscience) to a final density of 5-8x106 cells/ml. Cells were filtered through cell strainer caps (35μM mesh, Falcon) to remove the presence of cell doublets and clusters. Sorting was performed on a FACS Aria III using a 100-μM nozzle, sheath pressure of 17-22 psi. A fraction of cells was passed through the cell sorter, without selection, forming the unsorted group, whilst GFP+ and GFP- cells were isolated using a highly restrictive gating strategy to exclude doublets and debris based on forward and side-scatter parameters, as well as dead cells using the viability marker 4'-6-Diamidino-2-Phenylindole (DAPI). Background auto-fluorescence was compensated for by an empty auto fluorescence channel (FL2-580/30), and a H9 parental cell line at the same stage of differentiation was used as an GFP- control. FACS-isolated cell fractions were resuspended in maturation media containing ROCK inhibitor (Y27632, 10μM, Sigma) at 100,000 cells/μL and stored on ice until the time of transplantation. Flow cytometric analysis was conducted using FlowJo software.

2.3 Biomaterials

2.3.1 Preparation of self-assembling peptide scaffolds

A self-assembling peptide (SAP) for laminin was engineered as previously described [50]. The laminin-based epitope synthesized had the sequence isoleucine-lysine-valine-alanine-valine (IKVAV) and two aspartate residues were incorporated at the N-terminus of the peptide to lower the pH (7.4 – physiological conditions) upon which spontaneous assembly occurs, resulting in a final peptide sequence, DDIKVAV . Gelation was initiated using a well-established pH switch. Briefly, 1wt/v% hydrogels were prepared from amorphous Fmoc-DDIKVAV peptide powder. This was suspended in deionized water, then the pH was raised with a minimal amount of 0.5M NaOH to ensure solubilization. Gelation occurred spontaneously when the pH was lowered to 7.4 using dropwise 1M HCl, and

water used to ensure a concentration of 20 mg/mL. The final hydrogels were made with mixing at a 1:1 ratio with magnesium and calcium-free HBSS or cells. Following gelation, rheology confirmed a modulus similar to the rat brain [74]. Fourier transform infrared (FTIR), circular dichroism (CD) spectroscopy, and transmission electron microscopy verified synthesis and structure of the desired nanofibrillar structure. The resultant hydrogels could be reversed to an aqueous state by application of shear force (achieved via repeated titration or vortexing), such that the gel disassembled into a liquid solution. This unique property of hydrogel was advantageous, enabling incorporation of protein and cells into the polymer during its liquid phase, and resulting in homogenous distribution of the protein throughout the scaffold following its subsequent gelation, that was achieved upon removal of the shear force.

2.4 Immunohistochemistry

Animals received an overdose of sodium pentobarbitone (100mg/kg) followed by transcardial perfusion with Tyrode solution followed by 4% paraformaldehyde. Brains were coronally or horizontally sectioned (40µm; 12 series) on a freezing microtome (Leica) and immunohistochemistry performed as described below and previously by [50]. Primary antibodies and dilutions are shown in **Table 2**. The bound antibody complex was detected either indirectly through enzymatic conjugation of the diaminobenzadine chromagen or using directly conjugated fluorescent secondary antibodies (Jackson Immunoresearch).

Name	Target	Invitro	Chromogenic	Fluorescent	Company & Catalogue #
Beta-Tubulin /Tujl (chk)	Neurons	1:500	1:1000	1:500	Millipore, AB9354
Calbindin (m)	Calbindin			1:1000	SWANT, CB300
CD11b (OX-42) (m)	CD11b (integrin) OX42			1:100	AbD Serotec, MCA275GA
cFOS (g)	Dopamine release		1:1000		Santa Cruz, sc-52
Dapi	Nuclear stain	1:5000 of 1mg/ml			Sigma Aldrich, D8417
FoxA2 (g) HNF-3β	FoxA2 (ventralization)	1:200		1:200	Santa Cruz, sc-6554
GFAP (Rb)	Astrocytes			1:200	DAKO, Z0334
GFP (Ch)	GFP	1:1000		1:1000	Abcam, AB13970
GFP (Rb)	GFP		1:200	1:200	Abcam, AB290
GIRK2 (Rb)	A9 Dopamine neurons (GIRK)			1:500	Alomone Labs, APC-006
Hu Nuclei (HNA) (m)	human cells		1:500	1:200	Millipore, MAB 1281
Ki67 IgG, SP6 (Rb)	Proliferating cells (M-phase)		1:1000	1:1000	Thermo Fisher #LBVRM-9106-S1
MBP myelin basic protein (m)	oligodendrocytes			1:200	Millipore, AB15542
NCAM / CD56 (ERIC1) (mouse)	PSA-NCAM (detects human	1:100	1:500	1:100	Santa Cruz, sc-106
Nestin human (m)	Human Neuronal precursor	1:800	1:1500	1:1000	R&D Systems, MAB1259
NeuN (m)	Neurons (nuclei)		1:500	1:200 + streptavidine	Millipore, MAB 377
NLGN3	Neuroligin3	1:200		1:200	Synaptic Systems
Oct-4 (m)	Embryonic Stem cell	1:100			Santa Cruz sc-5279
Olig1 (Rb)	neurons & glia			1:200	Millipore, AB15620
OTX2 (rb)	Midbrain precursors			1:4000	Millipore, AB9566
RECA-1 (Rat)	Blood vessels			1:500	Serotec, MCA970R
SOX2 (g)	stem cells	1:300		1:300	R&D Systems, AF2018
Synaptophysin human (m)	Synapse pre-synaptic terminal			1:1000	Enzo Life Sciences, ADI-905-782-100
TH (Rb)	catechol neurons (DA)	1:800	1:1000	1:1500	Pel-freeze, P40101-0
TH (Sh)	catechol neurons (DA)	1:800		1:800	Pel-freeze, P60101-0

Table 2. List of primary antibodies.

2.5 Microscopy and Quantification

Fluorescence images were captured on a Zeiss Axio ObserverZ.1 upright epifluorescence or Zeiss LSM 780 confocal microscope. Bright and darkfield images were taken on a Leica DM6000 upright microscope. Grafts were delineated by human PSA-NCAM expression and volume extrapolated using Cavalieri's principle. For GFP and TH quantification, all positive cells were counted from brightfield images (1:6 sections) and corrected for series number (number of cells x 6). For GIRK2 and Calbindin quantification, dopamine neurons were first identified using TH immunoreactivity from confocal images. For fibre density assessment, 10 z-stack-sections (1µm per section) were obtained and compressed. TH+ fibres were isolated on colour inverted images using the 'colour range' tool on Photoshop (Adobe). Data is expressed as percentage of immunoreactive pixels. All areas were captured in triplicate with conserved settings.

2.6 RNA Isolation and qPCR

The animals were killed, the brains removed and the striatum (containing the transplant) grossly dissected from surrounding tissues and snap frozen. The frozen tissue was homogenised using a TissueLyser LT (Qiagen) and total RNA extracted using the RNeasy Mini Kit (Qiagen) including DNase treatment. RNA yield and integrity were assessed using a Nanodrop One Spectrophotometer (ThermoFisher Scientific) and confirmed using a Qubit (ThermoFisher Scientific) and Tapestation (Agilent). The RNA was analysed by qPCR or RNAseq.

Species-specific primers were designed using Primer3 [75], aimed at containing a minimum of 5 bp mismatches between graft and host, or 2 mismatches in the 5 bp at the 3` end between species. Primers were targeted manually to regions of dis-similarity (identified by blasting paralogue genes) or using Primer-BLAST and selecting both the xenograft and host species (Homo sapiens and Mus musculus, respectively in the present context) under organism in the "Primer Pair Specificity Checking Parameters." This identified primers specific only to the xenograft species (i.e. human). All xenograft-specific primers used in this study are listed in **Table 3 (Chapter 5).**

First-strand reverse transcription of 500 ng of RNA into cDNA was conducted using the SuperScript® VILO cDNA Synthesis Kit (Invitrogen) according to the manufacturer's recommendations. Real-time qPCR was carried out on 25ng of cDNA using the SYBR GreenER™ qPCR SuperMix Universal (Invitrogen) and run on a Rotor-Gene 6000 (Qiagen). All qPCR data was analysed using the ΔΔCT method [76], using the xenograft-specific reference gene and expressed relative to the Undifferentiated grafts. Five independent biological replicates were analysed per group.

2.7 RNA sequencing

cDNA libraries (containing graft and host RNA) were prepared using the TruSeq stranded mRNA sample preparation kit (Illumina). For sequencing the final cDNA concentration of each sample adjusted to generate a target of 20 million xenograft-specific reads using the percentage xenograft RNA calculated from the qPCR data. Note, due to the low percentage of xenograft RNA in the Immature grafts, 5.5 million reads were targeted. Libraries were subject to paired-end, 75 bp sequencing on an Illumina HiSeq 2000 platform (Illumina) with 3 independent biological replicates analysed per group.

Analysis was conducted on the Galaxy web platform [77] using the Galaxy Australia server, and using Bioconductor Ref in the statistical analysis environment R (https://www.R-project.org/). Alignment to the human genome (Hg38) was performed using HISAT2 (2.0.3.3). Paired concordant reads were then mapped against the mouse reference genome (mm10). Under our high stringency approach, all reads that aligned to both the human and mouse genome were discarded, accounting for an average of 5% of human reads.

Read counts for each gene were generated using HTSeq-count (0.6.1) on union mode [78]. Differential expression analysis and Principal Component Analysis was conducted with DeSeq2 (2.11.38) [79]. Expression heat maps and unsupervised clustering were performed on log transformed row scaled expression values using the gplots package in R [76]. Gene ontology enrichment analysis on biological process was performed using DAVID gene ontology browser [80]. The RNA-seq data generated from this study has been deposited

in NCBI's Gene Expression Omnibus and are accessible through GEO Series accession number GSE126804.

2.8 Statistical Analysis

All data are presented as mean + SEM. Statistical tests employed (inclusive of one-way ANOVA and student t-tests) are stated in figure legends. Alpha levels of $p<0.05$ were considered significant with all statistical analysis performed using GraphPad Prism. *$p < 0.05$, **$p < 0.01$, ***$p < 0.001$ and ****$p < 0.0001$.

Chapter 3 - Extracellular matrix biomimetic hydrogels, encapsulated with stromal derived factor-1, enhance the A9 dopaminergic specification of fetal tissue grafts in a rodent model of Parkinson's Disease

3.1 ABSTRACT

Clinical studies have provided evidence for dopamine cell replacement therapy in Parkinson's Disease. However, grafts derived from fetal or PSC, remain heterogeneous with a high proportion of non-dopaminergic cells and display subthreshold reinnervation of target tissues, thereby highlighting an ongoing need to identify new strategies to promote graft outcomes. In recent work SDF1, secreted from meninges, has been shown to exert many roles during the ventral midbrain DA development, and DA-directed differentiation of PSCs. Furthermore, the co-implantation of meningeal cells can enhance the DA graft outcomes, however no direct evidence exists for the role of SDF1 in DA graft outcomes. Due to the rapid degradation of SDF1, we utilised a hydrogel to entrap the protein, sustaining delivery over 28 days, coinciding with the period of DA progenitor survival, differentiation and initial plasticity. Hydrogels were fabricated from the SAP, presenting an epitope for the brains main ECM protein laminin, thereby possessing the capacity to not only influence cell adhesion but additionally cell fate. Combined, we showed that SDF1-functionalised SAP hydrogels resulted in larger grafts, containing more TH+ neurons, as well as an increased number of A9 DA specification, the subpopulation of DA neurons responsible for controlling motor function. Moreover, we showed that the SAP hydrogel increased not only the number of A9 DAn but also the proportion of them. These findings demonstrate the capacity for functionalised, tissue-specific hydrogels to improve the composition of grafts targeted for neural repair.

3.2 INTRODUCTION

Parkinson's disease is a progressive neurodegenerative disorder where the loss of ventral midbrain dopamine neurons underpins disturbances in motor function. While dopamine pharmacotherapy is the mainstay in treatment, it presents waning efficacy over time and complications associated with systematic delivery. In contrast, cell replacement therapy offers sustained and targeted replacement of dopamine neurons. Experiments in animal models of PD, as well as a series of clinical trials, have provided the necessary evidence that transplanted dopamine progenitors, isolated from the developing ventral midbrain, are capable of surviving, releasing dopamine and improving motor deficits [15]. More recently, human pluripotent stem cells differentiated into VM progenitors have been shown to similarly alleviate motor symptoms in rodent and non-human primates, yet their functionality in a clinical setting remains to be observed [52] .

Despite these proof of principle studies and clinical trials, it was widely recognised that the survival of the dopamine neuron was low [24] [81], and was the most decisive factor in governing the success of a transplant. This poor survival was, in part, dictated by trauma to the cells during both isolation from the foetus and their physical implantation, yet also governed by the exposure of the progenitors to the adult environment of the host brain that was devoid of the many trophic cues normally present during the establishment of new neural networks in development [24]. Whilst DA neuron survival is critical for graft function, more specifically is the requirement for these cells to be of A9, rather than A10, subpopulation identity [82]. These A9 neurons, predominantly restricted to the substantia nigra pars compacta in the rodent, form the nigrostriatal pathway responsible for dopamine-modulation of motor function.

Over the past 30 years extensive efforts have been made to promote the survival and plasticity of DA progenitor grafts in PD models [83], in addition to understanding how to enrich for A9 neurons. In more recent years a series of studies have provided interesting insight into the role of the chemokine SDF1 (also known as CXCL12), and the meninges in midbrain DA development to suggest that SDF1 may improve grafting outcomes. The first evidence of SDF1

in VM DA development came from a series of studies demonstrating that the co-culture of embryonic stem cells on stromal cell feeder layers, or meningeal cells, promoted neural induction and induced DA differentiation via secreted factors termed stromal derived inducing activity (SDIA) [84]–[87]. Genome expression analysis revealed that SDF1 was one of the secreted factors required for DA specification [84]. Shortly thereafter SDF1, secreted from the meninges overlying the VM, and acting via the CXCR4 receptor expressed on DA progenitors and neurons (from E10.5-14.5) was shown to modulate migration and neuritogenesis [4] [49] [88]. Finally, meningeal cells, co-transplanted with VM progenitors influenced DA differentiation, increased A9 fate acquisition and promoted neurite extension and integration in a mouse model of PD [88]. The evident outstanding piece of the puzzle is whether SDF1 can directly influence DA graft outcomes.

In an effort to sustain SDF1 expression during periods of graft implantation and integration, and to avoid the complications associated with brain infusion kits or viral transduction, in the present study we incorporated the functional protein into a bioengineered hydrogel - an approached previously adopted by us to control protein delivery over defined temporal periods ranging from days, to weeks and even months [64] [65] [69] [68].

Additional to the benefits of temporally controlling protein delivery, biomaterials have the capacity to deliver structural and biochemical biomimetics of the ECM which can be advantageous in regenerative medicine to support both host and transplanted cells. These interfacing materials can provide further benefits, dependent on their mode of synthesis and structure, protecting transplanted cells against shear forces during implantation, shielding the graft from the host immune system, and/or dampen the host immunological response, for example [70]. Whilst a raft of biomaterials has been engineered and trialled for their regenerative capacity, those synthesised through processes that most closely mimic biology is evidently advantageous. With nature utilising supramolecular interactions to drive self-organisation of biological macromolecules such as peptides and proteins, these same principles can be applied to design synthetic peptides that can self-assemble into larger complex structures, similar to those normally found in biology. Various hydrogels have been formed from self-

assembling peptides, yet have most commonly utilized long, highly structured peptides such as RADA16, or peptide amphiphiles that require many steps in their synthesis and purification, resulting in increased costs and complexity. Consequently, there has been increasing interest into the fabrication of minimalist peptide sequences (<10 amino acids) that retain the ability to self-assemble and present bioactive sequences. Here we utilize our previously described Fmoc-based SAP system [89], to present a functional epitope sequence (IKVAV) of the α1 chain of laminin - the main extracellular matrix protein present in the brain. This IKVAV epitope has been shown to influence cell adhesion, proliferation, migration, differentiation and neurite plasticity [90], as well as influence graft outcomes in the intact and ischemic infarcted brain [91][92][50]. Here we utilize the neural tissue-specific SAP laminin-based hydrogel, shear-loaded with SDF1 to sustain delivery, to assess the beneficial impact on the survival, differentiation and integration of fetal tissue grafts in an animal model of Parkinson's Disease.

3.3 MATERIALS & METHODS

3.3.1 Self-assembling peptide hydrogel preparation and functionalisation

The neural tissue specific SAP hydrogel, presenting the laminin epitope sequence isoleucine-lysine-valine-alanine-valine (IKVAV), was fabricated using solid phase peptide synthesis, as previously described [93]. Two aspartate amino acid residues were added to the N-terminus of the peptide to lower the pKa, enabling spontaneous self-assembling to occur under physiological conditions (pH 7.4), and resulted in a final peptide sequence DDIKVAV. Importantly, by using this method of fabrication, the amino acid sidechains of the peptide moieties are presented on the outer edge of the nanofibres, to create a surface rich in bioactive molecules.

Gelation was initiated using a pH switch to yield a 20mg/ml stock [91]. Rheology was performed to verify that the modulus of the gel (stiffness) was similar to the mouse brain and thereby amenable to supporting the implanted cells. In addition, fourier transform infrared (FTIR), circular dichroism (CD) spectroscopy, and

transmission electron microscopy was conducted to confirm appropriate structure of the fabricated nanofibrils [93].

Application of shear force, through titration or vortexing, reversed the gel to an aqueous state and was necessary for the entrapment of SDF protein (100ng/ul, R&D Systems) for subsequent in vivo delivery. This shear-loading of the protein during the aqueous phase of the hydrogel enabled homogeneous distribution of the SDF1 protein throughout the gel. To assess the release kinetics of the protein from the gel, SDF1 (100 ng, R&D Systems) was loaded into the SAP (100 µL) by reverse shearing to an aqueous state and then cast into wells of a 96-well plate. PBS (200 µL) was added to the well and incubated at 37 °C. The supernatant was collected at pre-determined intervals over 28day period. All supernatant samples were stored at -20 °C until the time of analysis. The SDF1 levels were quantified by enzyme linked immunosorbent assay (ELISA), using previously described methods [64][94]. Release profiles were performed in triplicate wells for each time point and, repeated on 3 independent experiments.

3.3.2 Ventral midbrain specification of human pluripotent stem cells

The first post-mitotic TH+ DA neurons appears within the developing ventral midbrain at embryonic day 10.5 (E10.5) in mice, with DA neurogenesis peaking at E12.5 and ending by approximately E14.5. With expression of the SDF1 receptor, CXCR4, at its greatest from E10.5-12.5, and the established roles of SDF1 in migration, differentiation and plasticity reported at E11.5, E10.5/E12.5 and E10.5-E12.5, respectively [4][88][95], we nominally elected to utilize E11.5 VM progenitors for transplantation.

Mice expressing green fluorescent protein (GFP) under the tyrosine hydroxylase (TH) promoter were utilised for time mating, enabling tracking of graft derived (GFP+) DA neurons from host (GFP-) following transplantation. The TH-GFP mice were generated and obtained from Hideyuki Okano (Fukushima Medical University, Japan) [72]. Mice were time mated overnight and visualization of a vaginal plug on the following morning was taken as E0.5. At E11.5 pregnant dams were killed by cervical dislocation, GFP-expressing embryos isolated and the VM tissue micro-dissected, using our previously described methods [96]. The cells

were resuspended at 200,000cells/ul in magnesium and calcium-free Hank's buffered salt solution containing 0.1% DNase. Cells were stored on ice for the duration of the surgical procedures. At the time of in vivo delivery, the cells were either diluted 1:1 with (i) the SAP hydrogel, following shear reversal to an aqueous state (resulting in a gel concentration of 10mg/ml and cell density of 100,000/ul), or (ii) HBSS media (resultant cell density 100,000 cells/ul) .

3.3.3 Surgical Procedures

All animal procedures were conducted in agreement with the Australian National Health and Medical Research Council's published Code of Practice for the Use of Animals in Research, and experiments approved by The Florey Institute of Neuroscience and Mental Health Animal Ethics committee. Animals were group housed in individually ventilated cages with low irritant bedding on a 12:12-hour light/dark cycle with ad libitum access to food and water. Surgeries were performed on 28 athymic (BALB/c-Foxn1nu) nude mice under 2% isofluorane anaesthesia. All mice received unilateral injections of the selective catecholamine neurotoxin 6-hydroxydopamine (6-OHDA), into the substantia nigra pars compacta to ablate the midbrain dopamine neurons - using previously described methods [97]. Three weeks after lesioning, animals received transplants of one of the following 4 treatments: Cells, Cells + acute delivery of SDF1 (100ng, Cells+sSDF1), Cells + SAP or, Cells + SAP containing shear encapsulated SDF1 (Cells + SAP-shSDF1). All animals received a total of 100,000 cells and a final injection volume into the striatum of 1µl – **Figure 12A**.

3.3.4 Tissue Processing & histochemistry

At 12 weeks post-transplantation all animals received an overdose of sodium pentobarbitone (100 mg/kg) and were transcardially perfused with Tyrode buffer followed by 4% paraformaldehyde. The brains were post-fixed for 30mins and coronally sectioned on a freezing microtome (40µm thickness, 1:12 series) in preparation for histochemical analysis. Immunohistochemistry as previously described [50]. Primary antibodies and dilution factors were as follows: mouse anti-Calbindin (1:1,500: Swant), rabbit anti- G-protein-gated inwardly rectifying K+ channel subunit 2 (GIRK2, 1:500; Chemicon), chicken anti-GFP (1:1,000;

Abcam), rabbit anti-GFP (1:20,000; Abcam), mouse anti-NeuN (1:100; R&D Systems), rabbit anti-TH (1:500, Pel-Freeze), sheep anti-TH (1:800, Pelfreeze). Secondary antibodies for (i) direct detection were used at a dilution of 1:200—DyLight 488, 549 or 649 conjugated donkey anti-mouse, anti-chicken or anti-rabbit (Jackson ImmunoResearch); and (ii) indirect with streptavidin-biotin amplification—biotin conjugated donkey anti-rabbit (1:500; Jackson ImmunoResearch) followed by peroxidase conjugated streptavidin (Vectastain ABC kit, Vector laboratories), or 649 conjugated streptavidin (1:200; Jackson ImmunoResearch). Total cells within the grafts were visualized with 4', 6-diamidino-2-phenylindole (DAPI, 1:5000, Sigma-Aldrich). All fluorescent images were captured using a Zeiss Axio Observer.Z1 epifluorescence or Zeiss confocal microscope system. Bright and dark-field images were obtained using a Leica DM6000 upright microscope.

Total number of TH-GFP+, GIRK2+ and CALBINDIN+ neurons, as well as the proportion of NeuN+ (as a percentage of total DAPI) cells were counted from images captured at 20X magnification. Example: $\left(\frac{Number\ of\ TH-GFP+\ cells}{Number\ of\ DAPI+Cells}\right) x100.$ The density of graft-derived GFP+ DA fibers (% immunoreactive pixels) emanating from the graft was assessed within the dorsolateral striatum (the predominant target of A9 DA neurons and underpinning motor function) as well as immediately lateral to the graft-host border. Dark field images of GFP+ fibers were captured at 40X magnification on a Leica 6000 microscope and analysed using ImageJ software, using previously described methods [25]. The graft size was determined by ImageJ by selection of GFP+ region (mm^2) and corrected by the tissue thickness and number of series. Example: $\text{Area in mm2 x 40}\mu\text{m (thinkness) x 12 (number of sections)}.$

3.3.5 Statistical Analysis

All data are presented as mean + SEM. Statistical tests employed (inclusive of one-way ANOVA and student t-tests) are stated in figure legends. Alpha levels of $p<0.05$ were considered significant with all statistical analysis performed using GraphPad Prism. *$p < 0.05$, **$p < 0.01$, ***$p < 0.001$ and ****$p < 0.0001$.

3.4 RESULTS

3.4.1 Laminin-based IKVAV hydrogel fabrication and sustained SDF1 delivery

Here we utilize the Fmoc-SAP system to fabricate the Fmoc-DDIKVAV (**Figure 12B**), laminin epitope-presenting hydrogel for in vivo delivery of cells. The fabrication process involved the N-terminus of the peptide sequence being protected by an aromatic fluorenylmethoxycarbonyl (Fmoc) moiety. The aromatic groups of the Fmoc share electrons to form π-π interactions creating the backbone of the structures, while the individual peptides form hydrogen bonds with each other to create a secondary β-sheet protein structure. FTIR analysis of amide I region showed a characteristic peak for β -sheets with an observable carbamate peak (**Figure 12C**), and the stable formation of a dominant assembly confirmed by circular dichroism spectroscopy, showing transition peak at 200nm (**Figure 12D**). As result of several of these assemblies' individual nanofibres were formed that were nanometers in diameter and microns in length. These nanofibers then established supramolecular associations to create a highly branched nanofibrous network macroscale hydrogel whose structure was confirmed by transmission electron microscopy (**Figure 12E**). Rheological analysis of the elastic shear moduli of storage (G', black dots) and loss modulus (G", white dots) validated characteristic viscoelastic gel properties and demonstrated that the resultant gel had a modulus not dissimilar to the rodent brain (grey box, **Figure 12F**) [74], thereby presenting a hydrogel suitable for brain repair.

Critical for SDF1 to exert effects on the graft was the requirement for sustained presentation of the protein to the new cells acutely following implantation and during ongoing integration. In vitro, we demonstrated that recombinant SDF1 was rapidly degraded when added directly to the culture media, with less than 1% of the protein remaining after just 30 mins (**Figure 12G**). By comparison, shear encapsulation of the protein within the SAP hydrogel prolonged presentation, following an initial burst release. The burst release of the protein likely resulted from poorly entrapped SDF1 rapidly leaking from the SAP scaffold before it

reformed from its solution to gel state, yet had the benefit of prolonging the acute period of protein presentation over 4 hours (**Figure 12H**), and likely beneficial to the cells during the critically vulnerable phase of in vivo delivery. The majority of the SDF1 protein however interacted through absorption with the peptide fibrils within the scaffolds, resulting in a gradual release from the gel over 5-14 days, and corresponding to periods of DA progenitor maturation and integration. Ongoing release, of a slower rate, continued for at least 28 days (**Figure 1I**). Importantly, shear loading of SDF1 into the hydrogel had no impact on the assembly of the peptides or stiffness of the gels (data not shown).

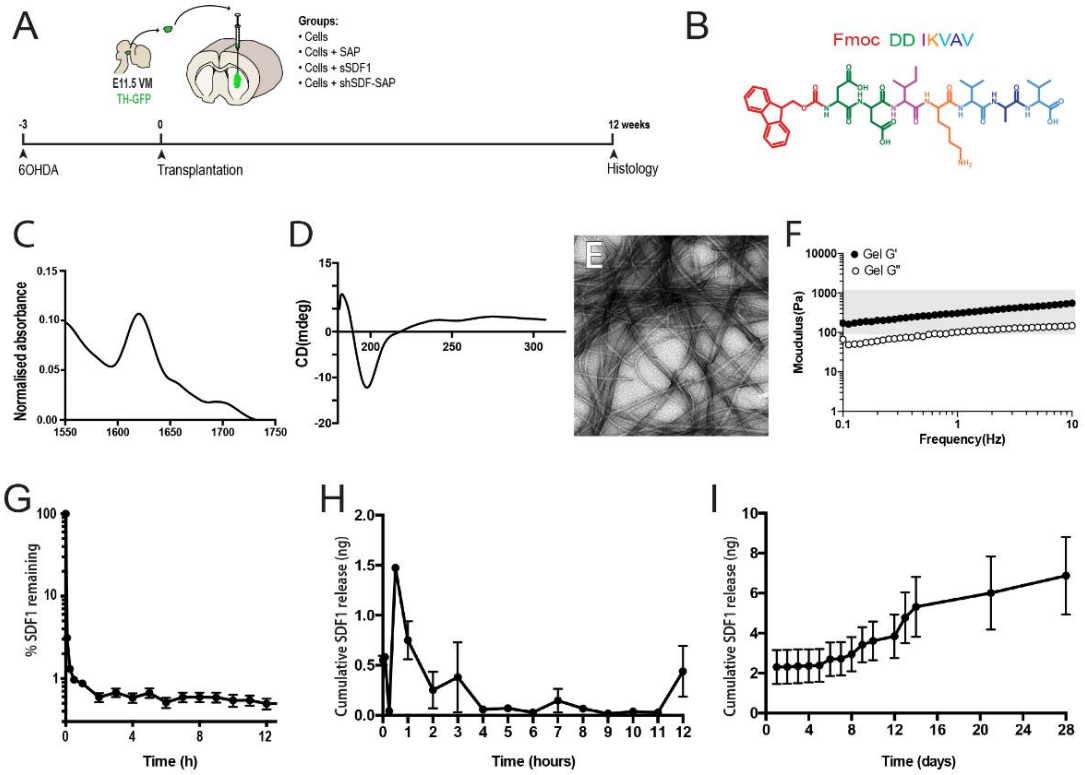

Figure 12. ***Laminin-based IKVAV hydrogel fabrication and sustained SDF1 delivery.*** *(A) Schematic picture of in vivo study design. (B) Schematic of the Fmoc-DDIKVAV peptide. (C and D) FTIR analysis of amide I region (C) showed characteristic peak for b sheets with an observable carbamate peak, and the stable formation of a dominant assembly confirmed by (D) circular dichroism spectroscopy, showing transition peak at 220 nm. (E) Assembly of the hydrogel's nanofibrils could be observed by electron microscopy. (F) Storage and loss modulus of the SAP hydrogel showed similarity to the rodent brain (grey box). (G) Soluble recombinant SDF1 protein in media showing rapid*

degradation within just 1 hour. (H-I) Shear entrapment of SDF1 within the hydrogel resulted in an initial burst release, yet sustained delivery over 28 days.

3.4.2 SDF1 functionalised scaffolds increases DA differentiation

At 12 weeks after receiving transplants of primary VM progenitors (+ SAP + SDF1) all animals were killed for histological analysis. Grafts could be identified in all brains by GFP labelling. Four animals were excluded from further analysis due to misplacement of the graft (residing outside the target striatal tissue) or due to the presence of obvious backflow of the GFP+ cells along the injection site (resulting in the presence of GFP cells in the overlying cortex and/or on the surface of the brain). Volumetric analysis revealed that graft size in the presence of either the SAP hydrogel (0.35 + 0.08 mm3) or sSDF1 (0.33 + 0.06 mm3) remained unchanged compared to grafts of cells alone (0.24 + 0.02 mm3), indicating that neither the gel or acute delivery of the protein impeded or promoted the survival (or proliferation) of the graft. In contrast, grafts in the presence of the SDF1-functionalised SAP hydrogel (Cells + shSDF1-SAP) were significantly larger (0.48 + 0.08 mm3), suggesting that the sustained presence of SDF1 influenced the proliferation or survival of the implanted progenitors- **Figure 13A-E**.

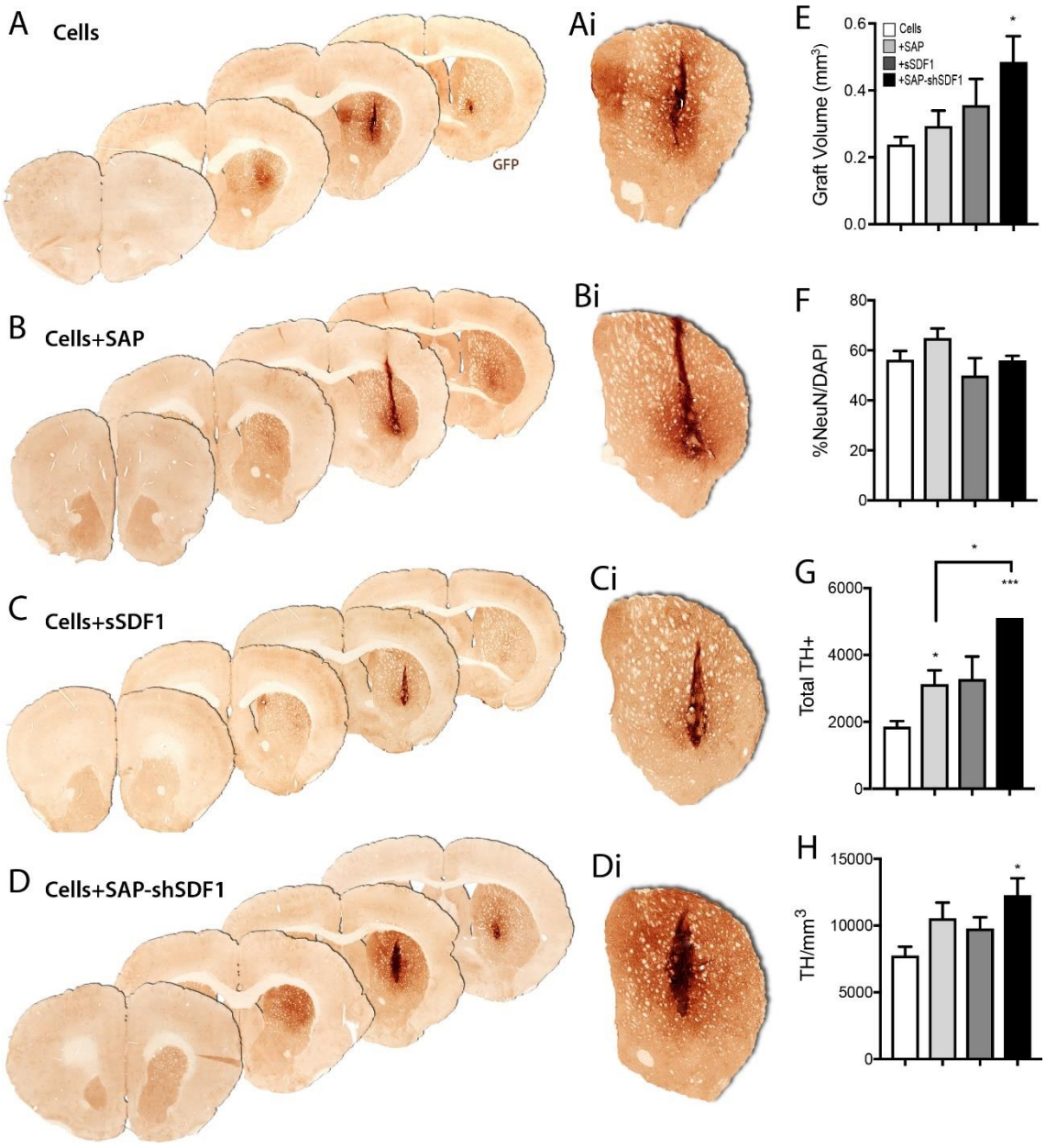

Figure 13. ***SDF1 functionalised scaffolds increase DA differentiation****. (A-D) Representative micrographs of primary VM progenitor grafts in the presence and absence of SAP and/or SDF1. Donor tissue, isolated from TH-GFP+ embryos, enable identification of the graft by GFP histochemistry. (E) Graph showing that the presence of the SDF1-functionalised SAP hydrogel (Cells + SAP-shSDF1) significantly influenced the graft volume. (F) Graph showing that neuronal maturation was not influenced by either the presence of the gel or SDF1 protein. (G) Graph of dopaminergic (GFP-TH+) cells quantification showing a significant increase of TH+ cells in the Cell+SAP grafts, an effect that was further increased in the presence of the funcitonalised hydrogel (Cell+SAP-shSDF1 group), highlighting the synergetic effect of SDF1 protein and the*

*hydrogel. (H) Quantification of TH cell density within the grafts, showing a significantly increase in cell+SAP-shSDF1 group, indicating that the increase in TH+ cells was due to enhanced differentiation, and not just increased graft size. 1:12 sections of 40µm. Data represents Mean +SEM, n=4-6/group, * p<0.05, *** p< 0.001.*

Density of NeuN+ neurons remained unchanged (ranging on average from 52-65%, **Figure 13F**) across all treatment groups, indicating that the majority of the graft acquired a maturing neuronal phenotype that was not influenced by either the presence of the gel or SDF1 protein. Consistency in NeuN+ cell density across the different graft groups also indicated that the presence of the hydrogel did not impede the capability of the implanted cells to migrate and integrate within the host tissue.

The use of the TH-GFP reporter mouse for isolation of donor tissue enabled clear visualisation of dopaminergic graft-derived (GFP+) integration, distinct from residual host dopaminergic neurons and fibers (GFP-). Quantitative assessment of GFP+ dopaminergic neurons within the grafts revealed that the presence of the SAP hydrogel, presenting the laminin epitope IKVAV, significantly increased the total yield (Cells: 1872 + 197, Cells + SAP: 3231 + 478). Acute delivery of SDF1 had no significant impact on DA neuron numbers (Cells + sSDF1: 3262 + 692). In contrast, the presences of the SDF1 functionalised SAP scaffold resulted in a 2.7-fold increase in GFP+ DA neurons (5092 + 560) compared to Cells alone, and increased compared to Cells + SAP, indicative of the synergistic effect of the SDF1 protein and the laminin-based scaffold, **Figure 13G**. Assessment of GFP+ cell density revealed an increase trend for grafts in the presence of the SAP, yet only significantly increased in Cells+SAP-shSDF1 (**Figure 13H**). Such observations suggest that the increased yield of TH-GFP+ neurons within these grafts was over and above the increase in graft volume, and that the functionalised scaffold was promoting DA differentiation.

3.4.3 Functionalised scaffolds have no impact on the density of dopaminergic innervation of the host striatum

Additional to the benefit of quantifying DA neuronal numbers within the graft, the GFP reporter enabled clear distinction of graft derived innervation of the host. Underpinning the capacity for grafted DA neurons to restore motor function, is their capacity to reinnervate the dorsolateral striatum. Assessment of this region of the host brain however revealed only sparse fibers (**Figure 14A**). Consequently, the capacity of the graft to innervate the host, and the impact of the IKVAV SAP hydrogel and/or SDF1 on graft plasticity was assessed at the graft-host border, as depicted in **Figure 14A**. No significant difference in GFP innervation was observed across the groups, suggesting that neither the laminin-epitope presenting SAP hydrogel or SDF1 had any influence on promoting graft plasticity, **Figure 14B-F**.

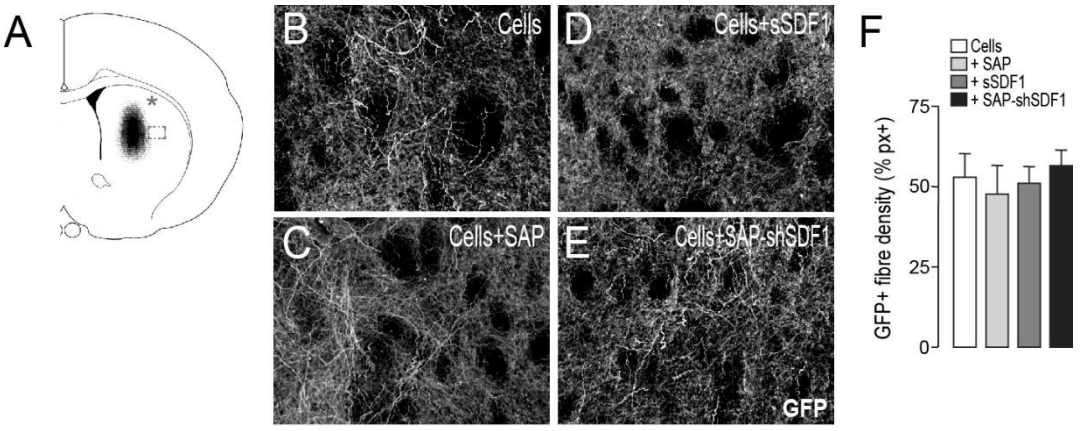

*Figure 14**. Functionalised scaffolds have no impact on the density of dopaminergic innervation of the host striatum**. (A) Schematic diagram illustrating the site of sampling for estimates of GFP+ fibre innervation. * indicates sampling site within the dorsolateral striatum, and boxed area shows sampling area adjacent to the graft core, depicted in (B-E). (F) Graph illustrating no significant difference in GFP+ graft-derived innervation of the host striatum across the groups. Data represents Mean +SEM.*

3.4.4 Functionalised scaffold increases the fate acquisition of A9 DA neurons, a subpopulation critical for motor function

Critical for the restoration of motor function following transplantation is not only the capacity for the new DA neurons to synaptically integrate, but more specifically the ability of the A9 DA neurons to form connections - a subpopulation of DA cells typically residing in the SNpc that form the nigrostriatal pathway. We therefore examined the number of A9 and A10-like neurons within the grafts, assessing GIRK2+GFP+, Calbindin+GFP+ and GIRK2+Calbindin+GFP+ cells, **Figure 15A**. Grafts in the presence of the SAP hydrogel showed a 2.6-fold increase in GFP+/GIRK2+ co-localised cells (Cells: 1013 + 121; Cells + SAP: 2589 + 461). In contrast, acute SDF delivery had no impact on A9 fate, failing to significantly increase the number of GIRK2+ cells within the graft (Cells + sSDF1: 1695 + 461) compared to Cells alone. However, SAP-delivered SDF1 had a significant effect on A9 specification, increasing the number of GIRK2+ cells compared to both Cells alone and Cells + sSDF1, (Cells + SAP-shSDF1: 3774 + 608), and highlighting the benefit of sustained protein delivery, **Figure 15A-C,F**. No reciprocal change in either GFP+/Calbindin+ or GFP+/GIRK2+/Calbindin+ neurons was observed, **Figure 15F**.

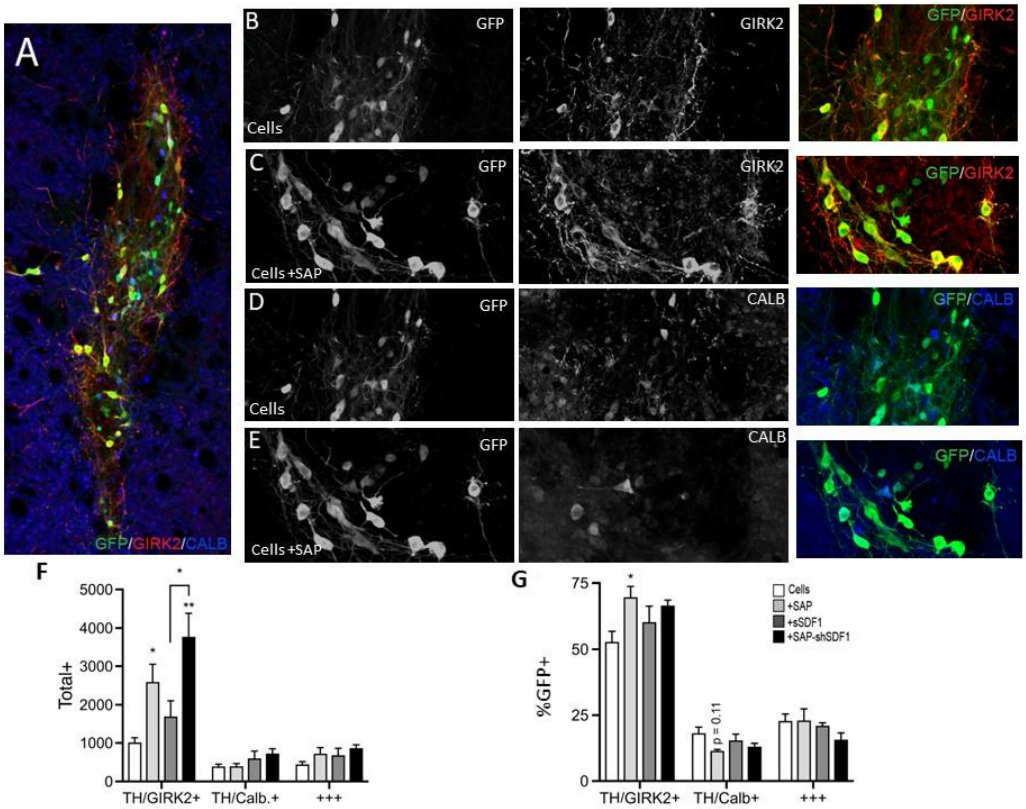

Figure 15. ***SAP scaffold, and sustained SDF1, increase A9 fate acquisition of DA neurons, a subpopulation critical for motor function****. (A) Representative picture of the graft showing the subpopulations of A9- and A10-like neurons identified by GFP (green), GIRK2 (Red) and Calb (blue). (B-E) Representative picture showing an increase in A9 cells (GFP+/GIRK2+) in Cells+SAP grafts compared to cells alone. (F) Graph of total number of cells expressing GIRK2 and/or Calbindin, highlighting a significant increase in A9 population (GFP+(TH+)/GIIRK2+) in the Cell+SAP and Cells+SAP-shSDF1 grafts. (G) Graph depicting the proportion of GFP+ cells co-expressing GIRK2, Calbindin+ or GIRK+/Calbindin+, where only grafts in the presence of the SAP showed a significant increase in the proportion of GIRK2+ cells. Data represents Mean +SEM, n=4-6/group, * p<0.05, ** p< 0.01.*

To assess whether the increase in A9-like GFP+/GIRK2+ cells was merely a consequence of increased GFP+ cells (observed to be significantly increased in both Cells + SAP and Cells + SAP-shSDF1 grafted animals, **Figure 13A-D, G**) A9 and A10 fated cells were expressed as a proportion of GFP+ cells within grafts. Only grafts in the presence of the SAP showed a significant increase in

the proportion of GIRK2+ cells (Cells: 53 + 4% GFP+GIRK2+/GFP+; Cells + SAP: 69 + 4%, p = 0.046; Cell + SAP-shSDF1: 67 + 2%, p = 0.125), suggesting that the laminin-based signalling presented by the SAP hydrogel was capable influencing DA fate acquisition, **Figure 15G**. Reflective of the total cell counts, no reciprocal change in either GFP+/Calbindin+ or GFP+/GIRK2+/Calbindin+ neurons was observed, **Figure 15G.**

3.5 DISCUSSION

The capacity to improve the survival, differentiation and/or integration of dopamine replacing cell grafts will have a significant impact on the number of cells required for grafting, and the predictability of graft function. While modifying one variable at a time can enable assessment of the impact in a biological context, presenting multiple biometric cues can often have a synergistic effect, such that the overall benefit is greater than the individual effects combined. With this in mind, here we sought to mimic key features of the physical and trophic ECM environment of neural tissue – fabricating a customised tissue-specific scaffold, presenting the functional laminin-binding epitope (IKVAV), known to influence cell adhesion, proliferation, differentiation and plasticity. Furthermore, we encapsulated SDF1 into the portion to sustain delivery. We showed the synergistic capacity of the SAP-shSDF1 hydrogel to increase graft size, DA neuronal numbers and most critically the number of A9-like neurons within a graft.

Since the first preclinical and clinical evidence for successful dopamine cell replacement there have been many efforts to improve transplant outcomes. Vulnerability of the donor cells is now recognised as one of the most critical factors contributing to graft success. When donor cells are isolated from fetal tissue, they are stripped of their anchorage to the ECM, activating cell death cascades. Cells then succumb to the physical shear forces of being injected through a fine needle/capillary, and finally these Immature progenitors are implanted into the adult host brain, devoid of age appropriate architecture or trophic support. Such traumas have highlighted the need for a more supportive environment for the donor cells, however the attention has remained on trophic

support, with little consideration for the physical environment. Evidence supporting the physical requirements of the graft are highlighted in series of additive studies showing that: (i) the co-grafting of unsheathing cells or sciatic nerve support DA grafts [98]–[101], (ii) newly integrating DA neurons utilise residual fibre bundles to act as scaffolding in axonal pathfinding [34] and that (iii) modulation of adhesion proteins L1 and ALCAM influence DA plasticity [102][103][104].

While biomaterials have been trialed and developed in other neural injuries – often to fill tissue voids and bridge gaps within fibre bundles, they have been less commonly employed to support grafts where the host tissue architecture remains intact. We were the first to demonstrate a benefit for utilising a (xyloglucan) hydrogel to support VM fetal tissue grafts [64], also demonstrated by others using a collagen-based gel [105]. In both instances the biomaterials provided only modest effects, likely underpinned by the gel composition and mode of synthesis, with the greatest benefit on graft outcome observed in their capacity to sustain the delivery of GDNF. A key goal of the present study was to utilise a scaffold that most closely mimicked the host tissue. As nanofibrous structural proteins are a major component of the ECM, and extensive effort has be invested in optimising the many properties of nanofibrous scaffold (such as tuning the stiffness to match the host tissue, as well as understanding the impact of nano- verses microscale morphology on cellular responsiveness), we elected to employ the Fmoc-based SAP system to fabricate a nanofibrous hydrogel, presenting the functional laminin epitope IKVAV. The selection of a laminin-based scaffold stemmed from recent observations for the roles of laminin in the survival and differentiation of DA neurons during VM development [63], as well as our observed improvement in the survival, differentiation and functional integration of stem cell-derived cortical grafts in a model of stroke [50]. The present findings showed the scaffold (SAP) to significantly increase DA neurons within the graft, and the first evidence of a biomaterial positively influencing A9 fate acquisition. Further work is required to understand the specificity of the laminin signalling for the A9 fate change, the impact of other laminin epitopes corresponding to alternate laminin subunits, namely laminin-521, implicated in human dopamine differentiation [44], and

whether distinct laminin-responsive transmembrane integrin proteins may be present on the surface of the subpopulations of DA progenitors.

Recent studies have highlighted the importance of SDF1 in DA development [88][106][95], and the DA differentiation of pluripotent stem cells [87][86][85][84]. Added to this, we previously demonstrated that the co-transplantation of meningeal cells, together with VM fetal grafts, significantly increased the proportion of A9 DA neurons within VM grafts – an effect that was speculated to be modulated via SDF1-CXCR4 signalling [95]. The capacity to directly address this question, however, required the ability to control the delivery of SDF1 over a timeframe relevant to the regenerative period, as well as targeted to the graft site, to ensure minimal off-target effects. This targeted temporal and spatial delivery of proteins, drugs and small molecules has, and continues to, be no small feat for regenerative medicine. Extensive efforts have been made to stabilize proteins and drugs for in vivo delivery – including the development of various biomaterials [70]. Here we provided evidence of the instability of SDF1, showing rapid degradation in vitro within minutes, highlighting the need for either sustained infusion in vivo (both a costly and cumbersome exercise) or our elected approach to incorporate the recombinant protein into the hydrogel by shear loading. The SAP hydrogel sustained SDF1 delivery over 28 days, showing a slowing in rate of release after 14 days. This window of delivery corresponds with the timeframe over which grafts differentiate and begin to integrate into the surrounding host – and could be validated here by the significant increase in the total number DA neurons, and GIRK2+ DA neurons. The lack of response of grafted cells to the acute delivery of SDF1, highlights the need to sustain delivery. The increased proportion of A9 DAn only present in the hydrogel group with a tendency in SAP hydrogel+SDF1 group indicates the need of establishing a correct SFD1 dosage. Further studies are required to confirm the functionality of these A9-enriched grafts, at the individual neuronal level as well as the greater functional integration and capacity to alleviate motor function.

SDF1 has previously been reported to strongly influence the plasticity of DA neurites in vitro and within the developing brain [106][88][95]. Surprisingly, despite an almost 3-fold increase in DA neurons in Cells+SAP-shSDF1 grafts, no

significant increase in DA fibers density within the surrounding host tissue was observed, or any other groups. Such observations were likely underpinned by insufficient duration, suboptimal dose, and/or the localisation of delivery to influence plasticity. SDF1 has been shown to attract DA neurites [95][88][106], yet was delivered here within the graft core, thereby failing to provide the necessary gradient to draw fibres into the host tissue. In other efforts to promote plasticity of DA neurons within grafts, trophic cues such as GDNF have been delivered within the target tissue (namely the dorsolateral striatum) - distant to the graft site, where they act to draw growing axons closer [33][34].

In summary, here we present a synergistic approach to improve graft outcomes, providing the first evidence of a bioengineered scaffold, presenting structural and trophic mimetics of the ECM and surrounding trophic cue SDF1, to the A9 dopaminergic differentiation of grafted VM progenitors. The utility of such functional biomimetic scaffolds may significantly improve the functional outcome of cell therapy for neural injuries, including Parkinson's Disease.

Chapter 4 - Prolonged GDNF release from tissue-specific hydrogels improves the functional integration of human stem cell-derived progenitor grafts in a rodent model of Parkinson's Disease

4.1 Abstract

The survival and subsequent synaptic integration of transplanted DA progenitors is essential for ameliorating motor symptoms in PD. Yet similar to ventral midbrain fetal tissue, hPSC DA progenitors, are exposed to numerous stressors prior to and during implantation that result in poor survival and show axonal plasticity well below the intact brain, and inferior to fetal grafts. Such observations suggest that a more conducive environment, reminiscent of the developing brain, to support newly integrate hPSC-DA progenitors could improve the functional capacity of these transplants. Here we employed a tissue-specific hydrogel, engineered by the self-assembling of peptides for a laminin epitope, thereby mimicking the major ECM protein of the brain. The hydrogel was loaded with GDNF via shear gel-solution transition, to sustain delivery. In an animal model of PD, the hydrogel provided protection of the progenitors during implantation, laminin-signalling influence an A9 DA neuron fate specification, while sustained GDNF contributed to enhanced survival and plasticity of DA neurons, collectively contributing to improved motor function. These findings highlight the potential therapeutic benefit of employing customised tissue-specific hydrogels to improve the standardisation, predictability and functional efficacy of hPSC transplants for PD.

4.2 Introduction

Clinical trials have provided proof of principle that the transplantation of new dopamine neurons into the striatum of PD patients can survive, integrate and restore motor function [54]. Initially demonstrated using fetal tissue, yet hindered by challenges of standardisation, ethics and availability, more recent years have seen a rapid advancement in the use of pluripotent stem cells as a viable donor source. Current differentiation protocols show high proportions of correctly specified ventral midbrain progenitors that, when implanted into animal model of Parkinson's disease, are capable of functionally integrating [21][22][25], with similar efficacy to human fetal tissue [53]. These exciting observations have resulted in the recent commencement and plans for multiple clinical trials [52].

A major challenge that persists for the field, however, is low survival rates of the donor cells. Yet the number of DA neurons that survive in a graft is recognized as the most decisive factor in governing whether a transplant is successful in ameliorating symptoms. Preclinical and clinical studies report cell survival rates of ranging from 1-20% for fetal tissue grafts [24] [81], and average dopamine neuron yields of <5% for hPSC-derived DA progenitor grafts [21][22] [25][37][43]. In addition to the physical trauma during harvesting of the cells from culture, two key events that impact on survival donor cells are the process of implantation, noting the shear forces exerted on the cells during injection, as well as the integration of the progenitors, acknowledging that the adult host brain into which transplants are placed lack many cues that are normally present during development when DA neurons are born and navigate their axons in situ to appropriate forebrain targets.

Another major deciding factor in the functional efficiency of these grafts is the capacity of the implanted cells to integrate into existing host circuitry, with evidence highlighting the necessity for synaptic connectivity of A9-like subpopulation of DA neurons in the graft with host striatal neurons [51]. While the requirement for this specific synaptic integration is known, the level of reinnervation of the host tissue by fetal derived grafts remains well below that of the intact brain – a phenomena that has been termed the 'ceiling effect' [107],

and is likely underpinned by the absence trophic cues that are typically present in developing brain when neurons integration, yet absent in adulthood. Added to this, more recent studies have observed that hPSC-derived DA transplants show significantly poorer striatal innervation than their human VM fetal counterparts [53]. Recognising that neural circuits established during development requires a tightly orchestrated physical and trophic environment, suggest that greater attention to the host milieu is required to promote survival, plasticity and integration of hPSC-derived DA neurons.

A number of efforts to inhibit cell death cascades and deliver trophic proteins have been investigated to promote the survival of the donor cells during the various stages of preparation and implantation and influence plasticity. One of the most heavily investigated proteins has been GDNF – first shown to promote survival and plasticity of cultured midbrain DA neurons [26], and subsequently employed to in preclinical and clinical studies to slow PD progression, as well as enhance grafting outcomes [27][28][83]. However, a persistent challenge in the application of proteins and small molecules has been their controlled delivery – recognising the limitation of cumbersome infusion kits, and while successful outcomes have been achieved using viral delivery to the host tissue, this presents its own challenges associated with sustained transgene expression.

While GDNF, as well as with a raft of other trophic and guidance proteins, have been explored for their capacity to improve graft outcomes in PD, considerably less attention has been paid to the extracellular matrix environment and its importance in providing both physical and chemical support for neurons and their axons. Recent studies have highlighted the role of cell adhesion proteins in DA differentiation and axonal pathfinding [108][102], and most recently laminin, the principle ECM protein in the central nervous system, has been shown to specifically influence survival and differentiation of fetal and PSC-derived midbrain DA neurons during development [63]. Such observations infer that greater attention to the biomimetics of the ECM may improve cell grafts.

In this regard, biomaterials have the potential to overcome many of the challenges associated with neural transplantation and have been utilized to

restore tissue architecture where necessary, enhance cell survival and differentiation as well as promote plasticity and integration of transplanted neurons [70][109]. Furthermore, functional proteins capable of influencing cellular fate, such as neurotrophic factors and morphogens, can be incorporated into bioengineered scaffolds to control temporal and spatial delivery. Recently GDNF-functionalized polymer hydrogels were shown to improve the survival and integration of rodent fetal VM tissue grafts in models of PD [110][111][64]. In parallel work, tissue-specific laminin-based hydrogels have been shown to improve hPSC-derived cortical progenitor grafts in stroke models [50][91], raising the question whether similar neural tissue-specific biomaterials, functionalised with GDNF might overcome many of the challenges currently hindering hPSC-derived VM progenitor grafts in PD.

4.3 Materials and Methods

4.3.1 Self-assembling peptide hydrogel preparation

A tissue specific self-assembling peptide (SAP) for the brain's major ECM protein - laminin, was fabricated using solid phase peptide synthesis, as previously described [91]. The laminin-based epitope synthesized had the sequence isoleucine-lysine-valine-alanine-valine (IKVAV), a fragment of the a1 chain of the protein. To ensure self-assembling under physiological conditions, two aspartate residues were incorporated at the N-terminus of the peptide to lower the pH at which spontaneous assembly occurred. Gelation was initiated using a well-established pH switch, as previously described, to yielded a 20mg/ml stock [91]. The final hydrogels were made with mixing at a 1:1 ratio with magnesium and calcium-free HBSS or cells. Following gelation, rheology was conducted to confirm a modulus similar to the rat brain [50][91]. Fourier transform infrared (FTIR), circular dichroism (CD) spectroscopy, and transmission electron microscopy verified synthesis and structure of the desired nanofibrillar structure [50]. The resultant hydrogels could be reversed to an aqueous state by application of shear force (achieved via repeated titration or vortexing), such that the gel disassembled into a liquid solution. Reversal of the gel into a liquid state

enable incorporation and homogeneous distribution of GDNF recombinant protein into the polymer. We refer to this incorporation of the functional protein into the polymer as shear loading or shear containment. Shear reversal of the gel also enabled incorporation of cells into the aqueous polymer solution for efficient delivery into the brain.

4.3.2 Assessment of GDNF release, and function, from SAP hydrogel

To assess the release kinetics of GDNF from the scaffold, GDNF (100 ng, R&D Systems) was loaded into the SAP (50 µL) by reverse shearing of the gel to an aqueous state prior to casting the gel into a well of a 96-well plate. PBS (200 µL) was added to the well and incubated at 37 °C. The supernatant was collected at pre-determined intervals over a 4-week period. All supernatant samples were stored at -20 °C until the time of analysis. The GDNF levels (protein unfolding and cumulative release) was quantified by enzyme linked immunosorbent assay (ELISA), using previously described methods [64], [89]. Release profiles were performed in triplicate wells for each time point and, repeated on 3 independent experiments.

The functionality of the GDNF released from the hydrogels was confirmed using previously described methods [91]. As above, GDNF was shear-loaded into SAP, cast into a 48 well plate and 100ul of media added. Conditioned media (shGDNF-CM) was collected after 12 hours and applied to primary ventral midbrain neurons for comparison to untreated cultures as well as those treated directly with recombinant GDNF protein (soluble GDNF, sGDNF, 20ng/ml). Primary VM cultures were performed and assayed as previously described [59]. In brief, VM tissue was microdissected from the brains of embryonic day 11.5 (E11.5) embryos that were obtained from time-mated mice expressing GFP under the tyrosine hydroxylase promotor. The VM tissue was dissociated using 0.05% trypsin and 0.1% DNase, digest subsequently arrested using 10% serum, and the cells resuspended in N2 media. Cells were seeded at a density of 125,000 cells/well in 48 well plates (coated with PDL/laminin). After 72 hours, cultures were fixed with 4% paraformaldehyde and assessments of TH+ neuron number and neurite length assessed.

4.3.3 Ventral midbrain specification of human pluripotent stem cells

The H9 human embryonic stem cell (hESC) reporter line expressing GFP under the LMX1A promotor (LMX1A-GFP) was expanded and differentiated to a ventral midbrain progenitor identity as previously described [25]. In brief, the cell line, confirmed to be karyotypically normal and routinely tested for absence of mycoplasma, was cultured on laminin 521 in mTeSR supplemented with 0.4% penicillin-streptomycin. To promote neural induction, cells were exposed to dual SMAD inhibition using LDN193189 (200nM, Stemgent; from 0-11 days in vitro, DIV) and SB431532 (10µM, R&D Systems; 0-5DIV). Ventral patterning was achieved by addition of sonic hedgehog (C25II, 100ng/ml, R&D Systems; 1-7DIV) and purmorphamine (2µM, Stemgent; 1-7DIV), and the cells caudalised to a midbrain identity by Wnt activation using CHIR99021 (3µM, Miltenyi Biotech; 3-13DIV). Regional identity of the differentiating cells was confirmed at 11DIV. At 21 DIV cultures were dissociated using Accutase (Life Technologies) and correctly specified ventral midbrain progenitors isolated by fluorescent activated cell sorting (FACS) based upon expression of LMX1A-GFP, using previously described methods (de Luzy et al., minor revisions submitted 25 June 2019).

4.3.4 Surgical Procedures

All animal procedures were conducted in agreement with the Australian National Health and Medical Research Council's published Code of Practice for the Use of Animals in Research, and experiments approved by The Florey Institute of Neuroscience and Mental Health Animal Ethics committee. Animals were group housed in individually ventilated cages with low irritant bedding on a 12:12-hour light/dark cycle with ad libitum access to food and water. Surgeries were performed on 55 athymic (CBHrnu) nude rats under 2% isofluorane anaesthesia. Rats received unilateral 6-OHDA (3.5µl, 3.2 µg/µl) lesions of the medial forebrain bundle at the following stereotaxic co-ordinates: 3.4mm caudal, 1.4mm lateral to bregma, and 6.8mm below the surface of the dura. Human ESC-derived LMX1A-GFP expressing VM progenitors were transplanted into the denervated striatum (1 µ l; 100,000 cells/ µl) at the following co-ordinates: 0.5mm anterior, 2.5mm lateral to Bregma and 4.0mm below the dura.

Treatment groups were as follows: Lesion, Lesion + LMX1A-GFP+ VM progenitors (subsequently referred to as 'Cells'), Lesion + Cells+ DDIKVAV SAP (referred to as 'Cells + SAP'), Lesion + Cells + soluble GDNF ('Cells + GDNF'), and Lesion + Cells + SAP shear loaded with GDNF (Cells + SAP-GDNF), n=7-11 rats per group.

GDNF was delivered (mixed with cells or shear loaded into the IKVAV polymer) at a final concentration of 1ug/injection. A total of 150,000 cells were injected per animal, delivered within the IKVAV polymer (at a final concentration of 10mg/ml) or HBSS media. All animals received a final injection volume of 2µl.

4.3.5 Behavioural testing

Behavioural assessment of motor impairment was performed 3 weeks after unilateral 6-OHDA lesioning using the amphetamine-induced rotation and cylinder tests, as previously described [25]. In brief, for rotational testing, net rotations over 60 minutes were analysed 10 minutes after intraperitoneal injection of D-amphetamine sulfate (5mg/kg; Tocris Bioscience). For the cylinder test, rats were placed within a clear glass cylinder and the first 20 forepaw touches recorded over three consecutive days. Data was presented as left paw ratio (Left/(Left + Right)) × 100. Animals displaying a functional deficit (>300 rotations/hr), indicative of extensive unilateral ablation of the midbrain dopamine pathway, were included in the study. The 33 rats reaching criteria were ranked in order of the percentage rotational asymmetry and evenly distributed across the 5 treatment groups. Testing was repeated at 24weeks post-transplantation.

Note, the delivery of GDNF or SAP into 6-OHDA lesioned rats, in the absence of cells, bear no impact on motor performance, with stable motor deficits observed at 24 weeks, indistinguishable from Lesion only animals. Beyond motor assessment, these animals were not further analysed in the present study.

4.3.6 Tissue Processing and histochemistry

At 24 weeks post-implantation animals all animals received an acute injection of D-amphetamine sulfate (5mg/kg) prior to an overdose of sodium pentobarbitone (100 mg/kg). Animals were transcardially perfused with 4% paraformaldehyde

and the brains processed for immunohistochemistry as previously described [50]. Primary antibodies and dilution factors were as follows: mouse anti-CD11b (1:100, Serotec), goat anti-cFos (1:1000, Santa Cruz), goat anti-FOXA2 (1:200, Santa Cruz), rabbit anti-GFAP (1:200, DAKO), chicken anti-GFP (1:1,000; Abcam), rabbit anti-GFP (1:20,000; Abcam), mouse anti-human nuclear antigen (HNA, 1:300, Millipore), mouse anti PSA-NCAM (1:200, Santa Cruz), mouse anti-Nestin (1:200, Millipore), mouse anti-NeuN (1:100; R&D Systems), rabbit anti-OTX2 (1:4000; Millipore), anti-rat endothelial cell antigen-1 (RECA-1, 1:500, Serotec), rabbit anti-TH (1:500, Pel-Freeze), sheep anti-TH (1:800, Pelfreeze), mouse anti-Calbindin (1:1,500: Swant), rabbit anti- G-protein-gated inwardly rectifying K+ channel subunit 2 (GIRK2, 1:500; Chemicon). Secondary antibodies for (i) direct detection were used at a dilution of 1:200—DyLight 488, 549 or 649 conjugated donkey anti-mouse, anti-chicken or anti-rabbit (Jackson ImmunoResearch); and (ii) indirect with streptavidin-biotin amplification—biotin conjugated donkey anti-rabbit (1:500; Jackson ImmunoResearch) followed by peroxidase conjugated streptavidin (Vectastain ABC kit, Vector laboratories), or 649 conjugated streptavidin (1:200; Jackson ImmunoResearch). Total cells in vitro, and in vivo were visualized with 4', 6-diamidino-2-phenylindole (DAPI, 1:5000, Sigma-Aldrich). All fluorescent images were captured using a Zeiss Axio Observer.Z1 epifluorescence or Zeiss confocal microscope system. Bright and dark-field images were obtained using a Leica DM6000 upright microscope.

Total number of TH+, GIRK2+, Calbindin+ as well as density of NeuN+ and cFos+ cells were counted from images captured at 20X magnification. The density of graft-derived PSA-NCAM labelling (%immunoreactive pixels) within the dorsolateral striatum (the midbrain DA forebrain target that underpins gross motor function) was assessed from images captured at 20X magnification and analysed using ImageJ software.

The immunological response of the host brain to the implantation of the Cells and/or the SAP scaffold (including the presence of GDNF) was assessed at predetermined sites lateral to the graft-host border (delineated according to GFP labelling). The area covered by GFAP or CD11b immunoreactivity was expressed as a percentage of the total pixels, as previously described [89].

RECA-1 immunostaining was employed to identify blood vessels within the graft and host tissue. Vessel density (expressed as the percentage total area covered by RECA-1 staining), within graft and host tissue, was estimated using previously described methods [50].

4.3.7 Statistical Analysis

All data are presented as mean + SEM. Statistical tests employed (inclusive of one-way ANOVA and student t-tests) are stated in figure legends. Alpha levels of $p<0.05$ were considered significant with all statistical analysis performed using GraphPad Prism. *$p < 0.05$, **$p < 0.01$, ***$p < 0.001$ and ****$p < 0.0001$.

4.4 Results

4.4.1 Tissue-specific scaffolds deliver functional GDNF to promote DA survival and plasticity in vitro

The current study examined the capacity of GDNF functionalised scaffolds to support human pluripotent stem cell derived VM progenitor grafts in a rat model of Parkinson's disease, **Figure 16A**. To begin, a hydrogel capable of mimicking structural and functional attributes of the brain's native extracellular matrix was engineered. The hydrogel was synthesised by the self-assembling of the specific peptide sequence, isoleucine-lysine-valine-alanine-valine (IKVAV), encoding for an epitope for the binding domain of laminin - a major ECM protein required for cell attachment, proliferation, differentiation and plasticity [112]. To enable assembly under physiological conditions (pH 7.4), two aspartate residues were added at the beginning of the sequence to adjust the pKa, resulting in a final peptide sequence, DDIKVAV (**Figure 16B**). Aromatic fluorenylmethloxy carbonyl

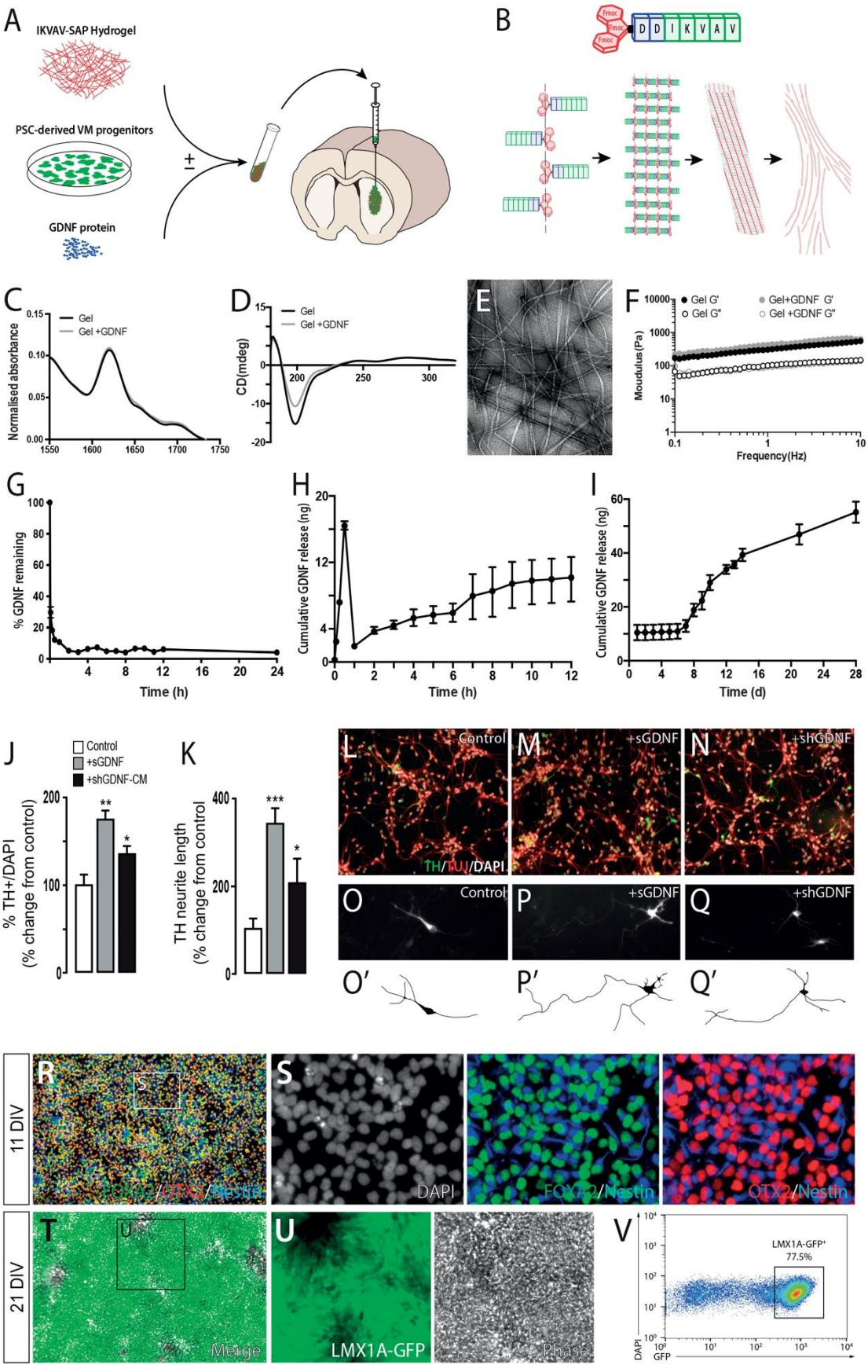
A
IKVAV-SAP Hydrogel
PSC-derived VM progenitors
GDNF protein
B
Fmoc
D D I K V A V
C
Gel
Gel +GDNF
Normalised absorbance
D
CD(mdeg)
E
F
Gel G'
Gel G"
Gel+GDNF G'
Gel +GDNF G"
Moudulus (Pa)
Frequency(Hz)
G
% GDNF remaining
Time (h)
H
Cumulative GDNF release (ng)
Time (h)
I
Cumulative GDNF release (ng)
Time (d)
J
Control
+sGDNF
+shGDNF-CM
% TH+/DAPI
(% change from control)
K
TH neurite length
(% change from control)
L
Control
M
+sGDNF
N
+shGDNF
TH/tUJ/DAPI
O
Control
P
+sGDNF
Q
+shGDNF
O′
P′
Q′
11 DIV
R
S
DAPI
FOXA2/Nestin
OTX2/Nestin
21 DIV
T
U
Merge
LMX1A-GFP
Phase
V
LMX1A-GFP+
77.5%
DAPI
GFP

*Figure 16 (From previous page)**. Generation of SAP hydrogel biomaterial and hESC-derived Vm progenitors suitable for transplantation**. (A) Schematic pictures of in vivo study design. (B) Schematic peptide structure showing its self-assembly, leading to a naturally nanofiber structure (combination of amphiphilic organisation, π-π interactions and the β sheet folding forming the nanofibrils). (C) Peptides interaction through hydrogen bonds forming a secondary β sheets that were confirmed by fourier transform infrared (FTIR) of amide I region showing characteristic peak for β sheets with an observable carbamate peak. (D) The stable formation of a dominant assembly, confirmed by circular dichroism spectroscopy, showing transition peak at 220 nm. (E) Hydrogel's nanofibrils, confirming appropriate assembly, could be observed using electron microscopy. (F) Storage and loss modulus of the hydrogel. (G) Soluble GDNF in media showing rapid degradation (>90% degradation within 2hrs). (H-I) Shear entrapment of GDNF within the hydrogel resulted in an initial burst release (within 15mins), followed by a delayed and sustained release, observed over 28 days. (J-K) VM primary cultures treated with soluble recombinant GDNF protein (sGDNF) and with conditioned media collected from SAP hydrogels shear loaded with GDNF (shGDNF-CM), confirming GDNF functionality – as revealed by increased TH+ cells and longer neurites. (L-Q) Representative pictures from Vm primary culture with and without sGDNF or shGDNF-CM. (R-S) VM fate specification of human PSCs at 11DIV confirmed by the co-expression of FOXA2, OTX2 and NESTIN. (T-U) Expression of the early intrinsic determinant transgene, LMX1A, at the time of transplantation (21DIV). (V) Use of an LMX1A-GFP reporter human PSC cell line enabled isolation of correctly specified VM progenitors, by FACS isolation, prior to transplantation. Data represents Mean +SEM. Figure J-K, n=3 independent cultures. * p<0.05, ** p< 0.01, *** p<0.001.*

(Fmoc) moieties were used to protect the amino terminal of the peptide, and provide shared electrons π-π interactions, creating the backbone structure (shown in red **Figure 16B**). The individual peptides interacted through hydrogen bonds to form secondary β sheets that were confirmed by fourier transform infrared (FTIR) and circular dichroism (CD), **Figure 16C-D**. Through a combination of amphiphilic organisation, π-π interactions and the β sheet folding, nanotubes were formed. These nanotubes interacted to create hydrated bundles

(**Figure 16A**), forming the matrix of the hydrogel, and could be visualised by transmission electron microscopy (**Figure 16E**).

Appropriate for in vivo delivery and the support of implanted neural progenitors, the resultant gels (at 10mg/ml) had a storage and loss modulus similar to the rat brain (SAP hydrogel: G' ~ 0.6kPa, G" ~ 0.1kPa; Rat brain: 0.3-1.1kPa [74]), **Figure 16F**. Note, shear-loading of the SAP hydrogel with GDNF had no impact on the assembly or mechanical properties of the gels (**Figure 16C-E**).

Importantly we confirmed the stability and functionality of GDNF released from the SAP hydrogels in vitro, prior to in vivo delivery. Surprisingly, recombinant GDNF protein added directly to the culture media, rapidly unfolded/degraded, with just 20% of the protein present after 15mins, and less than 3% at 24hours, **Figure 16G,** a possible multifactor combination result of degrading agents such as temperature and proteolytic enzymes normally present *in vitro and in vivo*. In contrast, shear entrapment of the protein within the hydrogel resulted in an initial burst release within the first 15 minutes, likely the consequence of poorly entrapped GDNF rapidly leaking from the hydrogel prior to reforming, that was followed by a delayed and sustained release from 7-14 days, **Figure 16H-I**.

To confirm the functionality of the GDNF protein released from the SAP hydrogels, prior to in vivo testing, we treated VM primary cultures, isolated from the developing embryo and rich in DA progenitors, with soluble recombinant GDNF protein (sGDNF) or conditioned media collected from GDNF shear loaded SAP gels (shGDNF-CM). As anticipated, sGDNF treatment resulted in a significant increase in the survival and/or differentiation of TH+ DA neurons in culture (%TH+/DAPI, **Figure 16J, L-N**), as well as TH+ neurite length (**Figure 16K, O-Q**), effects that were mimicked, although notably more modest, by treatment of the cultures with shGDNF-CM (**Figure 16 J-Q**).

Necessary for the generation of replacement neurons for transplantation, ventral midbrain DA progenitors were differentiated from LMX1A-eGFP human embryonic stem cells using an established xenogeneic-free protocol [23]. Appropriate and efficient VM fate specification of the cells in culture was validated at 11DIV by the co-expression of floor-plate marker FOXA2, forebrain-midbrain

transcription factor OTX2 and neural progenitor marker NESTIN – present in >85% of cells (**Figure 16R-S**). At the time of transplantation (21DIV), >75% of cells expressed the early intrinsic determinant transgene LMX1A (LMX1A-GFP, **Figure 16T-U**), a population that could be readily isolated by FACS **(Figure 16V**), for the purpose of VM DA neuron enrichment in grafts, as previously described (de Luzy et al., minor revisions submitted 25 June 2019).

4.4.2 GDNF-Functionalized scaffolds promote functional recovery and increased graft survival in Parkinsonian rats

Behavioural testing, for asymmetric motor function in unilaterally 6-OHDA lesioned rats, was performed four weeks after 6-OHDA lesioning (pre-transplantation, Pre-Tx) and repeated at 24 weeks after grafting, (**Figure 17A**). All animals receiving a cell graft showed significant correction of amphetamine-induced rotational asymmetry, whilst ungrafted animals displayed a persistent stable motor deficit (**Figure 17B**). In the stepping task, used to assess spontaneous motor function, all animals prior to transplantation showed a deficit in the contralateral forepaw use (<10% use of the impaired contralateral, compared to the unimpaired ipsilateral paw). Only animals receiving cell graft in the presence of GDNF-functionalised SAP scaffold (black bars), showed a significant improvement in limb use 24wks after grafting, **Figure 17C**.

In support of the observed improvement in rotational asymmetry, at 24 weeks after transplantation all animals displayed surviving grafts, predominantly confined to the striatum, as revealed by staining against the human specific neural cell adhesion protein, PSA-NCAM, **Figure 17D-G**. No evident tissue overgrowths were observed in any grafts, indicative that the implanted progenitors were sufficiently fate restricted in vitro prior to implantation. Volumetric assessment of the PSA-NCAM labelling revealed that grafts in the presence of the GDNF-functionalised SAP hydrogel (Cells + SAP-shGDNF) were significantly larger (2-fold) than cells in the absence or presence of SAP or sGDNF alone, **Figure 17H**.

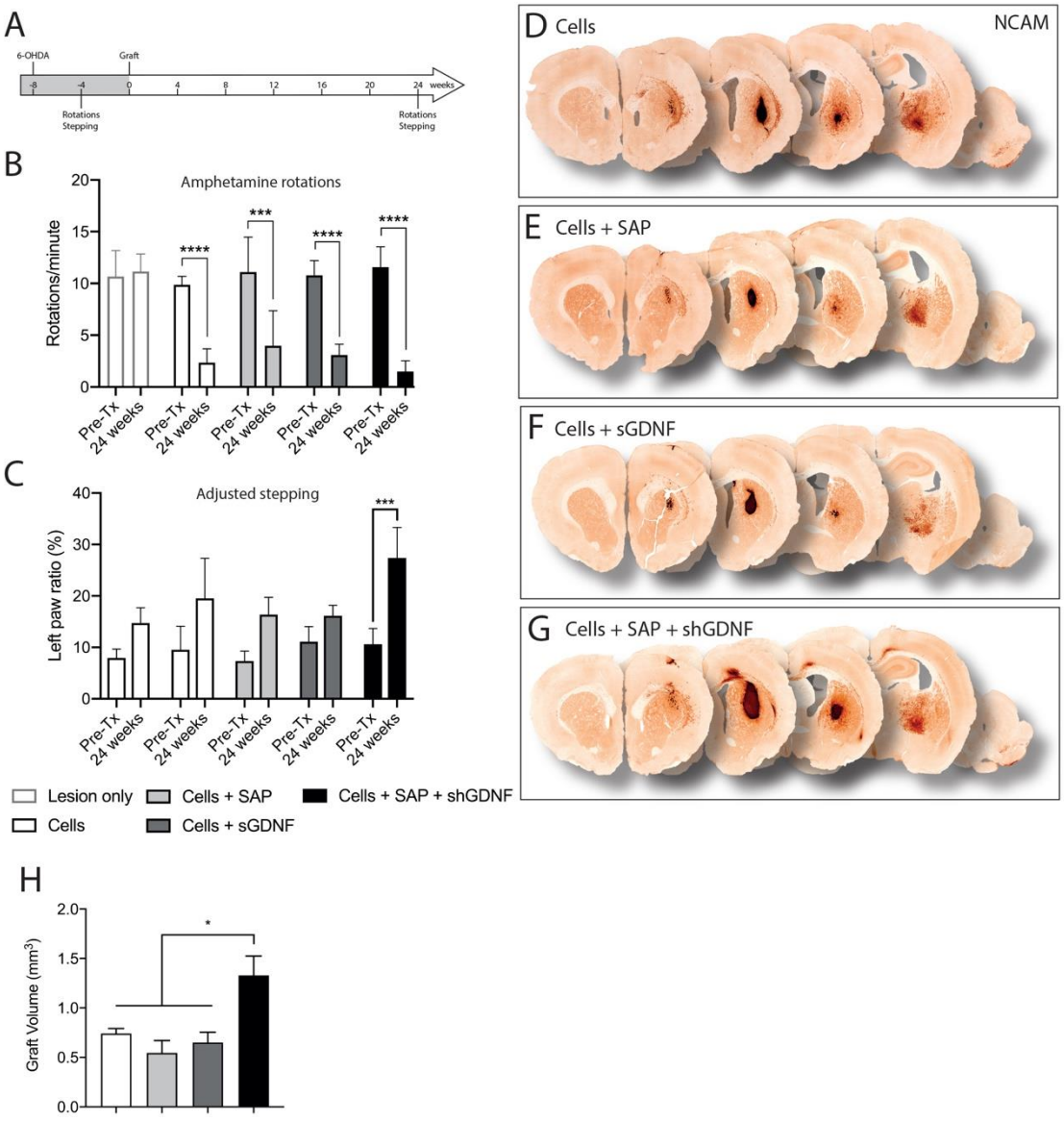

Figure 17. ***Implantation of human ESC-derived VM progenitors together with a GDNF functionalised tissue-specific scaffolds improves motor function in Parkinsonian rats****. (A) Schematic overview of in vivo study design. (B) All animals receiving a human PSC-derived VM progenitor cell graft showed significant correction of amphetamine-induced rotational asymmetry. (C) Only animals receiving cell graft in the presence of GDNF-functionalised SAP scaffold displayed a significant recovery in the spontaneous motor function adjusted stepping task at 24wks after grafting. (D-G) Representative picture of graft survival confirmed by PSA-NCAM staining after 24 weeks. (H) Graft volumetric assessment by PSA-NCAM labelling revealed that grafts in the presence of the GDNF-functionalised SAP hydrogel were significantly larger compared*

*to the other graft groups. 1:12 sections of 40µm. Data represents Mean +SEM, n=5-7 Grafts/group. * p<0.05.*

Despite the presence of viable grafts in all animals, necessary for understanding the potential utility of this biomaterial approach for cell delivery was as assessment of the biocompatibility of the implanted scaffolds. Previous findings have demonstrated the persistence of these SAP-based hydrogels up to 9 months after implantation [50], indicating that assessment of immunoreactive markers against reactive astrocytes (GFAP) and microglial at the 6 months after implantation would highlight a immunomodulatory response, if present. Compared to cell grafts alone (Cells), neither the presence of the unfunctionalized or GDNF-functionalised SAP augmented an inflammatory response, with GFAP and CD11b cell density not significant different across treatment groups, measured at both the graft-host interface (Field of View 1, FOV1, **Figure 18**), and at more protracted distance away from the graft core (FOV2, data not shown).

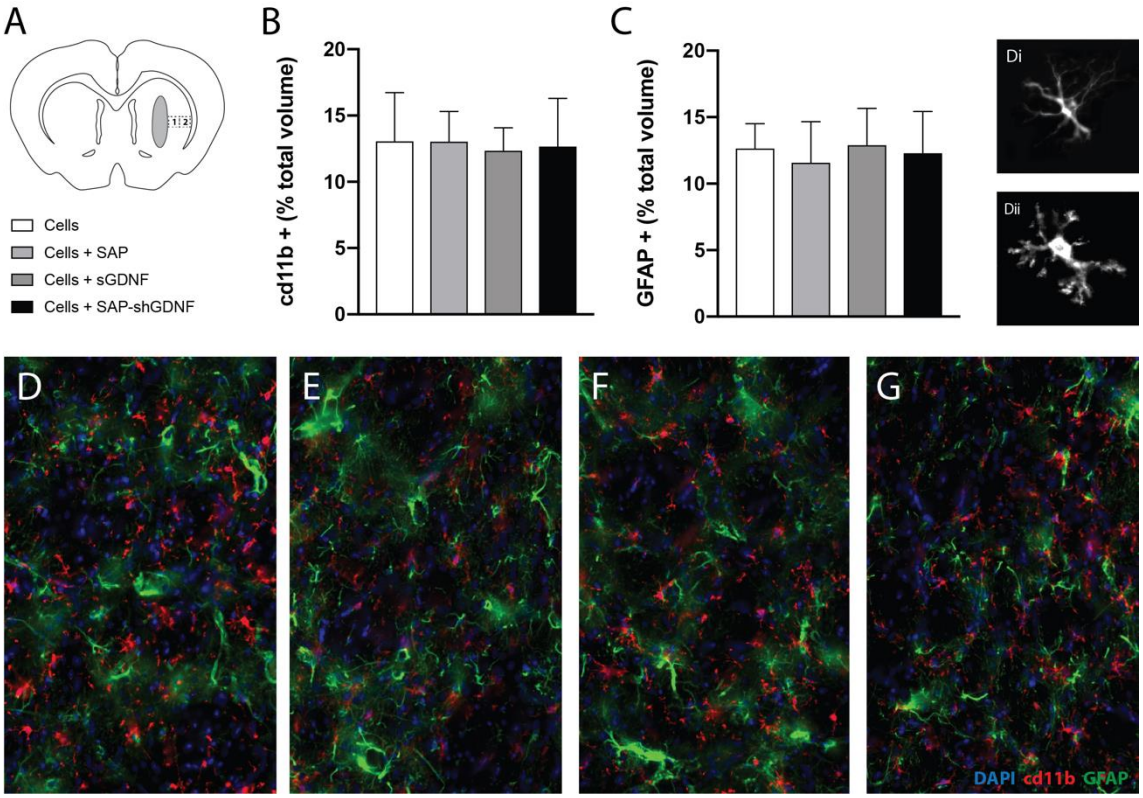

Figure 18. ***Tissue specific scaffolds show in vivo biocompatibility.*** *(A) Schematic figure showing the regions of sampling of GFAP and CD11b density – at the graft-host boundary (field of view 1, FOV1) and a more distal site away from the graft border (FOV2). (B-C) Assessment of immunoreactive markers against microglial - Cd11b (B), and reactive astrocytes – GFAP (C), at 24 weeks after implantation, showing no difference in inflammatory response across the groups. (D-G) Representative picture of GFAP (green) and Cd11b (red) among the groups, at 24 weeks. (D) Cells, (Di) Representative picture of GFAP, (Dii) Representative picture of Cd11b (E) Cells+SAP, (F) Cells+sGDNF, (G) Cells+SAP-shGDNF. Data represents Mean +SEM, n=5.*

As most death of DA progenitors occurs during preparation of the tissue/cell suspension, and acutely (within days) after implantation [24], in a separate cohort of animals the density of GFAP immunoreactive astrocytes was assessed at 2 weeks post-implantation. Similar to assessment at 6 months, the presence of the biomaterial imparted no inflammatory response above that observed in animals implanted with Cells alone (**Figure 19**).

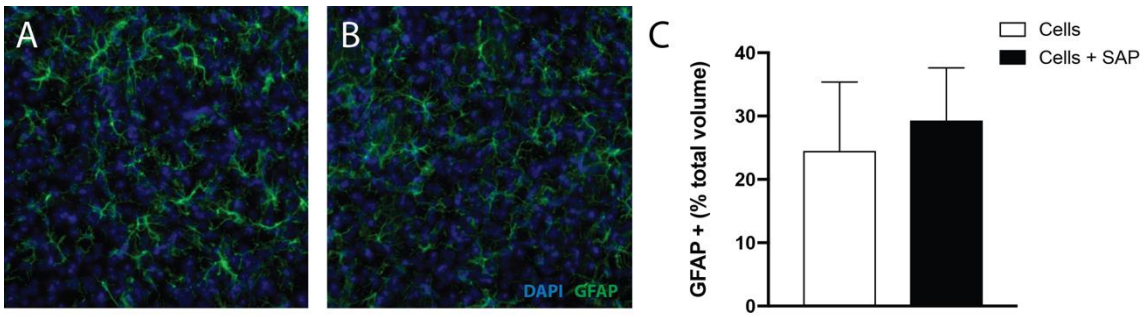

Figure 19. Tissue specific scaffolds show in vivo biocompatibility acutely after implantation. (A-B) Representative images of GFAP staining within FOV1 (as per Figure 18) showing similar GFAP+ immunoreactivity within (A) Cells and *(B) Cells+SAP implanted animals. (C) Quantification of GFAP+ density adjacent of the graft. Data represents Mean + SEM, n=4/group.*

Necessary for the survival of cells within large grafts is their juxtaposition to a vascular supply. Staining for RECA1+, to identify endothelial cells lining the vasculature, as well as GFP to demarcate the graft, revealed the presence of a vascular network within the grafts (**Figure 20A-F**). In comparison to the host brain, RECA1+ vessels were significantly less dense, with no difference between graft groups, indicating that neither the biomaterial nor the GDNF influenced vascularisation of the graft (**Figure 20G**). Similar to previous observations of large hPSC-derived neural grafts [50], the RECA1+ cells were GFP- (**Figure 20A**), indicative of the recruitment endothelial progenitors from the host tissue – an unsurprising observation in light of the in vitro neural fate restriction of the cells, and selection of LMX1A-GFP neural progenitors, prior to implantation.

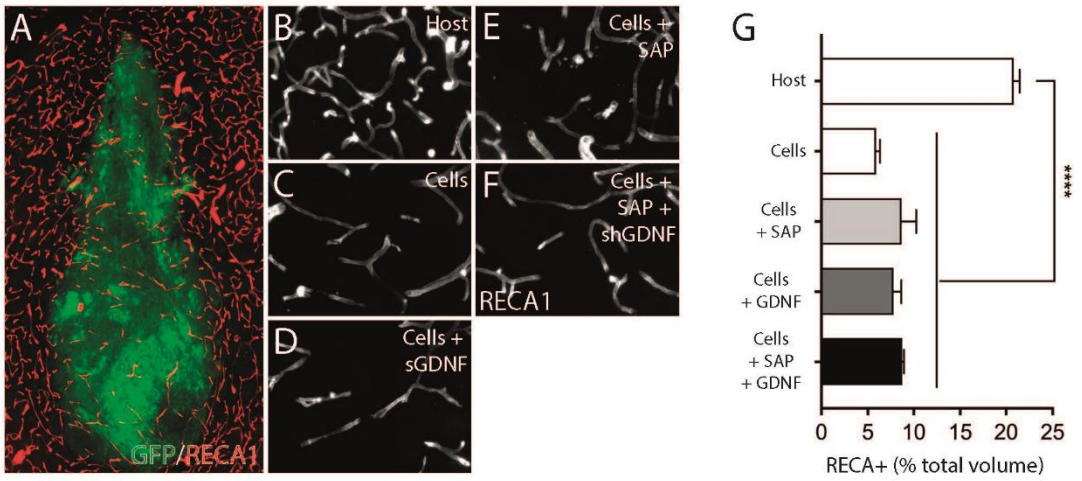

Figure 20. ***Human PSC-derived VM progenitor grafts show modest vascularisation that was not influenced by the presence of GDNF and/or the SAP hydrogel****. (A) Representative overview of a graft illustrating RECA1 + staining against endothelial cells, revealing the presence of a vascular network within the grafts. (B) the vascular network was visibly denser in the host, compared to the (C-F) grafts. (G) Quantitative analysis showed no difference in vascularization between grafted groups, indicating that neither the biomaterial nor the GDNF influenced vascularisation. Data represents Mean +SEM, n=5 Grafts/group. **** p<0.0001.*

4.4.3 Functionalized scaffolds promote survival of DA neurons and bias A9-specification

The function of PSC-derived VM neural progenitor graft is underpinned by their capacity to form mature neurons, specifically tyrosine hydroxylase-expressing DA neurons. NeuN+/HNA+ co-immunoreactivity revealed that approximately a third of the cells within all grafts adopted a mature neuronal phenotype, irrespective of the presence of the hydrogel or GDNF protein, **Figure 21A-C**. In contrast, while the acute delivery of GDNF or presence of the IKVAV SAP hydrogel alone had no impact on TH+ cell number, grafts in the presence of the functionalized SAP scaffold, sustaining GDNF delivery (Cells + SAP-shGDNF), showed a 2.7-fold increase in TH+ cells Figure **21D-H**. However, TH cells density had no significant improvement among the groups, suggesting that the likely effect of GDNF was on promoting survival during implantation and the acute days of graft integration **Figure 21I**.

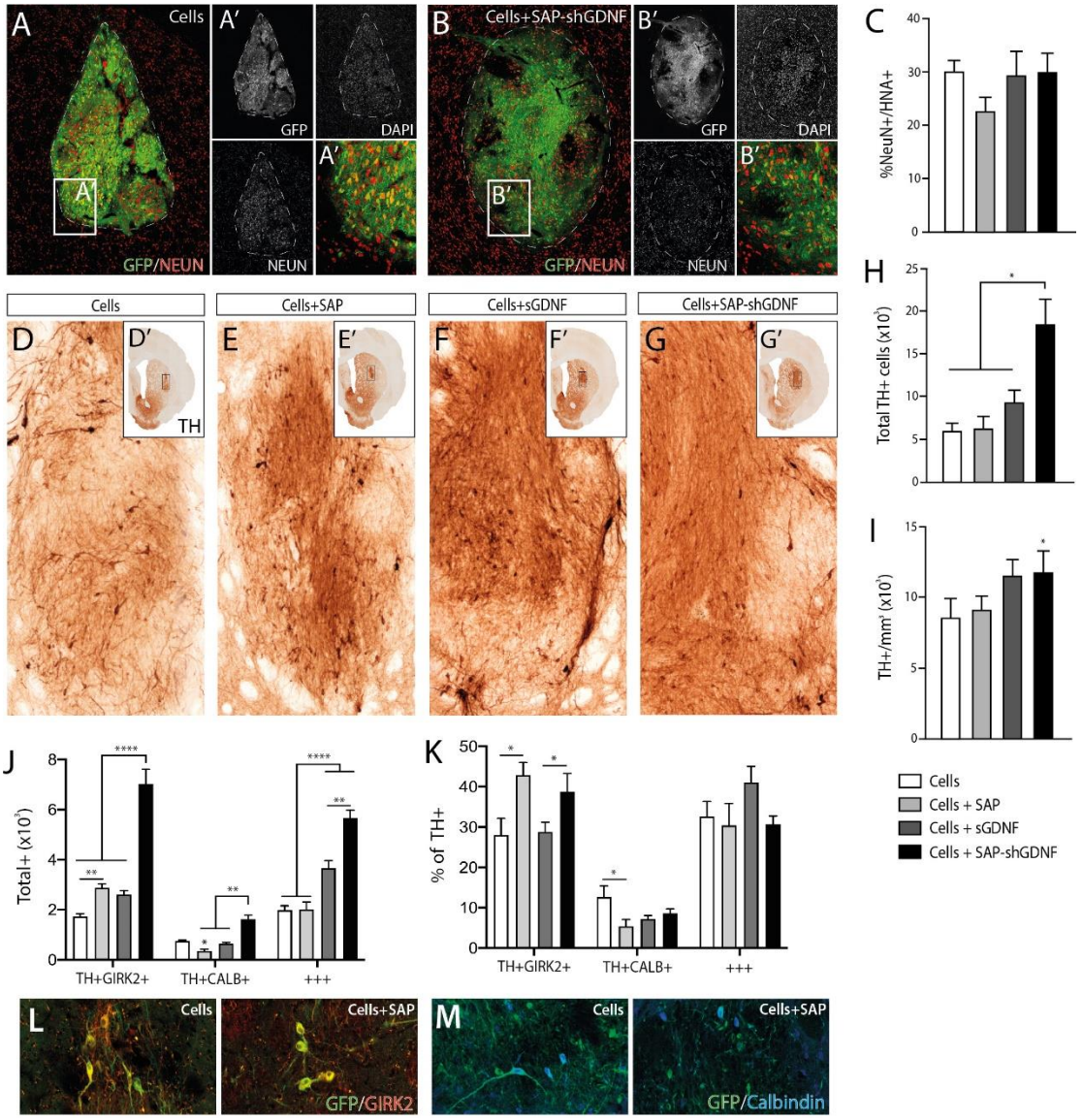

Figure 21. ***Functionalized scaffolds increase graft size, consequential DA neuron yield and bias A9-specification.*** *(A-C) Representative picture of NeuN+/HNA+ co-expression in a graft of (A) Cells alone and (B) Cells+SAP-shGDNF. (C) Approximately a third of the cells within all grafts adopted a mature neuronal phenotype, irrespective of the presence of the biomaterial and/or GDNF. (D-G) Representative picture of TH+ cells within grafts, at 24 weeks, showing that grafts in the presence of a GDNF functionalized SAP scaffold had increased TH+ cells. (H) Quantification of TH+ cells within the graft and (I) density of TH+ cells. (J) Grafts in the presence of a GDNF-functionalized SAP scaffold showed an increase in TH+/GIRK2+, TH+/CALB+ and TH+/GIRK2+/CALB+ cells, indicative of DA graft maturation. (K) Expressed as a proportion of TH+ cells, only grafts in the presence of the tissue-specific IKVAV SAP hydrogel showed a significant increase in the percentage of TH+/GIRK2+ (A9-like DA neurons), at the expense of*

*TH+/CALB+ (A10). (L-M) Representative photomicrographs of GIRK2, Calbindin (CALB+) and TH+ cells within a Cells- and Cells+SAP graft. Data represents Mean +SEM, n=5 Grafts/group. * p<0.05, ** p<0.01, **** p<0.0001.*

The presence of the hydrogel and/or GDNF had no impact on the capacity of the TH+ neurons within the grafts to acquire a mature fate, with >75% of all TH+ cells within the grafts, across all treatment groups, showing an GIRK2+ A9-like and/or Calbindin+ A10-like phenotype (data not shown). More detailed assessment of A9 and A10-like identity, however, reveal a significant shift in A9-fate in the presence of the SAP hydrogel (total TH+GIRK2+ cells: Cells, 1727 + 114; Cells + SAP, 2878 + 157; Cells + sGDNF, 2609 + 148; Cells + SAP-sh-GDNF, 7014 + 592). This increase in A9 fate acquisition was at the expensive of A10-like identity, with a reciprocal decrease Calbindin+TH+ cells (Cells: 750 + 32; Cells + SAP: 349 + 80; Cells + sGDNF, 637 + 63; Cells + SAP-sh-GDNF: 1618 + 157 TH+CALB+ cells), **Figure 21J-M**. Assessment of proportion of TH+ cells acquiring A9 or A10 fate revealed that this fate shift was specific to the presence of the SAP hydrogel, and not additive effects of sustained GDNF, as both Cells + SAP and Cells +SAP-shGDNF showed a significant increase in the proportion of GIRK2+ cells (43% and 38%, respectively), compared to grafts of Cells alone (28%), yet were not significant different from each other, **Figure 21K**.

4.4.4 Functionalized scaffolds support the integration of hPSC-derived VM graft

Following acute amphetamine administration, the upregulation of the intermediate early response gene, cFos, within DARPP32+ medium spiny neurons of the striatum has been shown to be an indirect measure of DA release, including from grafted DA neurons [113]. The density of cFos-immunoreactive cells within the striatum (adjacent to the graft) was assessed. Reflective of dopamine depletion within the striatum, ungrafted 6-OHDA lesioned animals showed a significant reduction in cFos, compared to the contralateral hemisphere of the brain, (**Figure 22 H, I**). All the animals in the presence of hPSC-derived VM grafts resulted in a significant increase in density of cFos immunoreactive levels compared to the lesion (ungrafted) brain. Moreover, animals receiving

grafts in the presence of the GDNF functionalised hydrogel (Cells + SAP-shGDNF) showed a trend for increased striatal cFOS+ cell density (**Figure 22 H, I**).

Finally, the capacity of the grafted neurons to innervate the host striatum was assessed. Reflective of the improvements in spontaneous motor function observed only in animals grafted with cells in the presence of GDNF-functionalised scaffolds (Cells + SAP-shGDNF) showed a significant increase in density of graft-derived human PSA-NCAM+ fibers (**Figure 22 A,D,F).** Surprisingly, no difference in the density of graft-derived human synaptophysin was observed, indicating that neither the presence of the SAP hydrogel or GDNF influenced synaptic maturity of the grafts **Figure 22 B**. Despite confirmation of ablation of the host midbrain neurons by TH histochemistry (data not shown) and significant motor deficits (**Figure 17B-C**), assessment of TH+ fiber density remains unable to discriminate between graft-derived DA fibers and what may be residual host TH+ fibers. Consequently, a more stringent assessment of graft-derived TH+ innervation was performed by assessment of density of co-localised human-specific synaptophysin (hSYP+) and TH+ puncta, specifically within the dorsolateral striatum - the target site for A9 DA neurons responsible for motor function. The synergy of the SAP hydrogel and sustained GDNF resulted in a significant (28%) increase in the percentage of TH+ puncta colocalised with hSYP, compared to Cells alone (**Figure 22 C,E,G**). Note that cell grafts in the absence of the SAP-shGDNF showed increased hSYP-immunoreactive puncta not colocalised with TH, indicative of increase non-DA synapses (**Figure 22 E**, arrowheads).

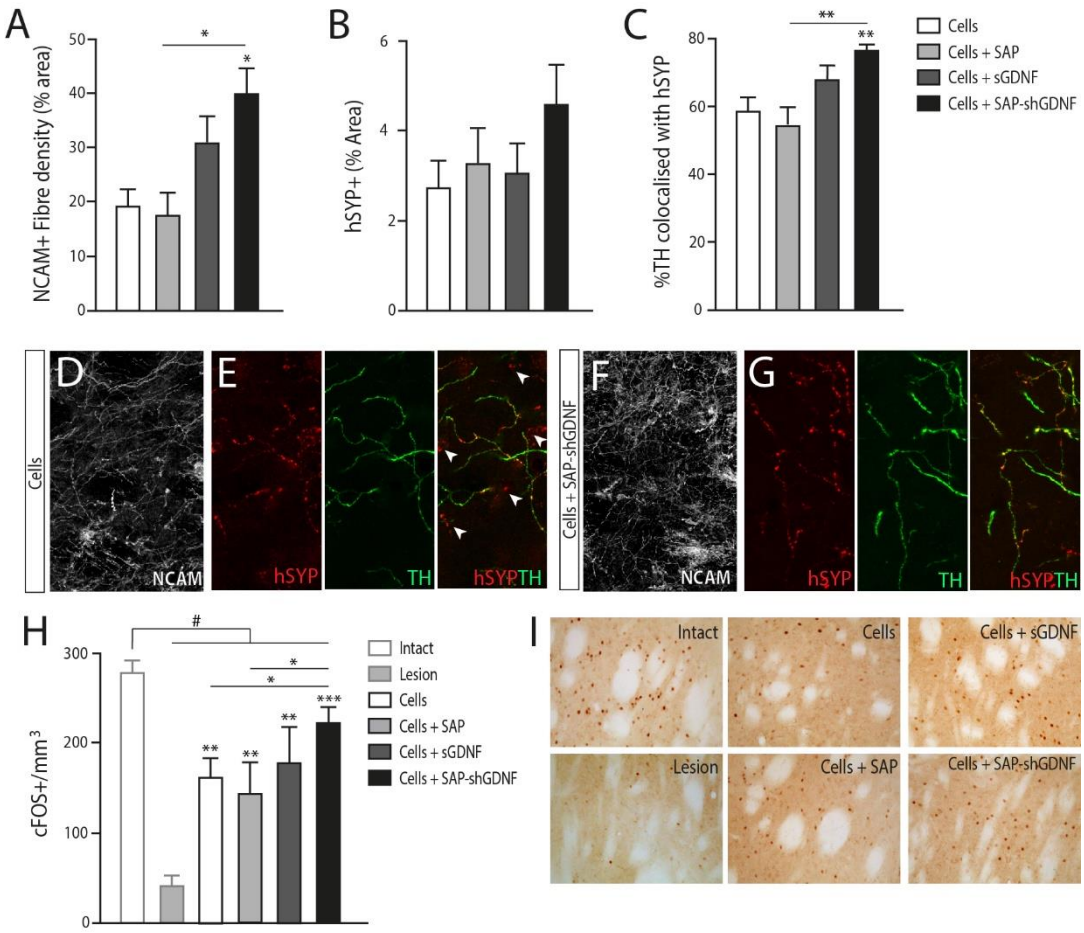

Figure 22. ***Functionalized scaffolds support the integration of hPSC-derived VM graft.*** *(A) Quantification of graft-derived human NCAM fiber density and (B) human synaptophysin (hSYP) within the host striatum. (C) Quantitative assessment of the proportion of TH immunoreactive puncta co-localised with hSYP within the host striatum, indicating that GDNF functionalized scaffolds promoted maturation of DA synapses. (D) Representative photomicrographs of NCAM-labeled graft fibers within the striatum of an animal grafted with cells alone, or cells+ SAPshGDNF. (F) Photomicrographs showing hSYP and TH labeling (plus merged images) taken from the host striatum of a rat grafted with Cells and, (G) Cells + SAP-shGDNF, noting the increased density of co-localised puncta in the present of the functionalized scaffold. (H) Quantification of c-FOS+ cells within the host brain revealed significant increases in activated cells in the dorsolateral striatum of grafted animals, irrespective of the presence of GDNF and or the SAP hydrogel. (I) Representative photomicrographs of cFOS-labeling in the host brain of*

*control (intact), Lesion, and grafted (+ SAP + GDNF) animals. Data represents Mean +SEM, n=5-6 Grafts/group. * p<0.05, ** p<0.01.*

4.5 Discussion

Biomaterials have the capacity to significantly improve cell transplantation for neural repair. Examined most extensively in their neural capacity to support cell transplants after stroke (see review – [70][114]), more recently functionalised natural and synthetic polymers, capable of recapitulating structural and biochemical elements of the extracellular matrix, have been shown to promote the survival, differentiation and functional integration of rodent fetal tissue grafts in models of PD [64][105], [111]. With hPSC rapidly advance towards the clinic for cell replacement therapy in PD patients there is an evident need to understand how biomaterials may also support and improve these graft outcomes. Recent efforts, utilising functionalised hyaluronic acid hydrogels, have attempted to support hPSC-derived DA progenitors/neurons during transplantation, yet showed notably small grafts with limited integration into the host tissue and functionality below standard levels, effects likely underpinned by the mature state of the implanted cells [115], [116]. Providing paradigm shifting evidence, we fabricated a shear-reversible neural tissue-specific laminin-based peptide hydrogel, sustaining the presentation of neurotrophic factor GDNF, to improve hPSC-derived DA graft outcomes. Only in animals receiving cell grafts in the presence of the GDNF-functionalised hydrogel were both induced and spontaneous motor deficits ameliorated. Underpinning these behavioural improvements were increased graft survival, DA fate acquisition and innervation.

Anoikis, a form of programmed cell death that occurs when anchorage-dependent cells are detached from their surrounding extracellular matrix, affects donor cells during their harvest from in vitro cultures (or dissociation of fetal tissue) as well as acutely post implantation if they fail to form local adhesions. While a range of soft hydrogels that gel in situ, have been trialled to protect cells against shear forces during implantation, and rebuild de novo tissue where necessary, their remains and underlying requirement for engineered scaffolds to provide cell adhesive matrix [117]. In this regard, the SAP hydrogels, presenting

a cell adhesive epitope (IKVAV) for laminin provided a tissue-specific biomimetic of the native neural ECM. In vitro, this functional epitope has been reported to promote neuronal adhesion and survival with greater efficiency than laminin protein itself, due to the high density of signals presented to the surface [118]. In vivo, IKVAV-presenting SAP hydrogels have been shown to promote the survival of hPSC-derived cortical progenitor graft survival [50][91], yet surprisingly in contrast had no impact on the survival of the present VM progenitors grafts. In addition to their necessary adhesive properties, ECM proteins (including laminins) also contribute to stem cell maintenance, differentiation and plasticity [62], roles that have been confirmed using IKVAV peptides for cultured neural progenitors [67] and transplanted cortical progenitors [50][91]. Within the present findings, IKVAV SAP hydrogels had no impact on the maturation of VM progenitors into postmitotic NeuN+ neurons or adoption of TH+ DA identity within grafts, however biased GIRK2+TH+ specification, at the expense of CALB+TH+ A10-like DA neurons. Likely underpinning these disparate outcomes is the complexity of the laminin family of proteins. Laminins are heterotrimeric proteins that contain an α-, β-, and a γ-chains, with the employed nomenclature describing the chains present (e.g. laminin-521 comprising of an α5, β2, and a γ1 subunit) – with a total of 15 laminin trimers identified to date. Interestingly, recent success in the directed differentiation of hPSC into VM DA progenitors/neurons has been underpinned by the culturing of cells on laminin substrates, with 4 specific laminins recognised in this capacity (Lam-111, Lam-421, Lam-511 and Lam-521). With hPSC-DA differentiation protocols varying between research groups differing success for the different laminins have been observed, indicating that identification of the necessary and optimal subunits remains to be determined and/or the existence of redundant roles. Added to this, recent deep-sequencing analysis of laminin subchain expression within the developing ventral midbrain has revealed the presence of α1, α4, α5, β1, β2 and γ1, and enriched mRNA for Lam-111, -411, -421, -511 and -521 [63]. Furthermore, culturing of rodent midbrain primary neurons on Lam521 promoted survival of DA neurons (by suppressing the cell death associated protein, PTEN), and promoted DA

differentiation (by increasing expression of genes critical for VM DA identity, inclusive of LMX1A and PITX3), superior to other VM present laminins [63].

In the present study the employed peptide sequence IKVAV (Ile-Lys-Val-Ala-Val) is derived from the α1 subchain, one of the most potent laminin subunits influencing adhesion, differentiation and plasticity. Whilst IKVAV/ α1 appeared to have no effect on survival or DA differentiation in the current context, the increase in A9 specification provides the first evidence, to our knowledge, of selectively enriching for this subpopulation DA neurons within hPSC-derived grafts. Recognising the importance of this population for alleviating motor symptoms [2], [82], may provide means for implanting fewer cells with more targeted function. Future efforts, exploring additional α subunits, such as α5, as well as inclusion of β and γ subchains epitopes, within composite peptide gels, the mimic naturally occurring, or artificially engineered, laminins may further enhance graft outcomes according to aforementioned mechanisms for VM progenitors, as observed in vitro.

Growth factor deprivation of progenitors isolated from the developing embryo or in vitro cultures is a major contributor to cell death during acute graft integration. Such observations justified a large body of work into the re-introduction of GDNF into the adult brain to support dopamine progenitor grafts [8], [35], [119]. Additional to the impact on graft survival is the role of GDNF in DA plasticity. In the present study, acute delivery of GDNF failed to influence survival or plasticity, a likely consequence of insufficient dose and/or duration of delivery, noting that former studies showing the benefit of recombinant protein delivery in vivo used repeated doses over weeks [29], or continual infusion [120]. In more recent years, viral delivery approaches have been employed to sustain GDNF level – targeted at slowing PD progression and supporting grafts [21][35] [32]. A key challenge of this approach is the inability to silence the transgene after graft integration, that can result in aberrant axonal growth and downregulation of DA synthesis associated genes in host and hPSC-derive DA grafts [121](Gantner et al., under review, submitted in August 2019). In support of fetal tissue graft studies [105] [64], we show prolonged delivery of GDNF from IKVAV-SAP promotes survival, increased TH+ DA neurons and plasticity of hPSC-derived VM progenitor grafts.

In vitro we showed an initial burst release of GDNF, followed by a delayed and sustained delivery beyond 28 days, with this biphasic delivery likely underpinning initial progenitor survival, and subsequent integration. The modest, but significant, effects on graft plasticity suggest that higher concentrations of GDNF, and/or the incorporation of other DA axonal growth promoting proteins, such as Wnt5a, may enhance graft plasticity and functional integration.

Vascularisation of solid tissue grafts is critical for their survival, yet surprisingly little attention has been paid to the vessel network within fetal or hPSC-derived VM progenitor grafts. We provide here the first characterisation of blood vessels within grafts, showing the presence of organised host-derived (HNA-) endothelial cells. Similar to observations that the presence of the biomaterial did not impede the capacity of transplanted cells to migrate within the host tissue (unchanged cell density within the graft core) nor extend axonal projections into the surrounding striatal target tissue, host-derived endothelial cells were capable of infiltrating into the graft core. The density of the vessel network across all graft conditions was significantly less than the host tissue, suggesting that delivery of additional trophic cues such as BDNF, VEGF and/or erythropoietin, targeted at promoting angiogenesis, may improve graft outcomes - as has been observed following SAP-sustained delivery of BDNF for hPSC-derived neural grafts in stroke [91].

Necessary for the success of all transplants is the hydrogel biocompatibility requirement. We have demonstrated that the immune response (CD11b and GFAP) was not significantly difference in the presence of the hydrogel, compared to grafts of cells alone, suggesting compatibility. However, the animals used in this chapter were immunocompromised and further assessments into non-compromised animals will reveal the true potential of these scaffolds in this regard. Additional advantages of working with SAP hydrogels, by comparison to many other tissue engineering scaffolds, is their degradation into predictable metabolites, their reproducibility in synthesis (with no batch variability), long shelf life, and cost effectiveness; all features that will be important for future clinical application.

Taken together, these findings provide the first convincing evidence for a functionalised, tissue specific hydrogel to improve the survival, differentiation and integration of hPSC-derived DA progenitor grafts in an animal model of PD. These findings highlight that additional efforts, to incorporate functionalised biomaterials to influence the donor cells and host tissue should be considered as the filed moves towards the clinic. While here we present findings for a laminin α1 subchain peptide hydrogel, it provide the impetus that greater attention to the ECM should be made when grafting cells, as well as the controlled delivery of additional/alternative proteins targeted at neuroprotection, plasticity and even vascularisation, to ensure maximal function benefits can be obtained from grafted progenitors – targeted not only for cell replacement therapy in Parkinson's disease, but other conditions were cell transplantation presents a therapeutically viable option.

Chapter 5 - Transcriptional profiling of xenogeneic transplants: a case study examining human pluripotent stem cell-derived grafts in the rodent brain

5.1 Abstract

Our increasing ability to fate restrict human pluripotent stem cells into defined lineages makes them a valuable resource for transplantation targeted at tissue repair. Despite progress in differentiation protocols and transplantation approaches, our ability to profile xenografts (notably human grafts in animal models) is limited largely to low throughput immunohistochemical analysis, and often restricted by the availability of appropriate antibodies against key phenotypic markers. Added to this, transcriptomic and proteomic profiling of xenografts remains hindered by our inability to easily isolate the graft from the surrounding host tissue. Here a novel approach is described that enables standardised and rapid characterisation of xenografts. The methodology employs bulk tissue dissection, inclusive of the graft and surrounding host tissue, and utilises differences in the RNA sequences between the species to discriminate the xenograft from host gene expression -using either qPCR or whole RNAseq. To demonstrate and validate this approach, grafts of undifferentiated human stem cells and neural progenitors in the rodent brain were assessed. Xenograft-specific qPCR provided sensitive detection of proliferative cells and identified germ layer markers across the graft types. Grafts derived from neural progenitors showed characteristic lineage specific neural gene expression that matured with time, including phenotypic markers for which reliable antibodies are not available. Xenograft-specific RNAseq expanded this approach, profiling the complete transcriptome of the transplant. The profile allowed the identification of novel gene expression and an unbiased characterisation of graft composition. Such specific profiling provides a valuable tool for the analysis of xenografts and will be especially crucial for pre-clinical characterisation of grafts and batch testing of therapeutic cell preparations to ensure maximal safety and functional predictability of transplants prior to translation.

5.2 Introduction

The use of embryonic [18] and pluripotent stem cells [19], differentiated into tissue-specific subtypes has raised much hope for their use in regenerative medicine. The ability to differentiate PSCs into a defined cell subtype population opens possibilities for treating chronic or acute disorders by transplantation. For example, recently, studies have been focusing on using hPSC differentiated into islet cells to treat diabetes and hPSC-derived dopamine neurons to replace the cells lost for Parkinson's disease [55].

However, before moving towards clinical application, it is necessary to know and understand what the graft composition is, certifying safety and functionality. In Parkinson's disease, advanced differentiation protocols result in a high yield of correctly specified dopamine progenitors *in vitro* [21][22][23][122], suitable for transplantation. Nonetheless, when transplanted and analysed after extended periods of time (> 6 months, a timeframe necessary for functional integration of the new DA neurons), only a small fraction of the total cells within the graft actually became dopaminergic neurons [25][37][43][44].

Such outcomes naturally lead to question about safety. What are the unknown cell types present in the graft? Could these cells overgrow? And what impact could these uncharacterized populations have on the transplant recipient and graft function? Striving to answer these questions, histochemical assessments have confirmed a predominantly neural origin to these VM progenitor grafts [21][43] but, detailed analysis has been limited by antibody availability, selectivity of antibodies to identify species-specific expression from the host (i.e. human and not host rodent cells) and there is the need to know what one is looking for (which is feasible, for example, when screening for neuronal subpopulations, but more challenging when identifying cells that are of 'off-target origin. Consequently, histochemical approaches have resulted in graft composition remaining largely unknown.

As an alternative, techniques of transcriptionally profiling the grafts to understand gene expression have been developed, for example, the use of reporter cell lines for donor tissue that enable the selective isolation of the graft tissue from the host,

using either gross tissue dissection or by laser capture. Whilst a feasible approach for encapsulated and largely contained graft tissue, such as teratomas, those transplants that integrate into the host (such as neural transplants) are significantly more challenging to assess. In these instances one either elects to isolate the graft core to eliminate the host contaminant, yet in this way fails to assess cells at the graft-host boundary that, in the context of VM progenitor grafts are often the most mature and rich in DA neurons or, perform a broader isolation of the graft, simultaneously removing a proportion of host-derived cells. Added to this, laser dissection approaches are often labour intensive, and the tissue processing challenging to ensure quality RNA is yielded. A related approach in the quest to characterise grafts is single cells analysis [40][41][42]. This similarly requiring isolation of single cells by laser dissection or alternatively dissociation of the tissue and cell sorting techniques to extract the graft cells – yet matured graft and host tissue, particularly neural, poorly survive the dissociation and sorting processes. Furthermore, just a small fraction of the graft can be assessed. Within VM progenitors transplants not uncommonly yielding grafts of 500,000-1 million cells, the labour intensive assessment of 2000 cells in fact represents just miniscule fraction of the graft [43][25].

Circumventing these challenges, we have developed a methodology that employs bulk tissue dissection, containing the graft and the host tissue, and a selective detection process to discriminate the graft genome within a mixed graft-host tissue pool. This technique is based on identifying base pair sequences that differ between the host and graft species, resulting in a species-specific qPCR or whole RNAseq. We demonstrate and validate this new technique by comparing different transplant populations of human cells in the rodent brain.

5.3 Materials and Methods

5.3.1 Cell culture, differentiation and Sorting

Mouse RNA was extracted from a mixed pool of undifferentiated mouse pluripotent stem cells (E14TG2a obtained from ATCC, USA) as well as cells from diverse maturation phases (from ecto, meso and endoderm germ line lineages)

– harvested from whole mouse embryos (embryonic day (E) 9.5 and E12.5), as well as maturing ventral midbrain tissue (isolated at E10.5, E12.5, E14.5 and postnatal day 1 pups).

Human RNA, containing mixed cell populations, was generated by a mix of undifferentiated human pluripotent stem cell together with embryoid bodies (consisting of all germ layers), and varying maturation stages of ventral midbrain neural progenitors and mature dopamine neurons – day 11, day 25, day 40 (derived from differentiated hESC, as described below).

The H9 human embryonic stem cell line, expressing a green fluorescent reporter under the LMX1A promoter (H9 LMX1A-GFP) [23], was expanded as an undifferentiated population on laminin-521 (5ug/ml; StemCell Technologies) in TeSR2 media (STEMCELL Technologies) supplemented with 0.4% Penicillin-Streptomycin. The pluripotency of the cell line was confirmed by morphology and the co-expression of pluripotency genes SOX2 (data not shown) and OCT4 **Figure 23 A-B**. Undifferentiated hPSCs targeted for transplantation were isolated by Accutase treatment and resuspended in maturation media at a density of 10,000 cells/µL.

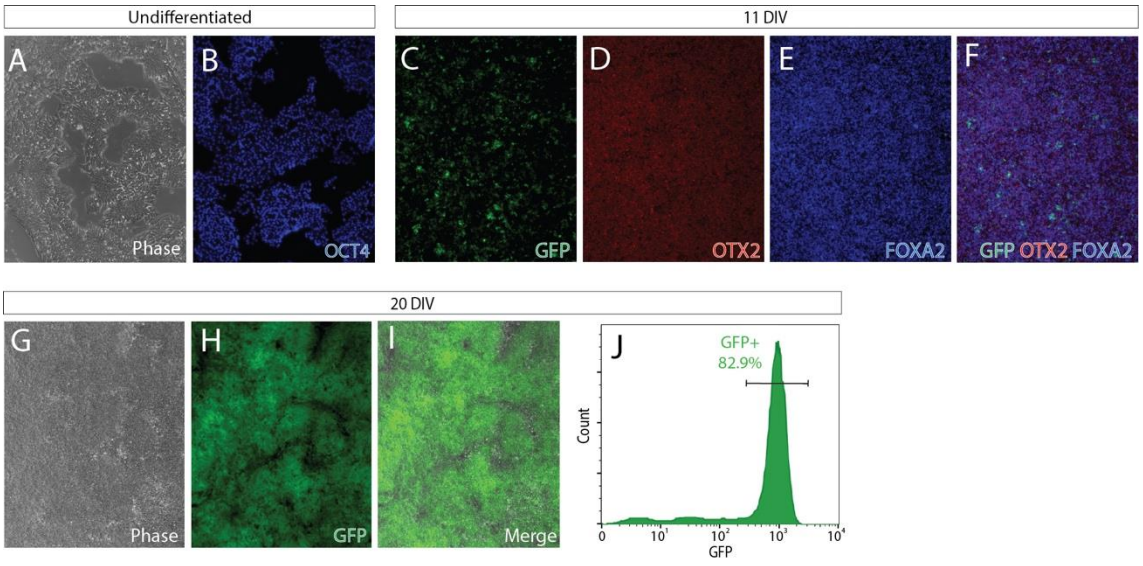

Figure 23. ***Characterization of undifferentiated and DAn progenitors in vitro. (A)*** *Phase contrast showing the morphology of undifferentiated human embryonic stem cells* ***(B)*** *and their expression of pluripotent gene OCT4.* ***(C)*** *VM specification of H9-LMX1A-GFP hESCs was confirmed at 11 days in vitro -by the co-expression of the GFP,* ***(D)***

*midbrain-forebrain gene OTX2 and **(E)** ventral identity transgene FOXA2. **(F)** Merged image of LMX1A-GFP, OTX2 and FOXA2 illustrating that most cells showed co-labeling, indicative VM Dan pattern. **(G)** Phase contrast and **(H)** GFP labeling **(I)** and merge, of day 20 VM progenitor cultures used for isolation of LMX1A-expressing cells for transplantation. **(J)** FACS plot showing >80% of cells in culture expressed GFP (LMX1A-GFP) at 20DIV.*

To obtain a pool of purified neural progenitors of known origin, hPSCs were differentiated to a ventral midbrain fate, with correctly specified cells isolated by fluorescent activated cell sorting (FACS) for the GFP reporter gene, LMX1A. To achieve this, cells were differentiated according to previously described methods [23]. In brief, hPSCs were seeded on Laminin-521 (5ug/ml; StemCell Technologies) in the presence of dual SMAD inhibitors (SB431542, 10μM, 0-5 days in vitro (DIV), R&D systems; and LDN193189, 200nM, 0-11DIV, Stemgent) to promote neural induction. Sonic hedgehog C25II (100ng/ml; R&D systems) and Purmorphamine (2μM; Stemgent) were added into the media from day 1-7DIV to promote ventralisation, and the caudalizing by the presence of Wnt agonist, CHIR 99021 (3μM; Stemgent, 3-11DIV). From 13DIV, cells were cultured in a 'maturation media' consisting of NBB27 supplemented with GDNF (20ng/ml; R&D systems), BDNF (20ng/ml, R&D system), TGFβ3 (1 ng/ml; PeproTech), DAPT (10 μM, Sigma-Aldrich), ascorbic acid (200nM; Sigma- Aldrich) and dibutyryl cAMP (0.05mM; Tocris Bioscience). At 21 DIV differentiating cultures were dissociated in Accutase (Innovative Cell Technologies) to a single-cell suspension and fluorescent activated cell sorting (FACS) performed on a MoFlo cell sorter (Beckman Coulter, MoFlo to isolate the LMX1A-GFP expressing progenitors, as described by Luzy et al., minor revisions submitted 25 June 2019). The co-expression of OTX2, FOXA2 and LMX1A (LMX1A-GFP+) verified the generation of neural progenitors (of ventral midbrain identity) **Figure 23 C-F**. As previously described, >95% of GFP+ cells immunolabeled for both FOXA2 and OTX2 (ventral floorplate marker and forebrain-midbrain marker, respectively), demonstrating that isolation of this GFP fraction (>80% of cells, Supplementary **Figure 23 G-J**) could enrich the specification of ventral midbrain progenitors from the heterogenous differentiated cultures by fluorescent activated cell sorting. The

FACS-isolated cell fraction was resuspended at 100,000 cells/μL in maturation media containing ROCK inhibitor (Y27632, 40μM, Sigma) and stored on ice until the time of implantation.

5.3.2 Cell transplantation

All animal procedures were conducted in agreement with the Australian National Health and Medical Research Council's published Code of Practice for the Use of Animals in Research, and experiments approved by The Florey Institute of Neuroscience and Mental Health Animal Ethics committee. Surgeries were performed on 30 athymic (Foxn1nu) nude mice under 2% isofluorane anaesthesia. Cells (1ul containing 100,000 cells) were stereotaxically injected into the brains of mice at the following co-ordinates relative to bregma: 0.5mm anterior, 2.0mm lateral and 3.0mm below the surface of the dura), as previously described [33]. Transplant groups (n=10/group) included: (1) undifferentiated hPSC implanted for a period of 1month; (2) LMX1A-GFP+ ventral midbrain progenitors, implanted for 1month; and (3) LMX1A-GFP+ ventral midbrain progenitors, implanted and left to mature for 6 months.

5.3.3 Tissue Processing and histochemistry

After the prescribed period of graft survival (1 or 6 months), half the animals from each group (n=5/group) were killed for immunohistochemical analysis. Animals received an overdose of sodium pentobarbitone (100mg/kg) and were transcardially perfused with Tyrode solution followed by 4% paraformaldehyde. The brains were then isolated and coronally sectioned (40μm; 12 series) on a freezing microtome (Leica). Immunohistochemistry was performed on fixed cell cultures of undifferentiated and VM differentiated hPSCs (4% paraformaldehyde for 10mins) or on brain sections as previously described [50]. Primary antibodies and dilutions were as follows: Goat anti-FOXA2 (1:200; Santa Cruz), chicken anti-GFP (1:1,000; Abcam), rabbit anti-GFP (1:20,000; Abcam), mouse anti-human nuclear antigen (HNA, 1:300; Millipore), rabbit anti-KI67 (1:1,000; ThermoFisher), mouse anti- NESTIN (1:200; Millipore), mouse anti-OCT4 (1:100, Santa Cruz), rabbit anti-OTX2 (1:4000; Millipore), goat anti-SOX2 (1:200; R&D), sheep anti-tyrosine hydroxylase (TH, 1:800, Pelfreeze), rabbit anti-TH (1:1,000, Pelfreeze),

mouse anti-myelin basic protein (MBP, 1:200, Millipore), rabbit anti-OLIG1 (1:200, Millipore), rabbit anti- Glial fibrillary acidic protein (GFAP, 1:800, DAKO), rabbit anti-Neuroligin3 (NLGN3, 1:200, synaptic Systems), goat anti-cFOS (1:1000, Santa Cruz), mouse ant- synaptophysin (SYN, 1:1000, Enzo life sciences) . Secondary antibodies for direct detection were used at a dilution of 1:200—DyLight 488, 549 or 649 conjugated donkey anti-mouse, anti-chicken, anti-rabbit or anti-rat (Jackson ImmunoResearch). All cultures and brain slices were stained with 4',6-diamidino-2- phenylindole (DAPI, 1ug/ml; Sigma Aldrich) to highlight total cell nuclei.

Fluorescence images, from in vitro cultures and brain sections containing the graft, were captured using a Zeiss Axio Observer Z.1 epifluorescence. Quantitative assessment of the total number of HNA+, KI67+, GFP+ and TH+ cells were counted from the images captured at 20X magnification. The density of Nestin-labeling (%immunoreactive pixels) was assessed from tiled images taken of the grafts, captured at 20X magnification, and analysed using ImageJ software.

5.3.4 RNA Isolation and qPCR

The remaining animals (n=5/group) were killed by cervical dislocation, the brains removed and the whole striatum (containing the transplant) grossly dissected and snap frozen. Total RNA was extracted from the frozen tissue using a TissueLyser LT (Qiagen) and the RNeasy Mini Kit (Qiagen, including DNase treatment). The integrity and yield of RNA was assessed using a Nanodrop One Spectrophotometer (ThermoFisher Scientific) and verified using a Qubit (ThermoFisher Scientific) and Tapestation (Agilent). The resultant RNA was analysed by qPCR or RNAseq, **Figure 24.**

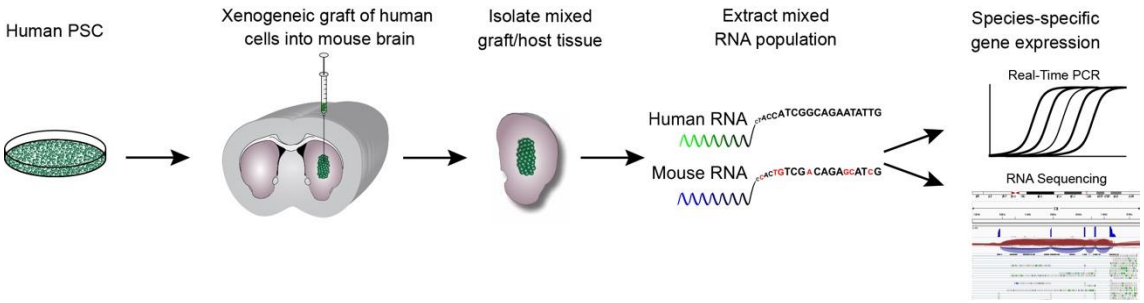

Figure 24. ***Experimental design.*** *Schematic illustrating the experiment paradigm. Human pluripotent stem cells (undifferentiated or VM differentiated) were transplanted into the brain of nude mice. Striatal tissue containing both the human graft and surrounding host mouse tissue was dissected, and the RNA isolated to produce a mixed species RNA population. Xenograft gene expression was discriminated from the host using species-specific primers for qPCR to profile individual genes, or by RNA sequencing to profile the whole transcriptome.*

Species-specific primers were designed using Primer 3 [75], aimed at containing a minimum of 5 base pair (bp) mismatches between graft and host, or 2 mismatches in the 5 bp at the 3` end between species. Primers were targeted manually to regions of dis-similarity. The first step was to blast the nucleotides of the paralogue genes of interest, we chose the platforms (i) NCBI (https://blast.ncbi.nlm.nih.gov/Blast.cgi?PAGE_TYPE=BlastSearch) or (ii) ENSEMBL (https://asia.ensembl.org/Homo_sapiens/Tools/Blast), the later used in cases where homology between the genes was particularly high and led us to target UTR regions. The mismatched nucleotides and indels between the two transcripts were then highlights. Subsequently the Primer3web software (http://bioinfo.ut.ee/primer3/) was used to design the primer at a specific region of interest (region containing the highest mismatch), adding the symbol “-" (this symbol is defined by the website protocol to force the primer design within this specific region). After designing the primers, we assessed their specificity by Primer-BLAST and selecting both the xenograft and host species (Homo sapiens and Mus musculus, respectively in the present context) under organism in the “Primer Pair Specificity Checking Parameters.” This identified primers specific only to the xenograft species (i.e. human). All xenograft-specific primers used in this study are listed in **Table 3**.

Gene	Forward Primer	Reverse Primer	Fold Specificity
Proliferation & Trilineage Markers			
MKi67	GCCTCCTAATACGCCTCTCA	CCTGATGGTTGAGGCTGTTC	2845005
AFP	CCCAGTTTGTTCAAGAAGCCA	ACACCCTGAAGACTGTTCATCT	9026
GATA6	AGAAGATGGAAGGGAAGGGC	GTCCTAGTCCTGGCTTCTGG	560
BRACHY	CGATCCTGGGTGTGCGTAAC	GCCGCAGTAGTAGTGCTGTT	4770
COL2A1	GCCGGTCTGCTTCTTGTAAA	GAGGGTGGGATGAATGGACA	1131652
NCAM1	TCCAGGCCAGGCAGAATATT	TCATCGTCTTCCTCTTGCTC	535304
NES	CTGGAGCAGGAGAAACAGGG	CTGAGGGAAGTCTTGGAGCC	1668361
Immature Dopaminergic Markers			
LMX1A	ATGAACCCCTACACGGCTCT	TAAGGGTGCATGTGGTCTCC	1916443
TH	GAGGCCATCATGGTAAGAGGG	CTGCCTGCGCCCAATGAAC	38699
OTX2	AGCTGCACTGAAACTTTACGA	CCAATGTCTCTTTACTGCTAGGC	2375830
EN1	AAGAAATAGCCAAGTGTCTCCA	GTCTGGCCTGGATCGCTC	3281
NEUROG2	CCCCTTTCTCTTTAACGCCG	ATGTAGAAGCAAAGGTGAAGAGA	3929
NR4A2	GGTGTCCGGGTTCCCTTC	TCCGCGTCTCTCTTCATTCA	81245
PITX3	CAGCCAACCTTAGTCCGTG	CGGAGGCTGTGAATCGTTG	4421
Mature Dopaminergic Markers			
DAT1	TTCCTCAACTCCCAGTGTGC	CCGTTCTGCTCCTTGACAAG	9027
VMAT2	ACAGCTAGTTCTCTCAAGTGTAG	GCCAACCAGATAACATGTTAACA	443938
GIRK2	TGCGGATTTCATGACGTCTC	TGGAATGAAGTGGGGGAAAGATAA	31433
CALB1	TCCAACAAACTTACTGTCAGAGA	CTAGACACCAGGATATGCAGTAT	129267
SYB2	TCTGTGCCATCATCGTGGTAG	CAGGCTTGGGACACATCGAG	1514070
Non-Dopaminergic Markers			
GFAP	TCTAAGGCCGAAGAAGGGTC	TTCCTCAGCGACTAAAGGCA	26068
EAAT1	GCTGGGGAATTCACCTCGTT	CCCCATCTTGGGCTCTTCTC	506428
OLIG1	AGACCAGCTGTTTGGAGAGC	GATGCAAGGCGGTTGGTTTT	11585
MBP	GAGGCACGGATCCAAGTACC	TTGTACATGTTGCACAGCCC	2062
Guidance Cues			
IGSF8	TGCCCTGGACACCCTATTTG	GGGATCACCGTTTTCGAAGC	558036
NLGN3	CCAACTCTCTCTGTGTCCGT	GCAAAACCCAGATCAGACCTG	218913
SEMA5A	CTGGACAAGTACGACTCGGT	GGAACTGGGGATTTACAAGAAGC	288557
Housekeeping Genes			
PSMB4	TGCACTTTACAGAGGTCCAATC	CGTAGGATCCCAGCATGTCT	5235877
MTHFD1	CAGTAGTGTGATCCCCTGGC	GCCTTTATTAGTCCGCTGCC	2005
CHMP2A	AGATGAGCTGTCGAACCTCC	GCAGGTTCTTAAGCCGTTCC	428816
HPTR1	GCTGAGGATTTGGAAAGGGTG	GCTACAATGTGATGGCCTCC	2201415

Table 3. Table of human xenograft-specific primers designed for the present study. Nucleotide bases shown in red correspond to mismatches between the human and mouse RNA sequence, and underlined bases represent the presence of insertions or deletions. Species-specific primers were optimally designed to contain a minimum of 5 base pair (bp) mismatches between graft and host, or 2 mismatches in the 5 bp at the 3` end between species.

First-strand reverse transcription of RNA into cDNA was conducted using the SuperScript® VILO cDNA Synthesis Kit (Invitrogen) according to the

manufacturer's recommendations. Real-time qPCR was carried out on 25ng of cDNA using the SYBR GreenER™ qPCR SuperMix Universal (Invitrogen) and run on a Rotor-Gene 6000 (Qiagen). To control for the size of the xenograft, a xenograft-specific reference (housekeeping) gene was identified. PSMB4, MTHFD1, CHMP2A and HPRT1 were tested and PSMB4 selected as the optimal housekeeping gene due to its high specificity and stable expression across the 3 graft types, **Figure 25**. All qPCR data was analysed using the ΔΔCT method [76], using the xenograft-specific reference gene and expressed relative to the Undifferentiated grafts. Five independent biological replicates were analysed per group.

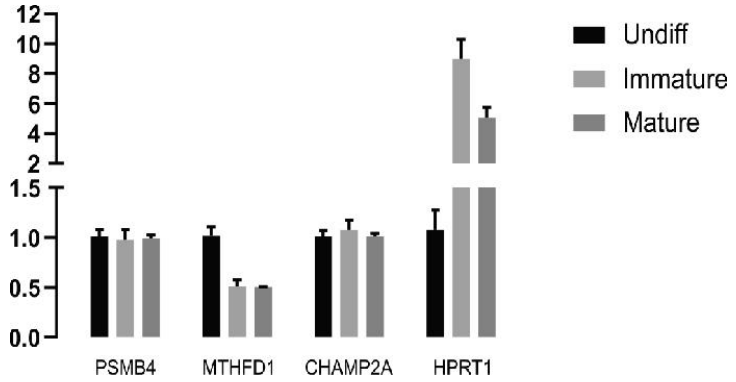

Figure 25. Screening of xenograft-specific reference (housekeeping) genes identified PSMB4 as having high specificity and stable expression across the 3 graft types assessed. N=3/group.

5.3.5 RNA sequencing

cDNA libraries (containing graft and host RNA) were prepared using the TruSeq stranded mRNA sample preparation kit (Illumina). For Sequencing the final cDNA concentration of each sample was adjusted to generate a target of 20 million xenograft-specific reads using the percentage xenograft RNA calculated from the qPCR data. Note, due to the low percentage of xenograft RNA in the Immature grafts, 5.5 million reads were targeted. Libraries were subject to paired-end, 75 bp sequencing on an Illumina HiSeq 2000 platform (Illumina) with 3 independent biological replicates analysed per group.

Analysis was conducted on the Galaxy web platform [77] using the Galaxy Australia server, and using Bioconductor [78] in the statistical analysis environment R (https://www.R-project.org/). Alignment to the human genome (Hg38) was performed using HISAT2 (2.0.3.3). Paired concordant reads (reads aligned with human genome) were then mapped against the mouse reference genome (mm10). All reads that aligned to both the human and mouse genome were discarded, accounting for an average of 5% of human reads.

Read counts for each gene were generated using HTSeq-count (0.6.1) on union mode [79]. Differential expression analysis and Principal Component Analysis was conducted with DeSeq2 (2.11.38) [80]. Expression heat maps and unsupervised clustering were performed on log transformed row scaled expression values using the gplots package in R [76]. Gene ontology enrichment analysis on biological process was performed using DAVID gene ontology browser [123]. Lists of human transcription factors and axon guidance cues and receptors were sourced from the HumanTFDB [124] and the KEGG PATHWAY Database [125] (hsa04360, Homo sapiens Axon guidance), respectively. The RNAseq data generated from this study has been deposited in NCBI's Gene Expression Omnibus and are accessible through GEO Series accession number GSE126804.

5.3.6 Statistical Analysis

All data are presented as mean + SEM. Statistical tests employed (inclusive of one-way ANOVA and student t-tests) are stated in figure legends. Alpha levels of $p<0.05$ were considered significant with all statistical analysis performed using GraphPad Prism. *$p < 0.05$, **$p < 0.01$, ***$p < 0.001$ and ****$p < 0.0001$.

5.4 Results

5.4.1 Design and validation of xenograft-specific primers for qPCR

To amplify xenograft-specific sequences by qPCR, we designed primers targeting regions that had the greatest difference between the 2 species. More specifically, the primers targeted a region of RNA containing a minimum of 5bp

mismatches between xenograft and host, or 2 mismatches within the final 5 bp at the 3` end of the primer, for example, the LMX1A and TH forward primer shown in **Table 3**.

The specificity of the primer for the human xenograft transcript was confirmed using *in vitro* pools of mouse or human cells known to express the genes of interest. A total of 30 primers were designed and tested (**Table 3**). The primer specificity for xenograft transcripts (over mouse) ranged from 500 to 10 million times greater, with a median specificity of 174,000 (**Table 3 and Figure 26**). Adopting an arbitrary cut-off of 1000-times greater expression within the human than mouse pool, the majority of primers designed (29/30) were classified as specific.

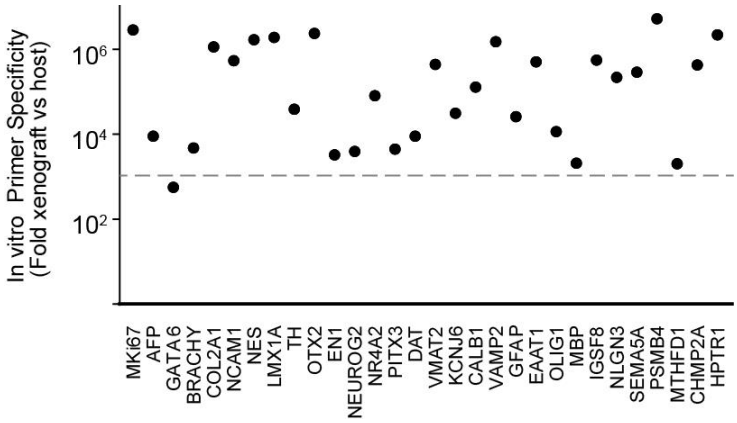

Figure 26. Graph of the specificity of xenograft-specific primers for human transcript relative to rodent host transcript in vitro showing an average specificity of 5,000 times that of the host (also represented numerically 'fold specificity' in panel.

After successful in vitro validation, next we tested the capacity of the primers to discriminate between xenograft and host transcripts within in vivo samples. In order to do so, we transplanted human stem cells in the striatum of immune-compromised athymic mice and assessed the ability for the designed primers to detect the expression of four selected constitutive genes expressed in the graft (PSMB4, MTHFD, CHMP2A and HPRT1), compared to an ungrafted tissue (mouse striatal tissue containing no xenograft – **Figure 27A**). Results showed that the 4 primers were capable of detecting significantly elevated expression of

the graft transcript compared to the host only tissue (PSMB4 10,349x; MTHFD 769x; CHMP2A 2,775x and HPRT1 1,726x times greater expression).

To evaluate if the species-specific primers could rapidly estimate a graft size, we transplanted a known number of human-derived neural progenitors (10,000; 30,000; 100,000 or 300,000 cells) into the mouse brain and analysed the expression of the house keeping gene, PSMB4, after two weeks. The human xenograft-specific PSMB4 primer enable predictions of graft size, while a non-specific primer (targeting the mouse and human PSMB4 gene) enabled assessment of the total amount of RNA within the isolated tissue. Using this approach we could express graft RNA as a proportion of total RNA, showing that xenograft RNA constituted 0.8% ± 0.60 of total RNA for grafts of 10,000 cells, 6.5% ± 2.48 (for grafts of 30,000 cells), 12.8% ± 1.78 (100,000 cells) and 18.1% ± 3.31 (300,000 cells) of the RNA population (**Figure 27 B**). This estimate of xenograft RNA showed a significant correlation with the number of cells implanted (r2 =0.78), demonstrating the capacity of the method to estimate graft size.

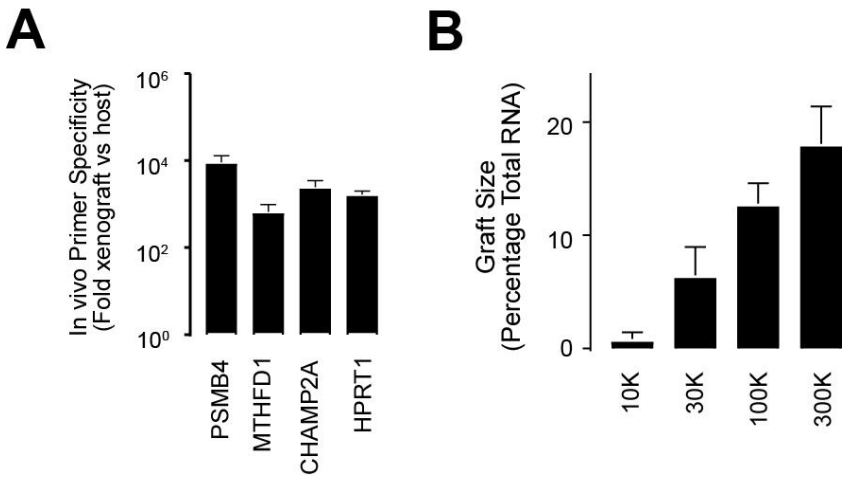

Figure 27. (A) Graph representing the in vivo specificity of xenograft-specific primers for 4 constitutively expressed transcripts, showing an average specificity of ~4,000 times greater in the transplanted, compared to untransplanted host. (B) Estimation of xenograft size using a xenograft-specific primer, PSMB4, showed a significant correlation (r2 =0.78) with actual number of cells implanted into the host. Data represents mean ± SEM, n=4.

5.4.2 Characterisation of xenografts using species-specific qPCR

In order to demonstrate and validate the usefulness of the species-specific transcriptional profiling approach, we subsequently compared the RNA from 3 different xenografts that we could anticipate composition and some gene expressions. Grafts for analysis were generated from (i) transplants of undifferentiated pluripotent stem cells (referred to as the 'Undifferentiated' grafts), analysed 1 month after implantation. These grafts were anticipated to contain highly proliferative populations and the presence of cells from all 3 germ layers (ecto-, endo- and mesoderm) (ii) Transplants of hPSC-derived ventral midbrain progenitors analysed 1 month after implantation (referred to as 'Immature Neuronal' grafts), and anticipated to show Immature/neuronal progenitor neurons gene expression and, (iii) Grafts derived from the transplantation of hPSC-derived ventral midbrain progenitors, analysed after 5 months (referred to as 'Mature Neuronal' grafts, and anticipated to contain mature neuronal expression). In parallel, separate cohort of animals, with the same 3 grafts types (undifferentiated, Immature and Mature Neuronal) were taken for histological assessment, to verify gene expression findings.

5.4.2.1 Graft Size

Using a human specific antibody (human nuclear antigen, HNA) to delineate the graft core and allow cell counts, we were able to quantify the xenograft size. HNA immunostaining showed the undifferentiated grafts were large and expansive (7.0 ± 3.5mm3 containing 2.03 x 10^6 ± 0.43 x 10^6 cells), Immature Neuronal grafts were small and discrete (0.43 ± 0.07mm^3 with 0.49 x 10^5 ± 0.11 x 10^5 cells) and the Mature Neuronal grafts were of moderate size (2.4 ± 0.25mm^3 containing 1.51 x 10^5 ± 0.31 x 10^5), (**Figure 28A-C**). Reflective of the histological results, the transcriptional estimation of graft size (as described previously) measured the proportion of xenograft RNA at 33.0 ± 8.93% (of total RNA) for the Undifferentiated grafts, 1.8 ± 0.40% in the Immature Neuronal grafts and 9.2 ± 0.91% in the Mature Neuronal grafts (**Figure 28D,E**).

5.4.2.2 Graft composition

Critical in the advancement of any transplantation-based therapy is the safety of the donor cells and a reassurance of elimination of proliferative cells, or reduction to a low proportion, prior to implantation. Hence, an assessment of Ki67+ (a protein expressed in all phases of the active cell cycle) was performed. As anticipated, cell counts of Ki67-immunoreactive cells in the grafts (Ki67+/HNA+) showed a greater population of dividing cells in the Undifferentiated grafts (9.5% ± 1.0), that was significantly reduced to 0.74% ± 0.16 in Immature Neuronal grafts, and even more in the Matured neuronal grafts, to just 0.28% ± 0.06 of total cells (**Figure 28F**). In agreement with the immunostaining results, the gene expression (using our xenograft-specific qPCR, expressed relative to the Undifferentiated grafts), showed that the expression in the Immature neuronal grafts was reduced to 0.11 ± 0.02-fold, and to 0.05 ± 0.01-fold in Mature neuronal grafts (**Figure 28G**). These results highlight the xenograft-specific qPCR ability to detect rare cell populations within a tissue.

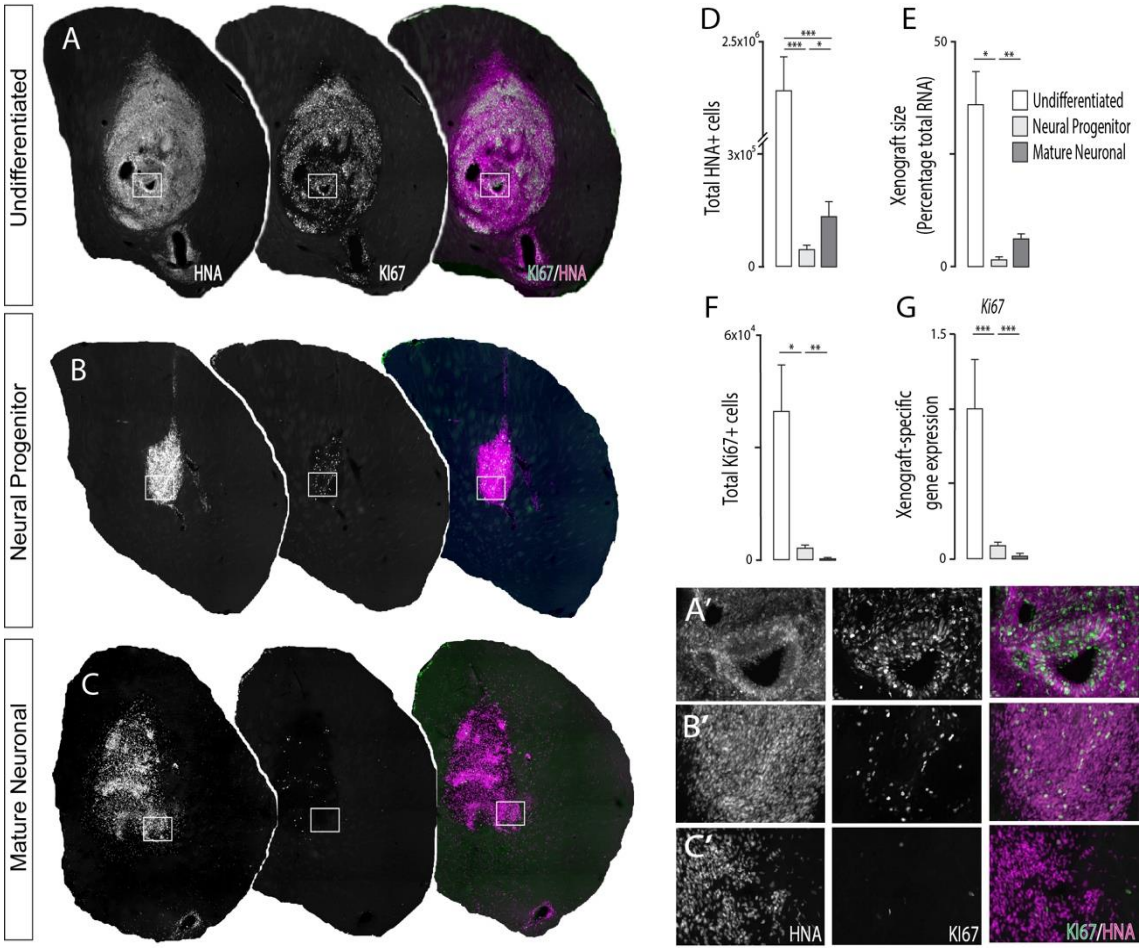

Figure 28. ***- In vivo validation of a xenograft profile using species-specific qPCR.*** *(A) Representative micrograph depicting a graft of undifferentiated human pluripotent stem cells (hPSC) 1 month after implantation. Human nuclear antigen (HNA) labelled all human-derived cells within the host tissue, while KI67 labelled proliferative cells. (B) Comparative grafts of hPSC-derived neural progenitors assessed at 1month and (C) 5months after implantation. (D) Quantification of HNA+ cells within the grafts (E) closely mirrored the proportion of human-specific transcript (as a percentage of total transcript). (F) Similarly, quantification of KI67+ proliferative cells, significantly elevated in grafts of undifferentiated hPSC, (G) reflected RNA transcript levels of the gene.*

To verify the technique capacity to identify different cellular population within a graft, we selected groups of genes that were anticipated to be expressed in each of the graft groups graft population. For example, we anticipated that genes related to defined germ layers (endoderm, mesoderm and ectoderm) would be highly expressed in the Undifferentiated grafts (resulting from the transplantation

of pluripotent cells and consequential teratoma formation), compared to the Immature and Mature Neuronal grafts which were restricted to an ectodermal/neural lineage prior to transplantation. The qPCR results validated the technique and predicted gene expression with the Undifferentiated grafts displaying high expression of endoderm (AFP and GATA6) and mesoderm (Brachyury and Collgen2A type 1, COL2A1) genes compared to the Immature and Mature Neuronal grafts (**Figure 29A-D**). In contrast, expression of neural cell adhesion marker (NCAM) was elevated in the Immature and Mature Neuronal grafts (2.25 ± 0.39 and 1.58 ± 0.38, respectively), **Figure 29E**. Not surprisingly, Nestin (neuroectodermal stem cell marker) was expressed in the Immature neuronal grafts, yet significantly reduced in the Mature graft (an anticipated result since the gene is downregulated during neuronal maturation [126], **Figure 29F**. These findings were confirmed by Nestin immunohistochemistry (**Figure 29G-J**). The xenograft-specific gene expression accurately identified changes in markers across the 3 germ layers that closely reflected the observed immunohistochemical labelling and quantification, demonstrating the veracity of the technique.

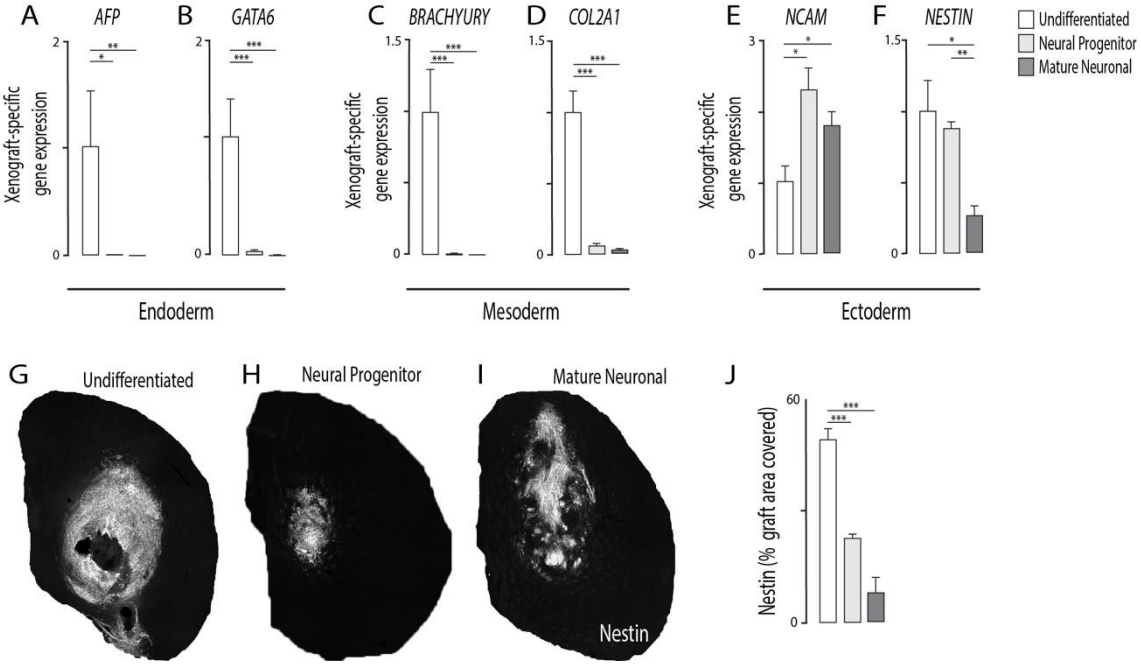

Figure 29. ***Capacity for qPCR technique to detect graft composition.*** (A-F) *Trilineage specification of cells within grafts of undifferentiated hPSCs was demonstrated*

*by high transcript expression of Endoderm (AFP, GATA6), Mesoderm (BRACHYURY, COL2A1) and ectoderm (NCAM, NESTIN) genes. Appropriately, neural progenitor grafts Immature and Mature Neuronal Grafts) contained only neuro-ectodermal gene expression. (*G-I*) Representative images of NESTIN-immunoreactive cells within Undifferentiated, Immature and Mature Neuronal grafts, respectively. (*J*) Comparative levels Nestin transcript was validated by the proportion of the graft showing NESTIN-immunoreactivity. Data represents mean ± SEM, One-way ANOVA with Tukeys posthoc testing, n=5. * p < 0.05, ** p < 0.01, *** p < 0.001*

To test if the technique was sensitive to detect more subtle changes present between Immature Neuronal and Mature Neuronal grafts, derived from the same VM progenitor pool, we subsequently performed immunohistochemistry against GFP (to identify LMX1A-GFP expressing Immature DA progenitors) and Tyrosine Hydroxylase (TH, to detect mature dopamine neurons in the grafts). Cell counts revealed that 21 + 4% of Undifferentiated grafts expressed the ventral midbrain progenitor marker (GFP+/HNA+), a proportion that was significantly increased in the Immature Neuronal grafts (82 + 1%) and maintained in the Mature Neuronal grafts (76 + 4%), (**Figure 30A-D)**. Reflective of the protein expression and cell quantification, LMX1A gene expression, relative to Undifferentiated grafts, showed LMX1A was increased 32.7 ± 1.7-fold in the Immature Neuronal grafts, and reduced to 17.2 ± 2.3-fold in the Mature Neuronal grafts (**Figure 30E**). This was in accordance to the literature, previously describing downregulation of the gene in maturing midbrain dopamine neurons during embryonic development.

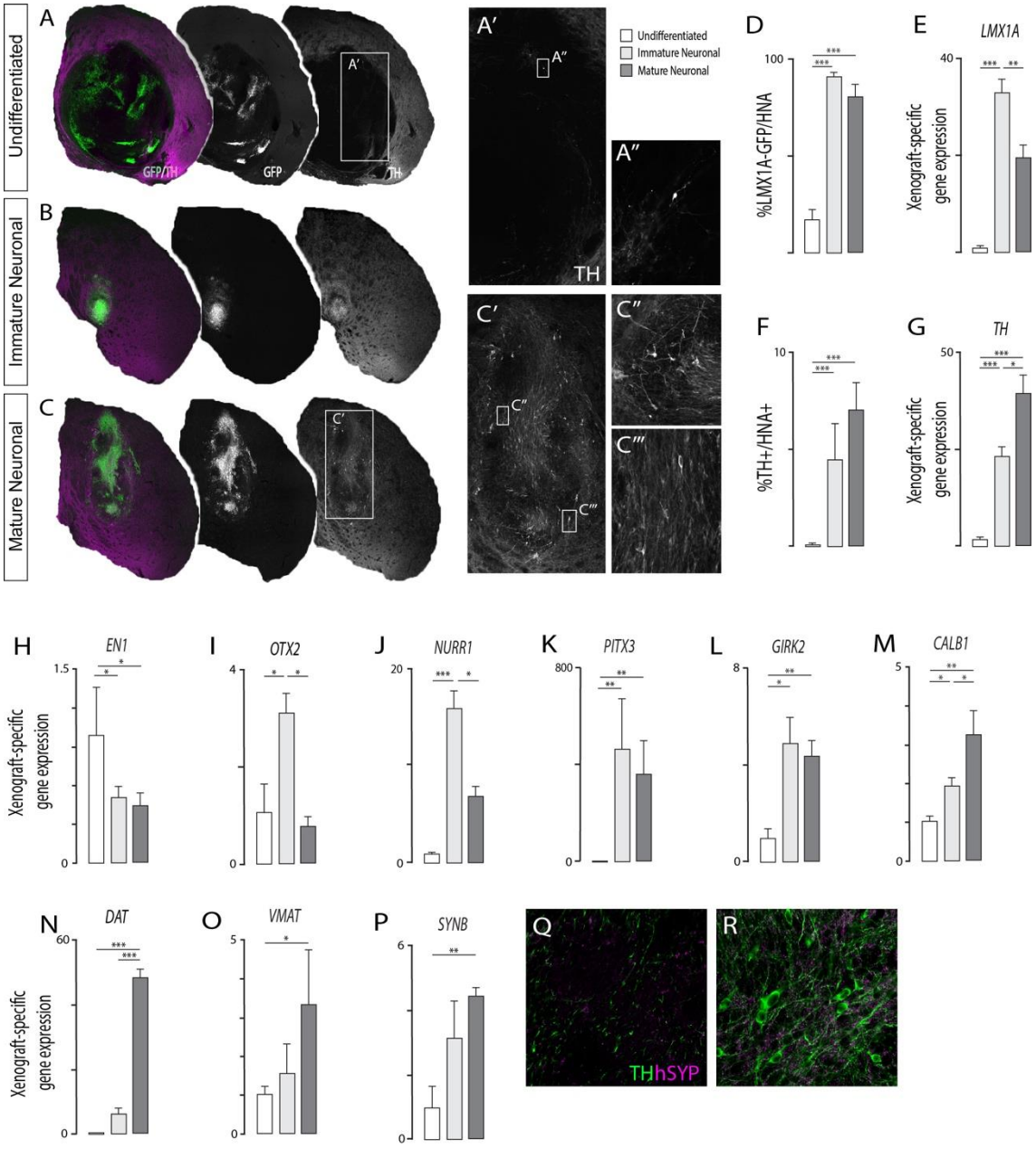

Figure 30. ***Validation of midbrain dopaminergic identity of xenografts using qPCR****. (A) Representative images from an undifferentiated hPSC, (B) Immature Neuronal and (C) Mature Neuronal graft depicting immunohistochemical expression of the early ventral midbrain progenitor protein – LMX1A (using an LMX1A-GFP reporter cell line) and mature dopamine neuron protein tyrosine hydroxylase (TH). (D) Neural specification of the cells prior to transplantation (to a ventral midbrain dopaminergic identity) resulted in a significant increase in LMX1A-labelled cells that could be validated by species-specific (E) LMX1A expression. (F) Similarly, TH cell counts significantly increased within ongoing maturation of the neuronal grafts, compared to undifferentiated cell grafts, (G) results that were validated by TH qPCR. (H) Graft expression of early ventral midbrain*

*progenitor transgenes as revealed by species-specific qPCR primers for EN1, (I) OTX2, (J) NURR1, (K) PITX3, as well as mature dopaminergic neuronal genes (L) GIRK2, (M) CALB, (N) DAT, (O) VMAT and (P) SYNB. (Q) Immunohistochemical labelling against tyrosine hydroxylase (TH, Green) and human synaptophysin (hSYP, magenta) in Immature and (R) Mature Neuronal grafts Data represents mean ± SEM, One-way ANOVA with Tukeys posthoc testing, n=5. * p < 0.05, ** p < 0.01, *** p < 0.001.*

TH cell counts in the Undifferentiated grafts were just 0.3% ± 0.04 of total cells (TH+/HNA+), a proportion that was significantly increased in the Immature Neuronal grafts (4.4 % + 1.5) grafts, with the greatest proportion observed in the Mature Neuronal grafts, accounting for 7.2% + 0.9 of all cells. Again, xenograft gene expression reflected the cell counts/proportions, with expression 8.0- and 12-fold greater in the Immature and Mature Neuronal grafts, respectively, compared to those grafts of Undifferentiated cells (**Figure 30F-G**).

To demonstrate the utility of the technique, to rapidly and comprehensively profile graft composition, 9 additional genes (anticipated to be expressed predominantly in neural specified grafts) were assessed. The first four gene were selective for their capacity to identify VM progenitors and included the forebrain-midbrain gene OTX2, the midbrain-hindbrain restrictive gene Engrailed- 1 (EN1), the dopaminergic precursor orphan nuclear receptor, Nurr1 (NR4A2), and pro-survival gene paired-like homeodomain 3 (PITX3), **Figure 30H-K**. As anticipated, compared to undifferentiated grafts, there was an upregulation of OTX2 (3-fold) and NR4A2 (16-fold) in the Immature Neuronal grafts, but not in the more Mature grafts. This is reflective of the transient expression of these genes in embryonic development [23]. The gene PITX3 was upregulated in both the Immature and Mature Neuronal grafts, compared to the undifferentiated grafts. Unexpectedly, EN1 was significantly downregulated in the neuronal grafts relative to undifferentiated grafts, but further trawling into the expression of this gene highlighted its many other roles in early development like embryonic segmentation [127]. Next, we assessed 5 genes reflective of neuronal maturation. Inclusive of GIRK2, CALB1, DAT, VMAT and VAMP2. The G-protein-regulated inward rectifier potassium channel 2 (GIRK2/KCNJ6) and Calbindin-1

(CALB) are mature midbrain dopamine neuron subpopulations markers; the dopamine transporter (DAT/SLC6A3) and vesicular monoamine transporter 2 (VMAT2/SLC18A2) are key for the recycling of dopamine; and finally, the vesicle-associated membrane protein Synaptobrevin 2 (SYNB/VAMP2), is a presynaptic protein involved in the docking of synaptic vesicles. The results showed that GIRK2 and CALB1 were significantly increased in the Immature and Mature Neuronal grafts. As anticipated, synaptic protein and transmitter associated genes DAT (49-fold), VMAT and SYB2 showed significantly elevated expression in Mature Neuronal grafts, compared to Undifferentiated and Immature neuronal grafts (**Figure 30L-P**). With the Mature neuronal graft showing increased gene expression indicative of synaptic integration (i.e. increased DAT, VMAT and SYNB transcript), we were able to confirm this observation by the increased histochemical labelling for human Synaptophysin in these Mature compared to Immature Neuronal grafts **(Figure 30Q-R)**.

5.4.3 Unbiased characterisation of xenograft composition and identification of novel transcriptional changes using RNAseq

Expanding on our species-specific transcriptional profiling, we elected to perform whole genome profiling using RNAseq to demonstrate the full capacity of the approach. The key difference between qPCR and RNAseq is that qPCR requires a gene of interest to be selected for assessment of transcript changes, while the later (RNAseq) enables for an unbiased characterisation of graft composition that can confirm both known/anticipated gene expression and the presence of previously unidentifiable cell populations. Moreover, RNAseq gives new insight into novel gene expression including recognition of mechanistic pathways contributing to graft function. Mixed species cDNA libraries (i.e. the human graft within the host mouse brain) were prepared from the 3 graft types and subject to paired-end, 75 bp sequencing to a target depth of approximately 20 million human reads (using the estimation of percentage xenograft RNA described in **Figure 28E**). A rapid and computationally efficient analysis pipeline was established and implemented on the Galaxy platform (freely available, thereby making it accessible and not requiring of a specialist bioinformatics infrastructure or

expert). Reads were first mapped against the human genome and only the successfully aligned reads were subsequently mapped to the mouse genome. Then, all human reads found to also map to the mouse genome were discarded, leading to a minimum risk of incorrectly specified reads. The reads that resulted from this approach were designated as unique to the human genome, and consequently originated from the xenograft. An average of 94.4 ± 1.5% of reads were identified as unique to the human genome under these criteria across the 3 graft groups, with 5.6 ± 1.5% of reads aligned to both human and mouse genomes, and therefore discarded from the analysis (**Figure 31A**). Noted the discarded reads mapped to 327 genes (defined as having an average of >10reads) and showed no enrichment for any gene ontology category or pathway. Nor did the reads map to highly conserved regions or repeated elements and showed profiles indicative of originating from mouse RNA (data not shown).

Comparing to the results of graft sizes originated from the qPCR-based estimation of human RNA, the number of unique human reads from the RNAseq were expressed as a percentage of the total reads (**Figure 31B**). The results were found to significantly correlate with the original estimation calculated using qPCR (r2 =0.94), showing the accuracy of both approaches. Furthermore, taking advantage of the variation in graft sizes across the groups, we were able to determine the percentage of xenograft RNA in a sample necessary to provide a sufficient level of unique reads. Samples where the human RNA was only 2.5% of the total RNA provided 86% reads unique to the human transcript using our high stringency approach. This specificity increased exponentially – observing that with 6.7% of human RNA, greater than 95% of the reads were classified as uniquely human, and samples of 35% human RNA yielded 99% unique reads (**Figure 31B**). These results showed that the analysis pipeline resulted in a highly efficient yield of species-specific reads from within a graft-host pool of tissue/RNA, including when the graft size was limited.

To verify if the xenograft-specific reads were consistent with the three distinct populations generated from the 3 grafted cell types, a global gene expression profile was analysed and resulted in 3 distinct clusters (**Figure31C**). It showed

the highest similarity between the replicates of each group, with Immature Neuronal and Mature Neuronal grafts the most closely related graft types (**Figure 31D**). Taking together, these findings demonstrate that at a global expression level, the xenograft specific RNAseq provided a highly specific expression profile consistent with the expected graft relationships.

A critical advantage of the RNAseq approach is the ability to investigate both known and novel genes. To demonstrate this, xenograft-specific differential expression analysis was conducted (**Figure 31E**). A total of 11,010 differentially expressed genes were identified between Undifferentiated and the Immature Neuronal grafts, and 12,449 genes between Undifferentiated and Mature Neuronal grafts (data not shown). Gene ontology categories between Undifferentiated and Immature Neuronal grafts identified, as anticipated, that genes related to synaptic signalling, axonal plasticity and neural development were upregulated in the Immature Neuronal graft. In contrast, RNA expression and regulation of cell cycle genes were downregulated (**Figure 31F**). Analysis of genes at this comparison identified 233 transcription factors possibly involved in development of ventral midbrain/mature dopaminergic populations, and 751 genes coding for axon guidance cues and receptors (data not shown). These results provide an extensive list of possible targets for the modulation of cell populations or plasticity in the maturation and integration of neuronal grafts.

To verify the utility of the RNAseq to provide an unbiased characterisation of the xenograft composition, we compared RNAseq results to the qPCR by assessing the known markers of germ layer lineages, Immature dopaminergic and mature dopaminergic neurons across the 3 graft types. In accordance to the qPCR results, the xenograft expression of cells proliferation marker Ki67 (**Figure 31G**) was highly expressed in the Undifferentiated grafts, and lowly expressed in the Immature Neuronal and Mature Neuronal grafts (**Figure 28G**). Two additional proliferative genes were also shown to be upregulated (PCNA and MCM2), supporting the findings. Also reflecting the qPCR results, endodermal and mesodermal genes were downregulated in the Immature and Mature Neuronal grafts, and ectodermal marker remained expressed, reflective of neural fate restriction (**Figure 31G**).

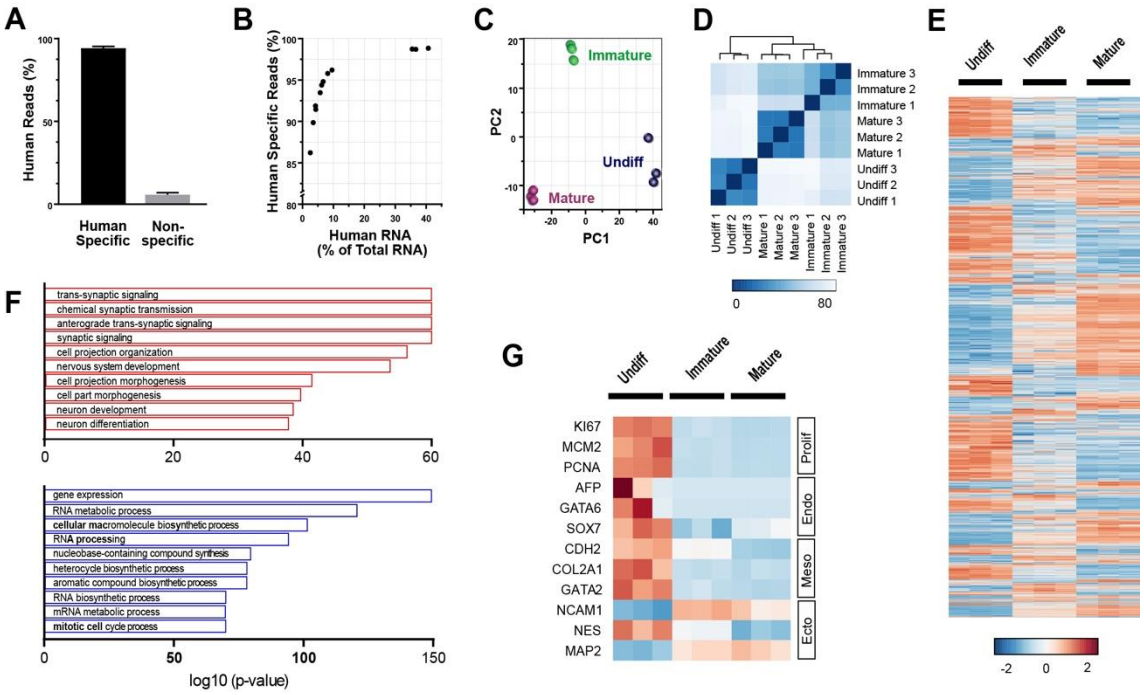

Figure 31. ***Unbiased Characterisation of xenograft composition (A)*** *Graph of xenograft-specific read yield showing 94.4% of the RNAseq reads were uniquely mapped to the human genome (xenograft-specific) compared to 5.6% mapping to both human and host (ambiguous origin) using our high stringency criteria.* ***(B)*** *Graph of the percentage of unique human reads (xenograft-specific) compared to the size of the xenograft showing that xenografts making up greater than 2.5% of the total RNA provide an economical yield of greater than 86% uniquely identified xenograft reads.* ***(C)*** *Principal component analysis comparing the global gene expression profile of each xenograft revealed the samples clustered into 3 distinct groups corresponding to the 3 graft types.* ***(D)*** *A dissimilarity matrix of the global RNA profile correlation and unsupervised clustering showed the highest similarity between the replicates of each group.* ***(E)*** *Heatmap of xenograft-specific gene expression.* ***(F)*** *Graph of enriched gene ontology categories between undifferentiated and Immature Neuronal grafts identified an upregulation of genes associated with synaptic signalling, axonal plasticity and neural development in the Immature Neuronal grafts while genes associated with RNA expression/processing and regulation of cell cycle genes were downregulated.* ***(G)*** *Heatmap of markers of germ layer lineages across the different graft types showed trilineage specification in the undifferentiated grafts, reflective of a teratoma, yet only*

ectoderm gene expression in the Immature and Mature neuronal grafts, reflective of their regional specification.

As anticipated, genes associated with dopamine development and function showed increased expression, in Immature and Mature Neuronal grafts compared to the Undifferentiated grafts. These expression levels were represented as a heatmap (**Figure 32A**) and graphed as fold change for each of the comparisons between the graft types (**Figure 32B**). Ventral midbrain dopaminergic progenitors' markers, inclusive of NEUROG2, FOXA2, and LMX1A were most highly expressed in the Immature Neuronal grafts. NR4A2, PITX3, and DRD2 were maintained at high levels in the both Immature and Mature Neuronal grafts, whilst the mature genes GCH1, SNCA (a-synuclein), VMAT2/SLC18A2 were expressed most highly in the Mature Neuronal grafts. Synaptic markers such as Synaptobrevin2 (SYNB/VAMP2) and SYP (Synaptophysin) were significantly upregulated in the Immature neuronal graft and presented an even greater fold change in the Mature Neuronal grafts (**Figure 32B**).

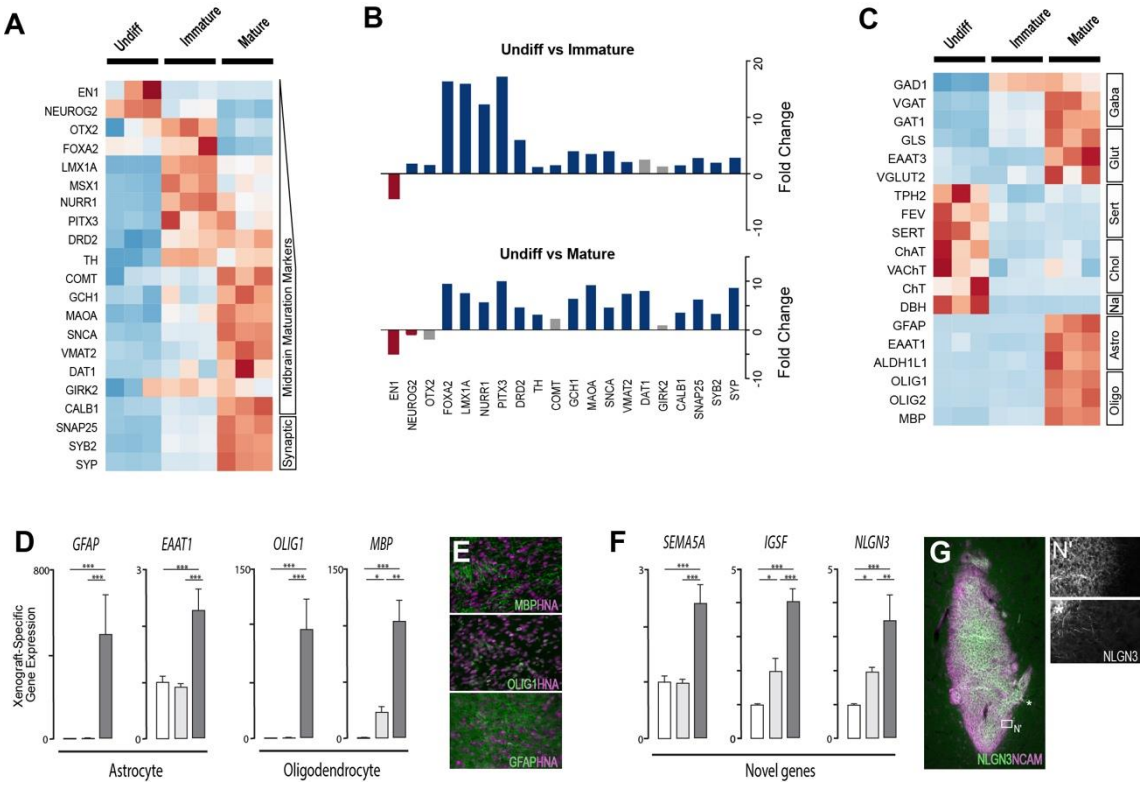

Figure 32. ***Identification of novel transcriptional changes using RNAseq. (A)*** *Heatmap showing higher expression in red and lower expression in blue and* ***(B)*** *fold change in gene expression for early and late ventral midbrain dopaminergic neuron markers across the 3 graft types. Low expression of most dopamine related genes was observed in the undifferentiated grafts, high expression of dopamine progenitor genes in the Immature grafts, and late dopamine genes were most highly expressed in the Mature grafts.* ***(C)*** *Heatmap (higher expression in red and lower expression in blue) of non-dopaminergic neural cell type markers across the 3 graft types revealed the presence of glutamatergic and GABAergic neurons within the Mature grafts, as well as astrocytes and oligodendrocytes.* ***(D)*** *qPCR verification of the expression of astrocyte (GFAP, EAAT1) and oligodendrocyte (OLIG1, MBP) genes.* ***(E)*** *Representative immunohistochemistry confirmed the presence of astrocytes and oligodendrocytes in the Mature grafts. RNAseq identified a number of novel genes expressed in the Mature neuronal grafts that were verified by* ***(F)*** *qPCR (SEMA5A, IGSF8, NLGN3) and* ***(G)*** *Immunohistochemical staining against NLGN3 (green) and human specific NCAM confirmed the presence of this novel plasticity gene within the Mature neuronal grafts. Gaba (GABAergic), Glut (Glutamatergic), Sert (Serotoninergic), Chol (Cholinergic), Na (Noradrenergic), Astro (Astrocytes), Oligo (Oligodendrocytes). Data represents mean*

*± SEM, One-way ANOVA with Tukeys posthoc testing. (C-J) n=3, (K,M) n=5. * p < 0.05, ** p < 0.01, *** p < 0.001.*

As described in this thesis introduction, despite the transplantation of seemingly correctly specified VM progenitors (typically 80% LMX1A/FOXA2/OTX2), after extended periods of time in vivo, less than 5% of the graft becomes mature dopaminergic neurons. These observations suggest that poorly specified cells in vitro, or alternate VM populations, expand to dominate the graft. Surprisingly, at a time when these cells are entering the clinic in Phase 1 clinical trials the identity of the remaining 95% are poorly characterized. In an effort to understand the graft composition, our data set was screened for markers of other neuronal (non-dopaminergic) cell populations in the 3 grafted cell groups (**Figure 32C**). We found GABAergic (GAD1,VGAT/SLC32A1, GAT-1/SLC6A1) and glutamatergic (GLS, EAAT2/SLC1A2, VGLUT2/SLC17A6) genes expressed in the Mature Neuronal grafts, and low expression of serotoninergic (TPH2, FEV, SERT/SLC6A4), cholinergic (CHAT, VAChT/SLC18A3, Ch/TSLC5A7) noradrenergic (DBH), relative to the Undifferentiated grafts. These results suggest the presence of different neuronal subtypes compositions rather than only dopaminergic. Unexpectedly, we observed high gene expression of other neural/non-neuronal cell types, such as astrocyte-associated genes GFAP, and ALDH1L1 as well as oligodendrocyte genes OLIG1, OLIG2 and MBP (**Figure 32D-E**). These results were confirmed by xenograft-specific qPCR profiling and immunohistochemistry for the astrocyte markers GFAP and EAAT1/SLC1A3, as well as oligodendrocyte markers OLIG1 and MBP (**Figure 32D-E**).

Finally, the RNAseq data was used to reveal novel candidate genes that could be related to the maturation and plasticity of hPSC-derived VM Immature grafts. We identified, selected and examined three genes that show significantly elevated expression within the Mature Neuronal graft – SEMA5a (Semaphorin 5A), IGSF8 (Immunoglobulin superfamily member 8) and NGLN3 (Neuroligin 3). These three genes expressions were verified by qPCR (**Figure 32F**) and, due to limited commercial antibody availability, only NGLN3 was further validated by immunohistochemistry - showing punctate protein expression in the graft and evident expression along graft-derived axonal fibres (**Figure 32G**).

Altogether, these findings provide the first evidence for identifying the composition of VM progenitor grafts and shows the utility for this transcriptional profiling methodology to understand graft composition. Moreover, the identification of new genes involved in graft maturation present novel candidates for manipulation to promote graft plasticity, integration and function in the future.

5.5 Discussion

Within the present study we developed and described a novel approach to transcriptionally profile xenografts by discriminating the graft species RNA from that of the host. The xenograft-specific qPCR technique provides a much-needed standardised method for characterisation of graft composition. The method is simple to implement within any standard laboratory, requires minimal expertise/experience and is highly reproducible. The relatively simple design of primers, ad large RNA yields, permits for a great number of genes to be analysed relatively quickly, allowing for efficient characterisation of grafts inclusive of proteins/genes that are currently difficult to discriminate. The combination of this technique with RNAseq, provides an unbiased means to screen graft composition, investigate their function, and provide insight to enhance grafting outcomes.

We have validated and demonstrated the use of this technique by comparing gene expressions, cross-validated by qPCR and RNAseq, of 3 distinct human grafts within the rodent brain - those grafts derived from undifferentiated human pluripotent stem cells, grafts containing Immature Neural progenitors, and grafts of neural progenitors left to mature in situ over several months. A number of transcriptional results were confirmed by immunohistochemistry, where antibodies were available, with quantification across the 3 methodologies generating highly correlated results.

The specificity of xenograft-specific qPCR primers designed for the 30 genes assessed in the present study showed 1000 to > 1,000,000-fold increased expression over the mouse host. Thus, the technique is sensitive enough to provide an estimate of the graft size that was demonstrated with the correlation of the predetermined cell numbers transplanted. Also, the cell counts in

experimental groups quantified in parallel using immunohistochemistry also matched these estimates as did the proportion of xenograft RNA estimated by RNAseq. Moreover, the specificity of the technique lead to an accurate detection of both large- and small-scale changes in graft cell populations, such as the expression of germ layer lineage specific markers in Undifferentiated cell grafts, compared to the more subtle changes between Immature and mature neuronal grafts.

A great advantage of this technique is the ease of tissue and RNA isolation – enabling greater standardisation of graft composition across research groups and by different scientists. Here we have placed the grafts into the striatum, a clearly identified structure that could be grossly dissected. From this tissue (irrespective of location in other adopted studies in the future) RNA could be readily isolated (consisting of both host mouse and human xenograft RNA) using a standard column-based protocol. This straightforward method prevents the RNA from degrading, ensuring enough RNA quality and quantity to be analysed using the commonly available nanodrop spectrophotometer (as opposed to TapeStation or Bioanalyser). After the extraction of a mixed species RNA population, a qPCR or RNAseq can be done as an easily achievable tool for most laboratories without necessary expertise in microdissection, single-cell sorting or RNA handling. Also, the RNAseq analysis methods described here are accessible without specialist bioinformatic experience or infrastructure necessity. The analysis pipeline was done in the freely available Galaxy web platform (www.usegalaxy.org/), which provides point-and-click access to all the required bioinformatic tools [77].

The difficulty to perform a high throughput gene or protein analysis on xenografts has been an obstacle in understanding graft integration, and to identify targets to enhance survival, maturation and plasticity which may interfere in graft function. Analysis of graft composition often needs the availability of reliable antibodies, or a species-specific antibody to discriminate the host from the graft proteins. The difficulty is even bigger where cells migrate and intersperse within host tissues, such as glioblastomas invading a host brain or grafted axons innervating the host tissue. However, xenograft-specific qPCR can readily detect any gene of interest within a graft, irrespective of the expression also in the host or localisation of the

cell within surrounding tissues. For example, here we successfully designed primers against PITX3, one example where the antibody is notoriously unreliable (personal observations and communications). Primers were also designed against genes expressed in both the graft and host tissue for which human specific antibodies are not available, for example, the broadly expressed neural gene Nestin, the mature dopamine gene TH and the synaptic gene SYB2/VAMP2. Moreover, we demonstrated the ability to detect rare events within transplants, such as proliferative KI67 cells, knowledge that may be critical in preclinical testing of cell batches for tumorigenic potential, prior to translation. Importantly, the species-specific qPCR technique was validated by close match in gene expression levels and in cell counts within the graft (in particular, total cells, KI67, LMX1A and TH).

Building on the advantages of the species-specific qPCR, xenograft specific RNAseq provides an easily accessible tool for the interrogation of the entire transcriptome of the transplant, enabling the previously elusive assessment and characterization of graft composition, as well as investigation into novel genes and pathways that may influence graft function. The importance of the coverage of the cells phenotypic markers was highlighted here by the surprising high expression of astrocyte and oligodendrocyte transcripts within grafts derived from FACS sorted VM progenitors, an interesting finding for long-term transplantation where small pools of poorly specified cells can expand to become a significant component of the graft at therapeutically relevant timeframes yet are not easily detected in vitro. Such cell types have been difficult to detect using conventional methods to date, as antibodies fail to discriminate graft from host derived cells and have therefore largely relied upon use of reporter lines – that are evidently less amenable to clinical translation. Hence xenograft profiling may present the only way to understand graft composition and is particularly relevant in the context of cell therapy for PD that are in or approaching clinical trial [128][52] using very similar differentiation protocols for the generation of donor VMDA progenitors.

Finally, we demonstrated the utility of the species-specific RNAseq approach to identify novel genes within cell graft populations, such as Nlgn3, Sema5A and

IGSF8 - encoding for the proteins neuroligin-3, Semaphorin5A and Immunoglobulin superfamily member 8- that were highly expressed in mature (DA) neuronal compared to the other groups. These proteins have been linked to axonal and synaptic plasticity [129][130] or shown to be expressed on dopaminergic progenitors [23], but their roles in dopaminergic graft maturation remains to be explored. Even more, as described before, human pluripotent stem cell-derived dopamine neurons show inferior plasticity compared to fetal tissue and the identification of such genes may present new targets for modulating axonal growth and graft integration.

5.5.1 Conclusion

In summary, we described a novel approach to aide in the profiling of xenografts in situ. While demonstrated in the context of pluripotent stem cell-derived dopamine grafts for cell therapy in Parkinson’s disease, this technique is amenable across xenotransplantation contexts, both within and outside the brain.

Chapter 6 - Discussion

6.1 Where are we now?

With a rapidly ageing population, the incidence of neurodegenerative disorders, such as PD, is anticipated to increase 3-fold in the next 25 years. Unlike many other tissues in the body, the central nervous system has limited capacity to self-repair and as such, highlights the need for development of new therapies.

Dopamine pharmacotherapy is the main therapeutic intervention for PD patients. However, the reliance of drugs such as levodopa on residual DA neurons, that are progressively dying, for the conversion into dopamine, results in waning efficacy over time. Added to this is the systemic delivery of dopamine modulating drugs in patients that underpin many of the side effects such as sleeping disorders, impulsive and compulsive behaviours and euphoria or depression.

In principle, however, these dopamine modulating drugs provide evidence that replacing dopamine in the PD brain can alleviate motor symptoms. The ectopic transplantation of dopamine progenitors can circumvent the primary challenges, providing localised dopamine delivery to the necessary target striatal tissue, with no reliance on residual host midbrain neurons. The past 40 years has observed proof of principle for dopamine cell replacement therapy in both preclinical and clinical studies. However, the results from the early open label and double blind clinical trials in the 1980s-1990s were highly variable as a consequence of notable lack of standardization in the preparation of the donor tissue (inclusive of dissection method, variation in donor age, tissue storage, number of donors, pieces/cell suspensions), immune suppression regimes, patient age as well as disease onset and disease duration. Recognising these variables, there has now been a revised effort to demonstrate the true benefit of DA cell replacement in PD patients using fetal tissue. This current trial (TRANSEURO, headed by Professor Roger Barker from the University of Cambridge, UK) seeks to employ the optimal patients (<65years, responsive to L-DOPA, within 10years of disease onset), tissue preparation (such as fresh tissue isolated from 6-9week gestation donors) and employ immunosuppression for 12 months [16].

In parallel, due to recognition that fetal tissue grafting still lacks the capacity for tight standardization and is limited by availability and ethics, the field of pluripotent

stem cells has rapidly progressed. hPSCs are now seen as the future of cell transplantation - for PD and a raft of other conditions. Amazingly, since the derivation of the first *bona fide* VM DA neuron from hPSC in 2011, in just 7 years the field has progressed to clinical trial, with the first patient transplanted in Japan in October 2018 [128].

Regardless of this progress and associated excitement in the community, there remain a number of poorly addressed challenges. This thesis addressed (i) the need to improve the survival and functional integration of the grafts, and (ii) the need to have a better understanding of the graft composition (to ensure safety and predictable functionality) prior to translation.

6.2 Summary of research findings, significance and future directions.

6.2.1 Improving fetal tissue grafts for PD

Despite the standardization and ethical challenges associated with fetal tissue grafts for PD, this approach remains the gold standard in CRT, and will remain so at least until we see the first patient evidence for functional outcomes following hPSC-derived grafts. It therefore remains highly valid to use fetal tissue grafts to understand and improve graft outcomes. In this way, the first study in this thesis aimed to determine if sustained SDF1, delivered by a tissue specific hydrogel, would improve the survival, differentiation and integration of VM fetal grafts in a mouse model of PD. The study assessed the benefits of (1) a tissue specific hydrogel (2) and the impact of SDF1 on the graft.

We demonstrated that, contrary to the rapid recombinant SDF1 degradation when added directly to the culture media (<30 minutes), the laminin-based IKVAV hydrogel was able to entrap SDF1, resulting in an initial protein burst release likely beneficial to the cells during the critically vulnerable phase of in vivo delivery, yet importantly sustained delivery for >14 days - corresponding to periods of DA progenitor maturation and integration.

The results showed that grafts in the presence of the SDF1-functionalised SAP hydrogel (Cells + shSDF1-SAP) were significantly larger, suggesting that the

SDF1 influenced the proliferation or survival of the implanted progenitors. In addition, the presences of the SDF1 functionalised SAP scaffold resulted in an increase in TH+ DA neurons compared to Cells alone, and to Cells + SAP, indicative of the synergistic effect of the SDF1 protein and the laminin-based scaffold. Moreover, the Cell+SAP+shSDF1 group showed an increase in TH+ density within the graft. These observations suggested that the increased yield of TH-GFP+ neurons within these grafts was over and above the increase in graft volume, and that the functionalised scaffold was promoting DA differentiation.

We also showed that the presence of SAP hydrogel increased the A9 DAn (Th/GIRK2 co-expression) compared to the Cell+SDF1 group or cells alone and that sustained SDF1 delivery further increased in A9 specification compared to Cells + SAP. Moreover, only grafts in the presence of the SAP showed a significant increase in the proportion of GIRK2+ over GFP+ (TH+) cells, demonstrating that the increased number of A9 cells was not a merely consequence of increased GFP+ cells, suggesting that the laminin-based signalling presented by the SAP hydrogel was capable influencing DA fate acquisition. This finding is of great importance as the A9 DAn, and not A10 or alternative DA cells, are critical for the restoration of motor function [82].

Surprisingly, no significant increase in DA fibers density within the surrounding host tissue was observed. This result was likely a due to an insufficient duration, suboptimal dose, and/or the localisation of SDF1 delivery to influence plasticity. SDF1 has been shown to attract DA neurites [95][88][106], yet was delivered here within the graft core (to influence survival and differentiation of DA neurons), thereby failing to provide the necessary gradient to draw fibres out of the graft core and into the host tissue. In the future, it would be interesting to deliver SDF1 within the targeted dorsolateral striatum in an attempt to attract axon growth.

With these findings in agreement to ours in demonstrating the benefits of the functionalised scaffold added to previous work examining biomaterials for fetal tissue [64] [105], the subsequent obvious step is to assess the influence of functionalised biomaterials in the next targeted cell source, the hPSC-derived grafts.

6.2.2 What is the future for hPSC-derived transplants in PD

Human PSC-derived grafting is the evident long-term goal for the CRT field. The ability to generate VM DA progenitors *in vitro* will not only overcome ethical concerns, but also standardization and industry-scale production. From the fetal tissue graft studies, we have understood the necessity of key guidance cues presence/delivery for a better cell survival, differentiation and integration, such as GDNF that has been used in non-human primates demonstrating the benefits of prolonged delivery into the host tissue (via injection of viral vectors) [35]. We have also learnt that physical environment/ECM has a crucial influence on these outcomes.

These knowledges lead us to the development of a tissue specific SAP hydrogel (also employed in the aforementioned fetal grafting) to mimic the brain ECM by the presentation of one of the laminin epitopes (recognising laminin as the main protein in the brains ECM). In parallel work, our group showed that this laminin-based tissue-specific hydrogel promoted human stem cell graft (cortical) differentiation, integration and functionally in a model of stroke. Consequently, chapter 4 looked to modulate hPSC-VM grafts using the same laminin-based hydrogel, as well as harnessing the capacity of the scaffold to deliver GDNF. Our aim was to understand if this sophisticated biomaterial would influence hPSC-derived grafts and if it would be able to impact graft-outcomes by sustaining protein delivery. Our results showed that only sustained delivery of GDNF, from the hydrogel, could improve both induced- and spontaneous motor deficits in Parkinsonian rats. The improvements were most likely a consequence of increased graft survival, DA fate acquisition and innervation.

Surprisingly, the unfunctionalized (-GDNF) hydrogel had no impact on survival and maturation (TH+ DAn) of VM progenitors *in vivo*. However, for the first time to our knowledge, a tissue-specific hydrogel could bias A9 (GIRK2+/TH+) specification, at the expense of A10 (CALB+/TH+) DA neurons, from hPSCs. Recognising the importance of the A9 population for alleviating motor symptoms

[82], the tissue-specific hydrogel may provide means for implanting fewer cells with more targeted function.

These findings are in contrast to recent work showing the influence of laminin in the survival and differentiation of DA neurons in the developing brain [63]. Likely underpinning these disparate findings is the complexity of the laminin family of proteins that has a total of 12 laminin trimers identified to date. Also, the different protocols existing for hPSC-DA differentiation presented differing success for the different laminins, indicating that identification of the necessary and optimal subunits remains to be determined and/or the existence of redundant roles. On the other hand, our results showed that prolonged delivery of GDNF from our tissue-specific SAP hydrogel promotes survival, increased TH+ DA neurons and plasticity of hPSC-derived VM progenitor grafts. *In vitro*, we showed an initial burst release of GDNF, followed by a delayed and sustained delivery beyond 28 days, with this biphasic delivery likely underpinning initial progenitor survival, and subsequent integration. The modest, but significant, effects on graft plasticity suggest that higher concentrations of GDNF, and/or the incorporation of other DA axonal growth promoting proteins, such as Wnt5a [59], may enhance graft plasticity and functional integration.

Our results also provided the first characterisation of vascularisation of hPSC-derived VM progenitor grafts, a feature surprisingly not studied to date but critical for their survival of large tissue grafts. We demonstrated that host-derived (HNA) endothelial cells infiltrate into the graft core to form a new vessel network. The density of the vessel network across all graft conditions was significantly less than the host tissue, suggesting that delivery of additional trophic cues such as BDNF, VEGF and/or erythropoietin, targeted at promoting angiogenesis, may improve graft outcomes.

Lastly, we have shown that the fabricated hydrogel had no significant impact on the immune response, with not dissimilar levels of reactive astrocytes and microglia to that observed for grafts of cells-alone. Biocompatibility of biomaterials is necessary for the success of all transplants may even provide means to protect the grafted cells from the host immune system. However, it should be noted that

the present study was done in immunocompromised animals that can mask some immune responses, thus, further assessment into non-compromised animals will reveal the true potential and compatibility of these scaffolds. Taken together, we have provided evidence for a functionalised tissue-specific hydrogel to improve the survival, differentiation and integration of hPSC-derived DA progenitor grafts in an animal model of PD.

These findings highlight efforts needed for the future directions as the field moves towards the clinic, such as the necessity to incorporate functionalised biomaterials to influence the donor cells and host environment. Here we have studied the laminin α1 subchain peptide hydrogel, recognized by the cells, but examining different peptide sequences for the various laminin subunits is another alternative. For example, the use of laminin 521 (comprised of the α5, beta2, gamma1 subchain) has been linked to more efficient midbrain dopamine differentiation in vitro [44] and the presence of α5 unit peptide within the hydrogel may lead to a better *in vivo* differentiation. Moreover, development of alternative biomaterials presenting other ECM components such as fibronectin and collagen should also be considered. Of great importance, another interesting alternative is the controlled delivery of additional proteins for neuroprotection, plasticity and even vascularisation, to ensure that maximal function benefits can be obtained from grafted progenitors. These future perspectives can be targeted not only for cell replacement therapy in Parkinson's disease, but other conditions were cell transplantation presents a therapeutically viable option.

The next step following transplantation is to identify the graft composition, guaranteeing efficacy and safety. This is needed not only for PD but for the broader CRT and regenerative medicine fields. Thus, the third study in this thesis focused on the development of a new method to address this challenge.

6.2.3 Understanding graft composition

The great potential that hPSC brings as a disease model and as a therapy has accelerated studies in the field. In PD, VM-derived from hPSC grafts are now

entering the clinic but, there are still outstanding concerns and room for improvements. In particular, when seemingly correctly specified ventral midbrain progenitors are transplanted into the striatum and analysed after extended periods of time, only a small fraction – approximately 5% - of the cells in the graft actually became dopaminergic neurons. Surprisingly little is known about the identity of the remaining 95% of cells and the impact they may have on both graft function and adjacent host tissues. For example, rogue, highly proliferative cells may lead to tumours or neural overgrowths, whilst off-target serotonergic neurons may lead to graft-induced dyskinesias.

To address this, we successfully designed a qPCR technique based on the ability of carefully designed primers to discriminate between xenograft (human) and host (mouse) transcripts. The technique was sensitive enough to estimate graft size and identify different cellular population within a graft, based upon transcript. Moreover, it is able to detect subtle changes present between different grafts. The technique was validated and demonstrated by RNA comparison from the 3 different xenografts (Undifferentiated, Immature neuronal and mature neuronal) that we could anticipate some gene expressions, known from the literature. We were not only able to detect major changes in gene expression between the populations (such as Ki67), but also more subtle changes (such as LMX1A in the Immature and mature neuronal grafts) or lower expression (such as AFP). The qPCR results were then verified by immunohistochemistry where antibodies were available.

Expanding on the idea of detecting transcript differences between the graft and host, we developed an RNAseq based approach to profile the entire genome. The highly specificity of the RNAseq technique showed 86% of reads unique to the human transcript when just 2.5% of the total RNA was of graft origin and >99% unique reads when the graft contributed 35% of the total RNA. This efficiency allows for quick, gross tissue dissection (in this instance the whole mouse striatum containing the human xenograft) with no need cell sorting, laser capture or alternate labour-intensive approaches. The easy technique prevents the RNA from degrading, ensuring enough RNA quality and quantity and even more important, allows the extraction using a standard column-based protocol.

The main difference between the two techniques (qPCR and RNAseq) is that the gene of interest must be known when using qPCR whereas the whole gene expression analysis can be performed using RNAseq, thereby giving insight into novel and/or unexpected gene expression. For example, we identified SEMA5a, IGSF8 and NGLN3 showing significantly elevated expression within the Mature Neuronal graft, as these genes are involved in neuronal maturation, they may present new candidates for manipulation to promote graft plasticity, integration and function in the future. In addition, we unexpectedly identified the presence a high expression of astrocyte-associated genes (GFAP and ALDH1L)1 as well as oligodendrocyte genes (OLIG1, OLIG2 and MBP), despite grafts of neuronal progenitors being implanted. Further studies are required to understand whether these populations present a benefit to the DA neurons (e.g. secreting trophic cues to influence plasticity), bare a negative impact, or have no influence on either the graft or host.

Importantly, the method is simple to implement at any regular scientific laboratory with a minimum required experience. The relatively simple design of primers permits a great number of genes to be analysed quickly, allowing a characterisation of grafts including the genes that are currently difficult to discriminate between the graft and host. Even more importantly, while demonstrated in the context of pluripotent stem cell-derived dopamine grafts for cell therapy in Parkinson's disease, this technique is amenable across xenotransplantation contexts, both within and outside the brain.

Although we highlight the many benefits of the developed techniques, there are also their limitations. The transcript levels fail to provide information at the cellular level. For example, is high gene expression seen in just a few cells within the graft, of low transcript in the majority of cells? In this regard we see the benefit of complementary single-cell sequencing to shed more light on a sample of cells within the broader population. We also recognise that RNAseq is expensive – especially when the numbers of grafted cells are low, requiring a much higher sequencing depth to achieve enough reads for accurate expression profiling. Thankfully, however, with time RNAseq is becoming increasingly affordable.

Taken together, these techniques will provide critical insight into the safety and functional predictability (based upon cellular composition) of a donor cell preparation in preclinical testing, prior to translation. It is important to highlight that this new profiling approach is not limited to CRT for PD but provides a powerful tool to examine other xenograft-based transplants in regenerative medicine.

6.3 Future directions

The neuroscience community has been extensively exploring hPSC differentiation protocols and now beginning to understand that the ECM context has a key impact on cells behaviour.

The newest protocols for VM DAn differentiation culture hPSC on laminin substrates to obtain high yields of dopaminergic cells. The presence of just one ECM element was a decisive factor for a good differentiation, however, in the context of cell preparation and *in vivo* implantation, the importance of the ECM-connection has been overlooked – rather cell are stripped from this underlying support during dissociation and in vivo transplantation, possibly contributing to suboptimal survival.

Perhaps future efforts could limit the requirement for single cell delivery of the donor preparation and rather deliver cells within small clusters so as to maintain some of the underlying matrix. Additional to this, as presented within the thesis, if the benefit of hydrogels to re-establish a de novo cell-matrix interaction, not only supporting cells but additionally shielding cells from the shear forces exerted during injection through fine cannulas. It is also interesting that studies have developed alternative cell culture dishes that allow the cells to detach without using proteolytic enzymes, such as the “Up-cell culture”, where the cells are released as cell-sheets, connected by the naturally produced ECM [131]. Moreover, it is also an option to use cell culture into hydrogels to be delivered as one unit, since the *in vitro* differentiation would minimize the complexity of delivering trophic cues and molecules *in vivo* to guide the final differentiation.

While the present thesis work sheds light on the composition of VM progenitor grafts for the first time, the outstanding question for the field is how to reduce the contribution of these non-DA cells. As mentioned, current protocols report >80% correctly specified VM progenitors at the time of transplantation. Key readouts to confirm 'correct identity' include expression of OTX2/FOXA2, and often also LMX1A, in addition to the absence of subthalamic genes (PITX2/BARHL1). Yet these collections of genes are notable broader in the developing brain that just restricted to the DA progenitors, and hence the presence of other VM populations in the graft. Added to this is the incorrectly specified cells that are in the minority at the time of grafting yet expand in situ. Surprisingly we have recently confirmed (unpublished data) that VM DA progenitors become post-mitotic within just 6 weeks yet, graft volume can increase 10-fold from 6 weeks to 6 months. In this regard, greater attention to eliminate these incorrectly specified cells (as well as non-DA VM progenitors) would have a major impact on the number of cells delivered and their predicted function. Within the thesis we make use of an LMX1A reporter hPSC line to enrich for VM progenitors. Many other sorting strategies have also been adopted over the year – with varying degrees of success. An alternative approach is to employ suicide genes (such as the thymidine kinase/ganciclovir of iCas9 based systems) that can be activated to eliminate proliferative or alternate unwanted populations, either prior to transplantation or at desired intervals after implantation.

Another challenge, partially addressed within the thesis findings, is how to promote the plasticity of the grafts and how to attract new DA axons to appropriate host targets (the striatum). Molecules associated with axon growth and guidance during development present obvious candidates to be delivered adjacent to the graft into the host striatum or even using the principle of a long-term biomaterial releasing these molecules [56]. For this to be of benefit it will be necessary to know if the donor cells express receptors relevant to the guidance cue.

Whilst the delivery of differentiated cells is seen as a challenge in neural transplantation, namely due to anoikis and shearing upon delivery, the next generation biomaterials could aide in survival during cell preparation and delivery.

Furthermore, the biomaterials can/could be designed to not only one guidance molecule but several proteins (absent in the adult brain) at the right time and concentration, mimicking the development processes. For example, early delivery of a molecule to influence survival (such as GDNF, lazaroids or Rho-associated, coiled-coil containing protein kinase inhibitors), followed by another to promote dopamine differentiation (e.g. SDF1, Wnt5a) and a subsequent one to influence connection with the host brain (e.g. Nertin-1 or re-expression of GDNF). Recent work from our group is beginning to assess the feasibility of such multimodal delivery systems [64], [70], and will an important area to continue investigating.

In complement, knowing the importance of ECM components, the biomaterials have been moving towards a costume-made ECM composition developed according to the targeted tissue. The CRT field is starting to consider delivering cells within the right ECM context, mimicking the environment that they are normally placed, connected and that the cells recognise *in vivo*. Adding another level of complexity, studies have shown that the 3D distribution structure changes completely the intracellular cell signals [132] mediated by cells receptors for ECM, such as integrins and syndecans, among others. Thus, it is not just about presenting all the ECM components but also presenting them in the right concentration and 3D physical distribution. Ignoring the microenvironmental importance for differentiation, cell signalling, tissue organization and believing that the key importance is the transplanted cell phenotype may have been the reason for some poor outcomes seen in the field.

Taking together, overcoming the residual challenges and optimising the functional efficacy of neural transplants for diseases such as PD will not be achieved alone by developmental scientists, neither material engineers, but given the complexity, it will be a multidisciplinary effort. If scientists and clinician want to truly advance new stem cell-based therapies into the clinic, it will be necessary to focus on multidisciplinary approaches to ensure the best complementary therapies are established.

References

[1] A. Dahlström and K. Fuxe, “A Method for the Demonstration of Monoamine-Containing Nerve Fibres in the Central Nervous System,” *Acta Physiol. Scand.*, vol. 60, no. 3, pp. 293–294, Mar. 1964.

[2] A. Bjo and S. B. Dunnett, “Dopamine neuron systems in the brain : an update,” vol. 30, no. 5, 2007.

[3] N. Prakash and W. Wurst, “Development of dopaminergic neurons in the mammalian brain,” vol. 63, pp. 187–206, 2006.

[4] E. Arenas, M. Denham, and J. C. Villaescusa, “How to make a midbrain dopaminergic neuron,” pp. 1918–1936, 2015.

[5] S. J. Chinta and J. K. Andersen, “Dopaminergic neurons,” *Int. J. Biochem. Cell Biol.*, vol. 37, no. 5, pp. 942–946, May 2005.

[6] L. Thompson, P. Barraud, E. Andersson, D. Kirik, and A. Bjo, “Identification of Dopaminergic Neurons of Nigral and Ventral Tegmental Area Subtypes in Grafts of Fetal Ventral Mesencephalon Based on Cell Morphology, Protein Expression, and Efferent Projections,” *J. Neurosci.*, vol. 25, no. 27, pp. 6467–6477, Jul. 2005.

[7] K. M. Money and G. D. Stanwood, “Developmental origins of brain disorders: roles for dopamine,” *Front. Cell. Neurosci.*, vol. 7, 2013.

[8] C. L. Parish and E. Arenas, “Stem-cell-based strategies for the treatment of parkinson’s disease,” *Neurodegener. Dis.*, vol. 4, no. 4, pp. 339–347, 2007.

[9] Deloitte Access Economics, “Living with Parkinson â€^{TM} s Disease – update Parkinson â€^{TM} s Australia,” no. October, pp. 1–80, 2011.

[10] J. Lotharius and P. Brundin, “Pathogenesis of parkinson’s disease: dopamine, vesicles and α-synuclein,” *Nat. Rev. Neurosci.*, vol. 3, no. 12, pp. 932–942, Dec. 2002.

[11] C. L. Parish and L. H. Thompson, “Modulating Wnt signaling to improve cell replacement therapy for Parkinson ’ s disease,” pp. 54–63, 2014.

[12] B. S. Connolly and A. E. Lang, “Pharmacological Treatment of Parkinson Disease,” *Jama*, vol. 311, no. 16, p. 1670, 2014.

[13] A. Bjorklund and U. Stenevi, “Reconstruction of the nigrostriatal dopamine pathway by intracerebral nigral transplants,” *Brain Res.*, vol. 177, no. 3, pp. 555–560, 1979.

[14] M. Perlow, W. Freed, B. Hoffer, A. Seiger, L. Olson, and R. Wyatt, “Brain grafts reduce motor abnormalities produced by destruction of nigrostriatal dopamine system,” *Science (80-.).*, vol. 204, no. 4393, pp. 643–647, May 1979.

[15] R. A. Barker, J. Drouin-Ouellet, and M. Parmar, “Cell-based therapies for Parkinson disease—past insights and future potential,” *Nat. Rev. Neurol.*, vol. 11, no. 9, pp. 492–503, Sep. 2015.

[16] R. A. Barker, J. Barrett, S. L. Mason, and A. Björklund, “Fetal dopaminergic transplantation trials and the future of neural grafting in Parkinson’s disease,” *Lancet Neurol.*, vol. 12, no. 1, pp. 84–91, Jan. 2013.

[17] C. Winkler, D. Kirik, and A. Björklund, “Cell transplantation in Parkinson’s disease: how can we make it work?,” *Trends Neurosci.*, vol. 28, no. 2, pp. 86–92, 2005.

[18] J. A. Thomson, “Embryonic Stem Cell Lines Derived from Human Blastocysts,” *Science (80-.).*, vol. 282, no. 5391, pp. 1145–1147, Nov. 1998.

[19] K. Takahashi *et al.*, “Induction of Pluripotent Stem Cells from Adult Human Fibroblasts by Defined Factors,” *Cell*, vol. 131, no. 5, pp. 861–872, Nov. 2007.

[20] S. M. Chambers, C. A. Fasano, E. P. Papapetrou, M. Tomishima, M. Sadelain, and L. Studer, “Highly efficient neural conversion of human ES and iPS cells by dual inhibition of SMAD signaling,” *Nat. Biotechnol.*, vol. 27, no. 3, pp. 275–280, Mar. 2009.

[21] S. Kriks *et al.*, “Dopamine neurons derived from human ES cells efficiently engraft in animal models of Parkinson’s disease.,” *Nature*, vol. 480, no. 7378, pp. 547–51, 2011.

[22] A. Kirkeby *et al.*, “Generation of Regionally Specified Neural Progenitors and Functional Neurons from Human Embryonic Stem Cells under Defined Conditions,” *Cell Rep.*, vol. 1, no. 6, pp. 703–714, 2012.

[23] A. JONATHAN C. NICLIS, a,* CARLOS W. GANTNER, a,* WALAA F. ALSANIE, a STUART J. MCDOUGALL, E. CHRIS R. BYE, a ANDREW G. ELEFANTY, b, c, d EDOUARD G. STANLEY, b, c, d JOHN M. HAYNES, and a C. L. Parish. COLIN W. POUTON, e LACHLAN H. THOMPSON, “Efficiently Specified Ventral Midbrain Dopamine Neurons From Human Pluripotent Stem Cells Under Xeno-Free Conditions Restore Motor Deficits in Parkinsonian Rodents.”

[24] R. F. Castilho, O. Hansson, and P. Brundin, “Chapter 10 Improving the survival of grafted embryonic dopamine neurons in rodent models of Parkinson’s disease,” 2000, pp. 203–231.

[25] J. C. Niclis *et al.*, “A PITX3 -EGFP Reporter Line Reveals Connectivity of Dopamine and Non-dopamine Neuronal Subtypes in Grafts Generated from Human Embryonic Stem Cells,” *Stem Cell Reports*, vol. 9, no. 3, pp. 868–882, Sep. 2017.

[26] L. Lin, D. Doherty, J. Lile, S. Bektesh, and F. Collins, “GDNF: a glial cell line-derived neurotrophic factor for midbrain dopaminergic neurons,” *Science (80-.).*, vol. 260, no. 5111, pp. 1130–1132, May 1993.

[27] A. Björklund, C. Rosenblad, C. Winkler, and D. Kirik, “Studies on Neuroprotective and Regenerative Effects of GDNF in a Partial Lesion Model of Parkinson’s Disease,” *Neurobiol. Dis.*, vol. 4, no. 3–4, pp. 186–200, 1997.

[28] D. Kirik, E. Cederfjäll, G. Halliday, and Å. Petersén, “Gene therapy for Parkinson’s disease: Disease modification by GDNF family of ligands,” *Neurobiol. Dis.*, vol. 97, pp. 179–188, Jan. 2017.

[29] C. Rosenblad, A. Martinez-Serrano, and A. Björklund, “Glial cell line-derived neurotrophic factor increases survival, growth and function of intrastriatal fetal nigral dopaminergic grafts.,” *Neuroscience*, vol. 75, no. 4, pp. 979–85, Dec. 1996.

[30] Y.-H. Ahn *et al.*, “Increased fiber outgrowth from xeno-transplanted human embryonic dopaminergic neurons with co-implants of polymer-encapsulated genetically modified cells releasing glial cell line-derived neurotrophic factor,” *Brain Res. Bull.*, vol. 66, no. 2, pp. 135–142, Jul. 2005.

[31] M. Johasson, M. Friedemann, B. Hopper, and I. Strömberg, “Effects of Glial Cell Line-Derived Neurotrophic Factor on Developing and Mature Ventral Mesencephalic Grafts in Oculo,” *Exp. Neurol.*, vol. 134, no. 1, pp. 25–34, Jul. 1995.

[32] S. R. Sinclair, C. N. Svendsen, E. M. Torres, D. Martin, J. W. Fawcett, and S. B. Dunnett, “GDNF enhances dopaminergic cell survival and fibre outgrowth in embryonic nigral grafts,” *Neuroreport*, vol. 7, no. 15, pp. 2547–2552, Nov. 1996.

[33] J. Kauhausen, L. H. Thompson, and C. L. Parish, “Cell intrinsic and extrinsic factors contribute to enhance neural circuit reconstruction following transplantation in Parkinsonian mice,” *J. Physiol.*, vol. 591, no. 1, pp. 77–91, Jan. 2013.

[34] I. Mendez, D. Sadi, and M. Hong, “Reconstruction of the nigrostriatal pathway by simultaneous intrastriatal and intranigral dopaminergic transplants.,” *J. Neurosci.*, vol. 16, no. 22, pp. 7216–7227, 1996.

[35] D. R. Wakeman *et al.*, “Human Neural Stem Cells Survive Long Term in the Midbrain of Dopamine-Depleted Monkeys After GDNF Overexpression and Project Neurites Toward an Appropriate Target,” *Stem Cells Transl. Med.*, vol. 3, no. 6, pp. 692–701, Jun. 2014.

[36] J. Kauhausen, L. H. Thompson, and C. L. Parish, “Primary tissue for cellular brain repair in Parkinson’s disease: Promise, problems and the potential of biomaterials,” *J. Physiol.*, vol. 591, no. 1, pp. 77–91, Jan. 2013.

[37] D. Doi *et al.*, “Isolation of Human Induced Pluripotent Stem Cell-Derived Dopaminergic Progenitors by Cell Sorting for Successful Transplantation,” *Stem Cell Reports*, vol. 2, no. 3, pp. 337–350, Mar. 2014.

[38] T. Carlsson, M. Carta, C. Winkler, A. Bjorklund, and D. Kirik, “Serotonin Neuron Transplants Exacerbate L-DOPA- Induced Dyskinesias in a Rat Model of Parkinson’s Disease,” *J. Neurosci.*, vol. 27, no. 30, pp. 8011–8022, Jul. 2007.

[39] M. Politis *et al.*, “Graft-induced dyskinesias in Parkinson’s disease: High striatal serotonin/dopamine transporter ratio,” *Mov. Disord.*, vol. 26, no. 11, pp. 1997–2003, Sep. 2011.

[40] M. Etzrodt, M. Endele, and T. Schroeder, “Quantitative Single-Cell Approaches to Stem Cell Research,” *Cell Stem Cell*, vol. 15, no. 5, pp. 546–558, Nov. 2014.

[41] G. La Manno *et al.*, “Molecular Diversity of Midbrain Development in Mouse, Human, and Stem Cells,” *Cell*, vol. 167, no. 2, p. 566–580.e19, Oct. 2016.

[42] F. Tang *et al.*, “Tracing the Derivation of Embryonic Stem Cells from the Inner Cell Mass by Single-Cell RNA-Seq Analysis,” *Cell Stem Cell*, vol. 6, no. 5, pp. 468–478, May 2010.

[43] B. Samata *et al.*, “Purification of functional human ES and iPSC-derived midbrain dopaminergic progenitors using LRTM1,” *Nat. Commun.*, vol. 7, no. 1, p. 13097, Dec. 2016.

[44] A. Kirkeby *et al.*, “Predictive Markers Guide Differentiation to Improve Graft Outcome in Clinical Translation of hESC-Based Therapy for Parkinson’s Disease,” *Cell Stem Cell*, vol. 20, no. 1, pp. 135–148, Jan. 2017.

[45] E. Andersson *et al.*, “Identification of Intrinsic Determinants of Midbrain Dopamine Neurons,” *Cell*, vol. 124, no. 2, pp. 393–405, Jan. 2006.

[46] C. H. Yan, M. Levesque, S. Claxton, R. L. Johnson, and S.-L. Ang, “Lmx1a and Lmx1b Function Cooperatively to Regulate Proliferation, Specification, and Differentiation of Midbrain Dopaminergic Progenitors,” *J. Neurosci.*, vol. 31, no. 35, pp. 12413–12425, Aug. 2011.

[47] C. R. Bye, L. H. Thompson, and C. L. Parish, “Birth dating of midbrain dopamine neurons identifies A9 enriched tissue for transplantation into Parkinsonian mice,” *Exp. Neurol.*, vol. 236, no. 1, pp. 58–68, Jul. 2012.

[48] I. Decimo, G. Fumagalli, V. Berton, M. Krampera, and F. Bifari, “Meninges: from protective membrane to stem cell niche.,” *Am. J. Stem Cells*, vol. 1, no. 2, pp. 92–105, 2012.

[49] J. A. Siegenthaler and S. J. Pleasure, “We have got you ‘covered’: how the meninges control brain development,” *Curr. Opin. Genet. Dev.*, vol. 21, no. 3, pp. 249–255, Jun. 2011.

[50] F. A. Somaa *et al.*, “Peptide-Based Scaffolds Support Human Cortical Progenitor Graft Integration to Reduce Atrophy and Promote Functional Repair in a Model of Stroke.,” *Cell Rep.*, vol. 20, no. 8, pp. 1964–1977, Aug. 2017.

[51] J. A. Steinbeck *et al.*, “Optogenetics enables functional analysis of human embryonic stem cell–derived grafts in a Parkinson’s disease model,” *Nat. Biotechnol.*, vol. 33, no. 2, pp. 204–209, Feb. 2015.

[52] R. A. Barker, M. Parmar, L. Studer, and J. Takahashi, “Human Trials of Stem Cell-Derived Dopamine Neurons for Parkinson’s Disease: Dawn of a New Era,” *Cell Stem Cell*, vol. 21, no. 5, pp. 569–573, Nov. 2017.

[53] S. Grealish *et al.*, “Human ESC-Derived Dopamine Neurons Show Similar Preclinical Efficacy and Potency to Fetal Neurons when Grafted in a Rat Model of Parkinson’s Disease,” *Cell Stem Cell*, vol. 15, no. 5, pp. 653–665, Nov. 2014.

[54] R. A. Barker, M. Parmar, A. Kirkeby, A. Björklund, L. Thompson, and P. Brundin, “Are Stem Cell-Based Therapies for Parkinson’s Disease Ready for the Clinic in 2016?,” *J. Parkinsons. Dis.*, vol. 6, no. 1, pp. 57–63, Mar. 2016.

[55] A. Trounson and C. McDonald, “Stem Cell Therapies in Clinical Trials: Progress and Challenges,” *Cell Stem Cell*, vol. 17, no. 1, pp. 11–22, Jul. 2015.

[56] D. VANDENHEUVEL, R. J. Pasterkamp, D. M. A. Van Den Heuvel, and R. J. Pasterkamp, “Getting connected in the dopamine system,” *Prog. Neurobiol.*, vol. 85, no. 1, pp. 75–93, May 2008.

[57] B. J. Dickson, “Molecular Mechanisms of Axon Guidance,” *Science (80-.).*, vol. 298, no. 5600, pp. 1959–1964, Dec. 2002.

[58] M. Tessier-Lavigne and C. S. Goodman, “The Molecular Biology of Axon Guidance,” *Science (80-.).*, vol. 274, no. 5290, pp. 1123–1133, Nov. 1996.

[59] B. D. Blakely *et al.*, “Wnt5a Regulates Midbrain Dopaminergic Axon Growth and Guidance,” *PLoS One*, vol. 6, no. 3, p. e18373, Mar. 2011.

[60] O. Guillame-Gentil *et al.*, “Engineering the extracellular environment: Strategies for building 2D and 3D cellular structures.,” *Adv. Mater.*, vol. 22, no. 48, pp. 5443–62, Dec.

2010.

[61] A. J. Maniotis, C. S. Chen, and D. E. Ingber, “Demonstration of mechanical connections between integrins, cytoskeletal filaments, and nucleoplasm that stabilize nuclear structure.,” *Proc. Natl. Acad. Sci. U. S. A.*, vol. 94, no. 3, pp. 849–54, Feb. 1997.

[62] U. Theocharidis, K. Long, C. Ffrench-Constant, and A. Faissner, “Regulation of the neural stem cell compartment by extracellular matrix constituents,” 2014, pp. 3–28.

[63] D. Zhang *et al.*, “Niche-derived laminin-511 promotes midbrain dopaminergic neuron survival and differentiation through YAP,” *Sci. Signal.*, vol. 10, no. 493, p. eaal4165, Aug. 2017.

[64] T.-Y. Wang, K. F. Bruggeman, J. A. Kauhausen, A. L. Rodriguez, D. R. Nisbet, and C. L. Parish, “Functionalized composite scaffolds improve the engraftment of transplanted dopaminergic progenitors in a mouse model of Parkinson’s disease,” *Biomaterials*, vol. 74, pp. 89–98, Jan. 2016.

[65] T.-Y. Wang, J. S. Forsythe, D. R. Nisbet, and C. L. Parish, “Promoting engraftment of transplanted neural stem cells/progenitors using biofunctionalised electrospun scaffolds,” *Biomaterials*, vol. 33, no. 36, pp. 9188–9197, Dec. 2012.

[66] N. Moriarty, C. L. Parish, and E. Dowd, “Primary tissue for cellular brain repair in Parkinson’s disease: Promise, problems and the potential of biomaterials,” *Eur. J. Neurosci.*, vol. 49, no. 4, pp. 472–486, Feb. 2019.

[67] A. Farrukh *et al.*, “Bifunctional Hydrogels Containing the Laminin Motif IKVAV Promote Neurogenesis,” *Stem Cell Reports*, vol. 9, no. 5, pp. 1432–1440, Nov. 2017.

[68] K. F. Bruggeman, Y. Wang, F. L. Maclean, C. L. Parish, R. J. Williams, and D. R. Nisbet, “Temporally controlled growth factor delivery from a self-assembling peptide hydrogel and electrospun nanofibre composite scaffold,” *Nanoscale*, vol. 9, no. 36, pp. 13661–13669, 2017.

[69] K. F. Bruggeman, R. J. Williams, and D. R. Nisbet, “Dynamic and Responsive Growth Factor Delivery from Electrospun and Hydrogel Tissue Engineering Materials,” *Adv. Healthc. Mater.*, vol. 7, no. 1, p. 1700836, Jan. 2018.

[70] K. F. Bruggeman, N. Moriarty, E. Dowd, D. R. Nisbet, and C. L. Parish, “Harnessing stem cells and biomaterials to promote neural repair,” *Br. J. Pharmacol.*, vol. 176, no. 3, pp. 355–368, Feb. 2019.

[71] M. Olsson, G. Nikkhah, C. Bentlage, and A. Björklund, “Forelimb akinesia in the rat Parkinson model: differential effects of dopamine agonists and nigral transplants as assessed by a new stepping test.,” *J. Neurosci.*, vol. 15, no. 5 Pt 2, pp. 3863–75, May 1995.

[72] K. Sawamoto *et al.*, “Generation of dopaminergic neurons in the adult brain from mesencephalic precursor cells labeled with a nestin-GFP transgene.,” *J. Neurosci.*, vol. 21, no. 11, pp. 3895–903, Jun. 2001.

[73] C. M. Nefzger *et al.*, “Lmx1a Allows Context-Specific Isolation of Progenitors of GABAergic or Dopaminergic Neurons During Neural Differentiation of Embryonic Stem Cells,” *Stem Cells*, vol. 30, no. 7, pp. 1349–1361, Jul. 2012.

[74] J. Weickenmeier *et al.*, “Brain stiffens post mortem,” *J. Mech. Behav. Biomed. Mater.*, vol. 84, pp. 88–98, Aug. 2018.

[75] A. Untergasser *et al.*, “Primer3—new capabilities and interfaces,” *Nucleic Acids Res.*, vol. 40, no. 15, pp. e115–e115, Aug. 2012.

[76] M. W. Pfaffl, “A new mathematical model for relative quantification in real-time RT-PCR,” *Nucleic Acids Res.*, vol. 29, no. 9, p. 45e–45, May 2001.

[77] E. Afgan *et al.*, “The Galaxy platform for accessible, reproducible and collaborative biomedical analyses: 2018 update,” *Nucleic Acids Res.*, vol. 46, no. W1, pp. W537–W544, Jul. 2018.

[78] W. Huber *et al.*, “Orchestrating high-throughput genomic analysis with Bioconductor,” *Nat. Methods*, vol. 12, no. 2, pp. 115–121, Feb. 2015.

[79] S. Anders, P. T. Pyl, and W. Huber, “HTSeq--a Python framework to work with high-throughput sequencing data,” *Bioinformatics*, vol. 31, no. 2, pp. 166–169, Jan. 2015.

[80] M. I. Love, W. Huber, and S. Anders, “Moderated estimation of fold change and dispersion for RNA-seq data with DESeq2,” *Genome Biol.*, vol. 15, no. 12, p. 550, Dec. 2014.

[81] P. Hagell and P. Brundin, “Cell Survival and Clinical Outcome Following Intrastriatal Transplantation in Parkinson Disease,” *J. Neuropathol. Exp. Neurol.*, vol. 60, no. 8, pp. 741–752, Aug. 2001.

[82] S. Grealish, M. E. Jonsson, M. Li, D. Kirik, A. Bjorklund, and L. H. Thompson, “The A9 dopamine neuron component in grafts of ventral mesencephalon is an important determinant for recovery of motor function in a rat model of Parkinson’s disease,” *Brain*, vol. 133, no. 2, pp. 482–495, Feb. 2010.

[83] L. Thompson and A. Björklund, “Survival, differentiation, and connectivity of ventral mesencephalic dopamine neurons following transplantation.,” *Prog. Brain Res.*, vol. 200, pp. 61–95, 2012.

[84] T. Vazin *et al.*, “A Novel Combination of Factors, Termed SPIE, which Promotes Dopaminergic Neuron Differentiation from Human Embryonic Stem Cells,” *PLoS One*, vol. 4, no. 8, p. e6606, Aug. 2009.

[85] A. Morizane, J. Takahashi, Y. Takagi, Y. Sasai, and N. Hashimoto, “Optimal conditions for in vivo induction of dopaminergic neurons from embryonic stem cells through stromal cell-derived inducing activity,” *J. Neurosci. Res.*, vol. 69, no. 6, pp. 934–939, Sep. 2002.

[86] H. Kawasaki *et al.*, “Induction of midbrain dopaminergic neurons from ES cells by stromal cell-derived inducing activity.,” *Neuron*, vol. 28, no. 1, pp. 31–40, Oct. 2000.

[87] H. Hayashi *et al.*, “Meningeal cells induce dopaminergic neurons from embryonic stem cells,” *Eur. J. Neurosci.*, vol. 27, no. 2, pp. 261–268, Jan. 2008.

[88] F. A. Somaa, C. R. Bye, L. H. Thompson, and C. L. Parish, “Meningeal cells influence midbrain development and the engraftment of dopamine progenitors in Parkinsonian mice,” *Exp. Neurol.*, vol. 267, pp. 30–41, May 2015.

[89] A. L. Rodriguez *et al.*, “In vivo assessment of grafted cortical neural progenitor cells and host response to functionalized self-assembling peptide hydrogels and the implications

for tissue repair," *J. Mater. Chem. B*, vol. 2, no. 44, pp. 7771–7778, 2014.

[90] K. Tashiro *et al.*, "A synthetic peptide containing the IKVAV sequence from the A chain of laminin mediates cell attachment, migration, and neurite outgrowth.," *J. Biol. Chem.*, vol. 264, no. 27, pp. 16174–82, Sep. 1989.

[91] D. R. Nisbet *et al.*, "Shear Containment of BDNF within Molecular Hydrogels Promotes Human Stem Cell Engraftment and Postinfarction Remodeling in Stroke," *Adv. Biosyst.*, vol. 2, no. 9, p. 1800113, Sep. 2018.

[92] A. L. Rodriguez *et al.*, "Using minimalist self-assembling peptides as hierarchical scaffolds to stabilise growth factors and promote stem cell integration in the injured brain," *J. Tissue Eng. Regen. Med.*, vol. 12, no. 3, pp. e1571–e1579, Mar. 2018.

[93] A. L. Rodriguez, C. L. Parish, D. R. Nisbet, and R. J. Williams, "Tuning the amino acid sequence of minimalist peptides to present biological signals via charge neutralised self assembly," *Soft Matter*, vol. 9, no. 15, p. 3915, 2013.

[94] T.-Y. Wang, K. A. F. Bruggeman, R. K. Sheean, B. J. Turner, D. R. Nisbet, and C. L. Parish, "Characterization of the Stability and Bio-functionality of Tethered Proteins on Bioengineered Scaffolds," *J. Biol. Chem.*, vol. 289, no. 21, pp. 15044–15051, May 2014.

[95] S. Yang *et al.*, "Cxcl12/Cxcr4 signaling controls the migration and process orientation of A9-A10 dopaminergic neurons," *Development*, vol. 140, no. 22, pp. 4554–4564, Nov. 2013.

[96] L. H. Thompson and C. L. Parish, "Transplantation of Fetal Midbrain Dopamine Progenitors into a Rodent Model of Parkinson's Disease," 2013, pp. 169–180.

[97] C. L. Parish, D. I. Finkelstein, J. Drago, E. Borrelli, and M. K. Horne, "The role of dopamine receptors in regulating the size of axonal arbors.," *J. Neurosci.*, vol. 21, no. 14, pp. 5147–57, Jul. 2001.

[98] C. G. van Horne, I. Strömberg, D. Young, L. Olson, and B. Hoffer, "Functional enhancement of intrastriatal dopamine-containing grafts by the co-transplantation of sciatic nerve tissue in 6-hydroxydopamine-lesioned rats," *Exp. Neurol.*, vol. 113, no. 2, pp. 143–154, Aug. 1991.

[99] S. Shukla, R. K. Chaturvedi, K. Seth, N. S. Roy, and A. K. Agrawal, "Enhanced survival and function of neural stem cells-derived dopaminergic neurons under influence of olfactory ensheathing cells in parkinsonian rats," *J. Neurochem.*, vol. 109, no. 2, pp. 436–451, Apr. 2009.

[100] F. H. Gage, U. Stenevi, T. Carlstedt, G. Foster, A. Bj�rklund, and A. J. Aguayo, "Anatomical and functional consequences of grafting mesencephalic neurons into a peripheral nerve ?bridge? connected to the denervated striatum," *Exp. Brain Res.*, vol. 60, no. 3, Nov. 1985.

[101] A. J. Aguayo, A. Björklund, U. Stenevi, and T. Carlstedt, "Fetal mesencephalic neurons survive and extend long axons across peripheral nervous system grafts inserted into the adult rat striatum," *Neurosci. Lett.*, vol. 45, no. 1, pp. 53–58, Mar. 1984.

[102] C. R. Bye, V. Rytova, W. F. Alsanie, C. L. Parish, and L. H. Thompson, "Axonal growth of midbrain dopamine neurons is modulated by the cell adhesion molecule ALCAM through trans -heterophilic interaction with L1Cam, ChL1 and Semaphorin," *J. Neurosci.*,

pp. 278–19, Jul. 2019.

[103] Y.-F. Cui *et al.*, “Embryonic stem cell-derived L1 overexpressing neural aggregates enhance recovery in Parkinsonian mice,” *Brain*, vol. 133, no. 1, pp. 189–204, Jan. 2010.

[104] V. Ourednik *et al.*, “Cross-Talk Between Stem Cells and the Dysfunctional Brain is Facilitated by Manipulating the Niche: Evidence from an Adhesion Molecule,” *Stem Cells*, vol. 27, no. 11, pp. 2846–2856, Nov. 2009.

[105] N. Moriarty, A. Pandit, and E. Dowd, “Encapsulation of primary dopaminergic neurons in a GDNF-loaded collagen hydrogel increases their survival, re-innervation and function after intra-striatal transplantation,” *Sci. Rep.*, vol. 7, no. 1, p. 16033, Dec. 2017.

[106] G. O. Bodea *et al.*, “Reelin and CXCL12 regulate distinct migratory behaviors during the development of the dopaminergic system,” *Development*, vol. 141, no. 3, pp. 661–673, Feb. 2014.

[107] D. Kirik, C. Winkler, and A. Björklund, “Growth and functional efficacy of intrastriatal nigral transplants depend on the extent of nigrostriatal degeneration.,” *J. Neurosci.*, vol. 21, no. 8, pp. 2889–96, Apr. 2001.

[108] W. F. Alsanie, V. Penna, M. Schachner, L. H. Thompson, and C. L. Parish, “Homophilic binding of the neural cell adhesion molecule CHL1 regulates development of ventral midbrain dopaminergic pathways,” *Sci. Rep.*, vol. 7, no. 1, p. 9368, Dec. 2017.

[109] P. Jendelová, Š. Kubinová, I. Sandvig, S. Erceg, A. Sandvig, and E. Syková, “Current developments in cell- and biomaterial-based approaches for stroke repair,” *Expert Opin. Biol. Ther.*, vol. 16, no. 1, pp. 43–56, Jan. 2016.

[110] N. Moriarty, S. Cabré, V. Alamilla, A. Pandit, and E. Dowd, “Encapsulation of young donor age dopaminergic grafts in a GDNF-loaded collagen hydrogel further increases their survival, reinnervation, and functional efficacy after intrastriatal transplantation in hemi-Parkinsonian rats,” *Eur. J. Neurosci.*, vol. 49, no. 4, pp. 487–496, Feb. 2019.

[111] N. Moriarty, C. L. Parish, and E. Dowd, “Primary tissue for cellular brain repair in Parkinson’s disease: Promise, problems and the potential of biomaterials.,” *Eur. J. Neurosci.*, Jun. 2018.

[112] J. B. Matson and S. I. Stupp, “Self-assembling peptide scaffolds for regenerative medicine,” *Chem. Commun.*, vol. 48, no. 1, pp. 26–33, 2012.

[113] M. A. Cenci, P. Kalén, R. J. Mandel, K. Wictorin, and A. Björklund, “Dopaminergic transplants normalize amphetamine- and apomorphine-induced Fos expression in the 6-hydroxydopamine-lesioned striatum,” *Neuroscience*, vol. 46, no. 4, pp. 943–957, Feb. 1992.

[114] K. F. Jensen and H. P. Killackey, “Terminal arbors of axons projecting to the somatosensory cortex of the adult rat. II. The altered morphology of thalamocortical afferents following neonatal infraorbital nerve cut.,” *J. Neurosci.*, vol. 7, no. 11, pp. 3544–53, Nov. 1987.

[115] M. M. Adil *et al.*, “Dopaminergic Neurons Transplanted Using Cell-Instructive Biomaterials Alleviate Parkinsonism in Rodents,” *Adv. Funct. Mater.*, vol. 28, no. 41, p. 1804144, Oct. 2018.

[116] M. M. Adil *et al.*, “Engineered hydrogels increase the post-transplantation survival of encapsulated hESC-derived midbrain dopaminergic neurons,” *Biomaterials*, vol. 136, pp. 1–11, Aug. 2017.

[117] B. Newland *et al.*, “Tackling Cell Transplantation Anoikis: An Injectable, Shape Memory Cryogel Microcarrier Platform Material for Stem Cell and Neuronal Cell Growth,” *Small*, vol. 11, no. 38, pp. 5047–5053, Oct. 2015.

[118] G. A. Silva, “Selective Differentiation of Neural Progenitor Cells by High-Epitope Density Nanofibers,” *Science (80-.).*, vol. 303, no. 5662, pp. 1352–1355, Feb. 2004.

[119] L. F. Lin, D. H. Doherty, J. D. Lile, S. Bektesh, and F. Collins, “GDNF: a glial cell line-derived neurotrophic factor for midbrain dopaminergic neurons.,” *Science*, vol. 260, no. 5111, pp. 1130–2, May 1993.

[120] D. M. Yurek, “Glial Cell Line-Derived Neurotrophic Factor Improves Survival of Dopaminergic Neurons in Transplants of Fetal Ventral Mesencephalic Tissue,” *Exp. Neurol.*, vol. 153, no. 2, pp. 195–202, Oct. 1998.

[121] C. Winkler, B. Georgievska, T. Carlsson, B. Lacar, and D. Kirik, “Continuous exposure to glial cell line-derived neurotrophic factor to mature dopaminergic transplants impairs the graft’s ability to improve spontaneous motor behavior in parkinsonian rats,” *Neuroscience*, vol. 141, no. 1, pp. 521–531, 2006.

[122] M. Denham, C. Bye, J. Leung, B. J. Conley, L. H. Thompson, and M. Dottori, “Glycogen Synthase Kinase 3β and Activin/Nodal Inhibition in Human Embryonic Stem Cells Induces a Pre-Neuroepithelial State That Is Required for Specification to a Floor Plate Cell Lineage,” *Stem Cells*, vol. 30, no. 11, pp. 2400–2411, Nov. 2012.

[123] D. W. Huang, B. T. Sherman, and R. A. Lempicki, “Systematic and integrative analysis of large gene lists using DAVID bioinformatics resources,” *Nat. Protoc.*, vol. 4, no. 1, pp. 44–57, Jan. 2009.

[124] H. Hu, Y.-R. Miao, L.-H. Jia, Q.-Y. Yu, Q. Zhang, and A.-Y. Guo, “AnimalTFDB 3.0: a comprehensive resource for annotation and prediction of animal transcription factors,” *Nucleic Acids Res.*, vol. 47, no. D1, pp. D33–D38, Jan. 2019.

[125] M. Kanehisa, M. Furumichi, M. Tanabe, Y. Sato, and K. Morishima, “KEGG: new perspectives on genomes, pathways, diseases and drugs,” *Nucleic Acids Res.*, vol. 45, no. D1, pp. D353–D361, Jan. 2017.

[126] C. Wiese *et al.*, “Nestin expression ? a property of multi-lineage progenitor cells?,” *Cell. Mol. Life Sci.*, vol. 61, no. 19–20, pp. 2510–2522, Oct. 2004.

[127] W. Wurst, A. B. Auerbach, and A. L. Joyner, “Multiple developmental defects in Engrailed-1 mutant mice: an early mid-hindbrain deletion and patterning defects in forelimbs and sternum.,” *Development*, vol. 120, no. 7, pp. 2065–75, Jul. 1994.

[128] D. Cyranoski, “‘Reprogrammed’ stem cells implanted into patient with Parkinson’s disease,” *Nature*, Nov. 2018.

[129] S. Bariselli *et al.*, “Role of VTA dopamine neurons and neuroligin 3 in sociability traits related to nonfamiliar conspecific interaction,” *Nat. Commun.*, vol. 9, no. 1, p. 3173, Dec. 2018.

[130] D. B. Kantor *et al.*, “Semaphorin 5A Is a Bifunctional Axon Guidance Cue Regulated by Heparan and Chondroitin Sulfate Proteoglycans,” *Neuron*, vol. 44, no. 6, pp. 961–975, Dec. 2004.

[131] V. Penna, M. V. Lipay, M. T. Duailibi, and S. E. Duailibi, “The likely role of proteolytic enzymes in unwanted differentiation of stem cells in culture,” *Futur. Sci. OA*, vol. 1, no. 3, p. fso.15.26, Nov. 2015.

[132] F. Karimi, A. J. O’Connor, G. G. Qiao, and D. E. Heath, “Integrin Clustering Matters: A Review of Biomaterials Functionalized with Multivalent Integrin-Binding Ligands to Improve Cell Adhesion, Migration, Differentiation, Angiogenesis, and Biomedical Device Integration,” *Adv. Healthc. Mater.*, vol. 7, no. 12, p. 1701324, Jun. 2018.